Distinct auxin signalling hubs modulate secondary growth and shape root architectures

Dissertation

der Mathematisch-Naturwissenschaftlichen Fakultät

der Eberhard Karls Universität Tübingen

zur Erlangung des Grades eines

Doktors der Naturwissenschaften

(Dr. rer. nat.)

vorgelegt von

Wei Xiao

aus

Zhuhai, China

Tübingen

2021

Gedruckt mit Genehmigung der Mathematisch-Naturwissenschaftlichen Fakultät der Eberhard Karls Universität Tübingen.

Tag der mündlichen Qualifikation:	08.02.2022
Dekan:	Prof. Dr. Thilo Stehle
1. Berichterstatter/-in:	Dr. Laura Ragni
2. Berichterstatter/-in:	Prof. Dr. Marja Timmermans

Table of Contents

1. Summary

Plant root morphogenesis, including primary patterning, secondary development and formation of lateral roots and root hairs, determines root system architecture, and hence the overall plant growth and performance. The root systems influence the efficiency of water uptake and acquisition of nutrients, and thereby plant adaptations to local environments. Therefore, decoding the regulation of root morphogenesis is of vital ecological and agronomic importance. Pericycle cells are deeply embedded in a distinctive layer of root, surrounding the procambium (i.e. primary xylem and phloem) and are crucial for the initiation of some key root tissues/structures. Particularly, lateral roots and phellogen (cork cambium) are initiated and differentiated from pericycle cells, producing root branching systems and a protective barrier of plant organ/tissue called periderm. Furthermore, secondary meristems indeed partially originate from pericycle cells that give rise to xylem and phloem, and ultimately contribute to the formation of vascular cambium.

Root morphogenesis is largely determined by the balance of stem cell proliferation and differentiation, which are largely regulated by phytohormones. Specifically, auxin-mediated signalling networks are commonly known to buffer the proliferation and differentiation of stem cells in many developmental contexts, including lateral roots development and vascular cambium establishment. Intriguingly, auxin is found to be enriched in pericycle cells. However, it remains unclear whether and how auxin and its downstream regulators coordinate and control the cell fate decisions of pericycle cells to the formation of distinct root organs/tissues, i.e. vascular cambium and phellogen, thereby promoting secondary growth.

Here, using the Arabidopsis root as a model, I showed that auxin is accumulated in phellogen and plays an essential role in phellogen establishment and maintenance. Based on my genetic and gene expression data, I demonstrated distinct IAAs-ARFs module and downstream targets control lateral roots versus vascular cambium and phellogen. Moreover, the initiation of the vascular cambium precedes, and is prerequisite to phellogen establishment. Interestingly, after the establishment of vascular cambium and phellogen, I found altering auxin signalling specifically in the phellogen affects the activity of the vascular cambium, hinting at a compensation mechanism balancing

secondary growth output. I further showed that several auxin-mediated downstream signalling regulators, including *KNAT1*/*BREVIPEDICELLUS* (*BP*), *WUSCHEL-RELATED HOMEOBOX 4* (*WOX4*), *ERECTA* (*ER*), and *AINTEGUMENTA* (*ANT*), accumulates in the vascular cambium and the phellogen. I found that *ER* may act as the upstream regulator of *BP*, *WOX4*, and *ANT*, and enlarges the girth of roots. Tissue specific overexpression of *BP* and *WOX4* in the phellogen and vascular cambium largely increased the periderm layers and the girth of the roots. Furthermore, ER-ANT module promotes vascular cambium proliferation and directs its differentiation, which influence phloem regulation and vascular cambium division, and largely increase the quantity of phloem and vascular cambium cell number, whereas ER-ANT module represses xylem cell formation and decreases xylem area.

To sum up, my studies here collectively demonstrate that the specificity of pericycle stem cell fate is achieved by distinct auxin induced modules; and the results provide molecular insights into how ER-ANT module modifies vascular cambium proliferation and differentiation.

2. Zusammenfassung

Die Morphogenese der Pflanzenwurzel beinhaltet das primär- und sekundäre Wachstum sowohl der Lateral- als auch der Haarwurzeln und bestimmt damit maßgeblich die Architektur des Wurzelsystems und des Pflanzenwachstums bzw. die Gesundheit der Pflanze. Das Wurzelsystem ist außerdem entscheidend für die Wasser- und Nährstoffaufnahme und außerdem für die Anpassung der Pflanze an den jeweiligen Standort. Das Verständnis der Wurzelmorphogenese ist damit von großer ökologischer und ökonomischer Bedeutung. Perizykelzellen sitzen eingebettet in einer bestimmten Schicht der Wurzel und umschließen das Prokambium (d.h. primäres Xylem und Phloem) und sind wesentlich für das Aktivieren von bestimmten Schlüsselstrukturen verantwortlich. Genauer, laterale Wurzeln und das Phellogen (Korkkambium) werden von Perizykelzellen dazu angeregt ein System aus Seitentrieben und einer schützenden Barriere zu bilden und auszudifferenzieren. Dieses System wird auch Peridem genannt. Darüber hinaus entsteht das sekundäre Meristem teilweise aus Perizyklezellen, die die Formation von Xylem und Phloem hervorrufen und so zur Ausbildung des vaskulären Kambiums beitragen.

Die Wurzelmorphogenese wird zum großen Teil von dem Gleichgewicht der Vermehrung und Ausdifferenzierung von Stammzellen bestimmt, was hauptsächlich von Phytohormonen reguliert wird. Besonders Auxin vermittelte Signalwege sind gemeinhin dafür bekannt, die Vermehrung und Ausdifferenzierung von Stammzellen in vielen Entwicklungszusammenhängen, insbesondere auch von der lateralen Wurzelbildung und des vaskulären Kambiums zu steuern. Interessanterweise wird gefunden, dass Auxin in perizyklischen Zellen angereichert ist. Allerdings, wie genau Perizykelzellen mittels von Auxin kontrollierten Regulatoren die bestimmte Ausbildung von Pflanzenorganen steuert ist immer noch unklar und es ist weiterhin unbekannt wie die zwei lateralen Meristeme (vaskuläres Kambium und Phellogen) koordiniert und zum sekundären Wachstum angeregt werden.

In der vorliegenden Arbeit mit der Wurzel von *Arabidopsis* als Modell konnte ich zeigen, dass Auxin im Phellogen angereichert wird und somit eine wichtige Rolle in der Ausbildung und dem Erhalt des Phellogens spielt. Basierend auf unseren genetischen Daten konnte ich zeigen, dass bestimmte IAAs-ARF Module und nachgeschaltete Objekte die Ausbildung von entweder lateralen Wurzeln oder Kambium und Phellogen steuern. Zudem, die Initiierung des vaskulären Kambiums ist

Voraussetzung für die Bildung des Phellogens. Danach werden ein gut etabliertes vaskuläres Kambium und Phellogen in den reifen Wurzeln präsentiert. Interessanterweise beeinflusst ein verändertes Auxinsignal vor allem im Phellogen die Aktivität des vaskulären Kambiums, was auf einen Kompensationsmechanismus für das sekundäre Wachstum spricht. Weiterhing konnte ich zeigen, dass mehrere Auxin gesteuerte Regulatoren, unter anderem *KNAT1/BREVIPEDICELLUS* (*BP*), *WUSCHEL-RELATED HOMEBOX 4* (*WOX4*), *ERECTA* (*ER*) und *ANTIGUEMENTA* (*ANT*), im vaskulären Kambium und dem Phellogen angereichert werden. Meine Ergebnisse zeigen, *ER* agiert im Signalweg oberhalb von *BP*, *WOX4* und *ANT* und erhöht den Umfang der Wurzeln. Gewebespezifische Überexpression von *BP* und *WOX4* im Phellogen und dem vaskulären Kambium zeigten eine Überlappung und bestimmte Signalziele, was zum Verständnis der Stammzellenspezifität beiträgt. Außerdem konnte gezeigt werden, ER-ANT Module regulieren das Phloem und das vaskuläre Kambium positiv, während ER-ANT Module die Formation von Xylemzellen vermindert.

Zusammenfassend zeigen meine Studien einerseits, dass die Spezifität von Perizykelsammzellen von bestimmten Auxinabhängigen Modulen gesteuert wird und bringen weiterhin neue Erkenntnisse inwiefern ER-ANT module das vaskuläre Kambium bilden und differenzieren.

3. Introduction

Root system architecture influences water up-take and nutrient acquisition, thereby impacting plant development and adaptations to the fluctuating environments. In plants, three types of meristems are found, including root apical meristem (RAM), forming the underground root system, shoot apical meristem (SAM) forming the above-ground tissues, and secondary meristems that contribute to secondary growth (cork cambium [i.e. phellogen] and vascular cambium) and hence radial thickening of the plant organs/tissues (Smit & Weijers, 2015; Ragni & Greb, 2018; Campilho *et al.*, 2020). Root system architecture is largely determined by activities of RAM and secondary meristems, that is, main root and secondary root growth that leads to the elongation and increases in the girth of the root, respectively. Particularly, pericycle cells (consist of xylem pole pericycle (XPP) cells and phloem pole pericycle (PPP) cells) are embedded deeply in root as one-layered meristematic cells that is surrounded by a three-cell layers (epidermal, cortex, and endodermal cells) and itself encircles the central stele (xylem and phloem) in a typical *Arabidopsis* root (Fig 1A). Pericycle cells are essentially meristematic cells that give rise to various distinct root structures, such as lateral roots, phellogen (cork cambium) and vascular cambium, and are of particular importance in regeneration processes, as an adaptation to the changing environments (Fig 2) (Che *et al.*, 2007; De Smet *et al.*, 2007; Atta *et al.*, 2009; Beeckman & De Smet, 2014; Shang *et al.*, 2016; Shin & Seo, 2018; Campilho *et al.*, 2020). However, it remains poorly known how the cell fate decisions in pericycle cells are specified and coordinated to produce distinct root structures.

Auxin-centered regulatory networks are widely known to play a major role in stem cell establishment, maintenance and regeneration in plant development. In RAM, phytohormones (such as auxin and cytokinin) are key regulators that coordinate stem cell proliferation and differentiation, thereby establishing the root system. Intriguingly, auxin is indeed found to be enriched in pericycle cells where it also likely promotes cell proliferation and differentiation that ultimately contributes to secondary thickening (Barra-Jimenez & Ragni, 2017; Ragni & Greb, 2018; Campilho *et al.*, 2020).

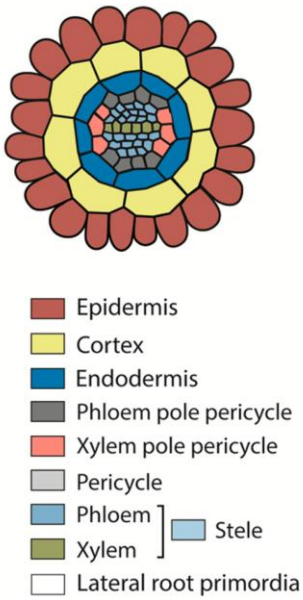

Figure 1. Morphological changes during lateral roots (Jing & Strader, 2019).

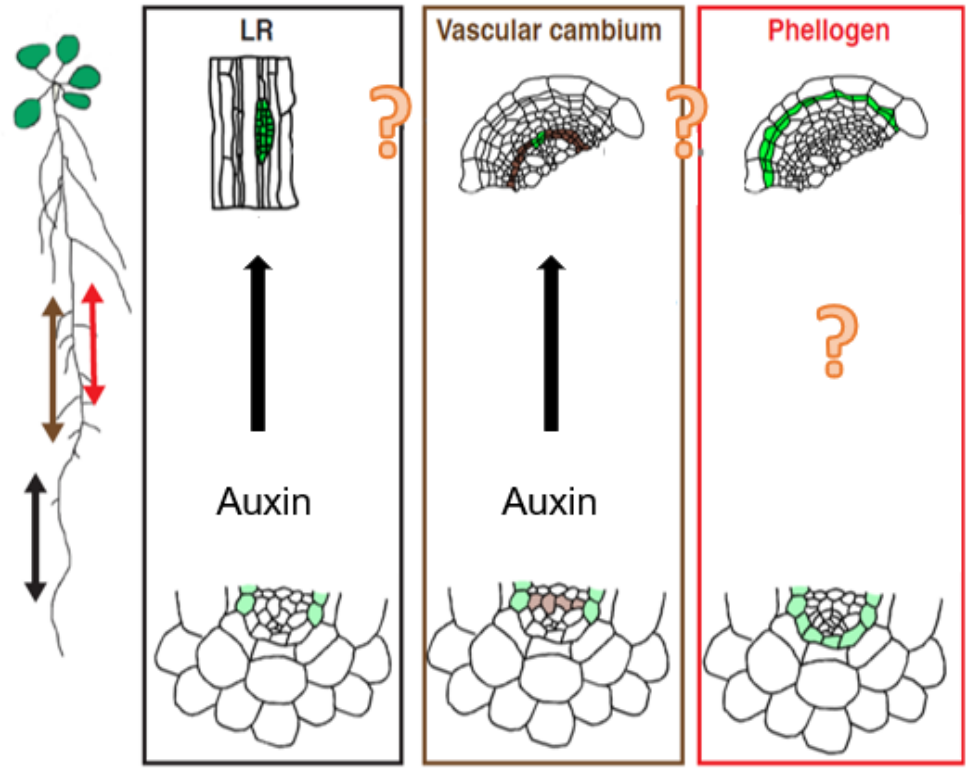

Figure 2. Model explaining pericycle output specificity, modified from (Xiao *et al.*, 2020)

Therefore, in this thesis, I endeavoured to investigate how auxin coordinates with other hormones and triggers meristem establishment and differentiation to form distinct plant organs/tissues that ultimately result in secondary thickening and the formation of lateral roots. To address these, I summarised the current understanding of the patterning of vascular cambium, periderm and lateral root in the following three sections: 1). vascular cambium establishment and maintenance requires auxin and its crosstalk with other phytohormones; 2). periderm, a key protective organ, contributes to secondary growth; 3). Lateral roots formation is largely determined by IAA-ARF modules. I also highlighted some outstanding questions that remain to be addressed which are also the focus of this thesis: how periderm is established and how auxin directs bilateral meristem (i.e. vascular cambium and periderm) differentiation.

3.1 Vascular cambium establishment and maintenance requires auxin and its crosstalk with other phytohormones

Secondary growth, the increase in girth of plant organs provides efficient long-distance transportation of water, nutrient, salts, and photo-assimilates and thereby contributes to successful colonization of vascular plants on Earth. The woody part of the plant is essentially the result of secondary growth and provides the physical support (Barra-Jimenez & Ragni, 2017; Ragni & Greb, 2018; Campilho *et al.*, 2020). Therefore, secondary growth in plant produces the vast diversity of trees and partly shapes the earth's biosphere as we know it today. The secondary growth is the principal site of biomass accumulation, in addition to its economic value in the forestry industry, provides a means for the durable sequestration of CO2. The storage of CO2 in woods also provides an effective solution to addressing climate change and global warming on the earth.

Therefore, secondary growth is of pivotal importance to our humankind and the sustainability of the planet we live in, however, the regulation of secondary growth remains poorly understood even in model species.

Secondary growth is found in root, branches, and stem in most woody dicotyledonous plants and gymnosperms (Barra-Jimenez & Ragni, 2017). Two bilateral meristems (i.e. vascular cambium and phellogen) give rise to secondary thickening and produce inward xylem and phelloderm and outward phloem and phellem/cork, respectively. Many studies focused on how vascular cambium is established and indicated that auxin is an

instrumental phytohormone in establishing vascular cambium and regulating secondary meristem activities in *Arabidopsis* (Ragni & Greb, 2018).

AUXIN RESPONSE FACTOR (ARF) and AUXIN/INDOLE-3-ACETIC ACID (Aux/IAA) proteins are the key players in auxin regulatory networks. In *Arabidopsis*, *Aux*/*IAA* gene family consists of 29 members encoding short-lived transcriptional repressors and is divided into seven subclades (Overvoorde *et al.*, 2005; Li *et al.*, 2017). Aux/IAA and ARF proteins form heterodimers wherein Aux/IAA represses the activities of ARF protein at low auxin level (Tiwari *et al.*, 2001). In *Arabidopsis*, 23 *ARF* genes were described including one pseudogene (*ARF23*), and roughly divided into 5 different subclades in phylogenetic analysis (Okushima *et al.*, 2005; Guilfoyle & Hagen, 2007). 5 out of 23 *ARF* genes (*ARF5*, *ARF6*, *ARF7*, *ARF8*, and *ARF19*) work as transcriptional activators and the other 18 *ARF* genes were summarized as transcriptional repressors (Ulmasov *et al.*, 1999; Tiwari *et al.*, 2003). IAAs with *ARF5*, *ARF6*, *ARF7*, *ARF8*, and *ARF19* regulate many aspects of plant developmental processes including RAM establishment, secondary growth and lateral roots initiation (Guilfoyle *et al.*, 1998; Ulmasov *et al.*, 1999; Tiwari *et al.*, 2001).

Recent studies have revealed that Aux/IAA negatively regulates vascular cambium establishment (Uggla *et al.*, 1998; Hamann *et al.*, 2002, Smetana *et al.*, 2019). For example, BODENLOS (BDL)/IAA12 module regulates the vascular formation (Uggla *et al.*, 1998; Hamann *et al.*, 2002) and SHORTHYPOCOTYL 2 (SHY2)/IAA3 module controls cambial growth in Scots Pine (Bianco, *et al.*, 2013), indicating IAAs are involved in vascular cambium establishment.

MONOPTEROS (MP)/ARF5, repressed by BDL, directly binds to the promoter of *WUSCHEL HOMEOBOX RELATED 4* (*WOX4*) and regulates its activities (Brackmann *et al.*, 2018). MP activates TDIF/CLE41/44-PXY/TDR signalling pathway, which promotes the expression of *WOX4*, promoting the cell proliferation (Hirakawa *et al.*, 2010; Suer *et al.*, 2011; Etchells *et al.*, 2013). Additionally, WOX4 and its homologue WOX14 redundantly promote proliferation on vascular cambium (Etchells *et al.*, 2013). Moreover, MP also regulates *KNAT1* (*KNOTTED-like from Arabidopsis thaliana 1*)/*BP* (*BREVIPEDICELLUS*), which belongs to Class I KNOX transcription factors. MP-BP is involved in meristem activities and promote many developmental processes in plants including secondary growth (Ori *et al.*, 2000; Hay *et al.*, 2006). BP and WOX4 work as the master cambial regulators and promote vascular cambium establishment and proliferation (Liebsch *et al.*, 2014; Zhang *et al.*, 2019). Altogether, it appears an auxin-

centered regulatory network: plant controls vascular development through IAAs-MP module and its main downstream targets *BP* and *WOX4*.

Auxin is involved in vascular cambium differentiation. MP, ARF7, and ARF19, the downstream regulators of IAA, induce five *CLASS III HOMEODOMAIN-LEUCINE ZIPPER* (*HD-ZIPIII*) genes maintain cellular quiescence in the xylem and guide xylem development (Carlsbecker *et al.*, 2010; Nieminen *et al.*, 2015; Fischer *et al.*, 2019; Smetana *et al.*, 2019).

Intriguingly, other hormones like cytokinin and SLs are involved in vascular cambium proliferation and differentiation, respectively. Cytokinin has a positive role on secondary growth via regulating cambial activity. TARGET OF MONOPTEROS5 (TMO5)/TMO5-LIKE1 (T5L1) and LONESOME HIGHWAY (LHW), as heterodimer complexes comprising two basic helix–loop–helix protein families, are master transcriptional regulators of the initial process of vascular development. TMO5/LHW are upregulated by cytokinin and promote cell division and differentiation to form cambial/pro-cambial in embryos, root apical meristem (RAM), and mature main root (Ohashi-Ito and Bergmann 2007; De Rybel *et al.,* 2013; Ohashi-Ito *et al.,* 2013; De Rybel *et al.,* 2014; Ohashi-Ito *et al.,* 2014). Interestingly, TMO5 is also stimulated by MP, indicating auxin induces vascular cambium and is cooperated with the cytokinin signalling pathway (Schlereth et al., 2010).

Cytokinin controls vascular cambium differentiation through *ER* (*ERECTA* receptor kinases) and the transcription factor *ANT* (*AINTEGUMENTA*). *ER* with its legend (EPFLs) and promotes phloem tissues regulation (Torii *et al.*, 1996; Bergmann *et al.*, 2004; Shpak *et al.*, 2004; Shpak *et al.*, 2005; Meng *et al.*, 2012; Uchida & Tasaka, 2013; Ikematsu *et al.*, 2017; Wang *et al.*, 2019). *ANT* and the cell cycle regulator CYCD3 (CYCLIN D3) act as two cytokinin downstream cambium regulators that increase cambium cell number and vascular expansion (Randall *et al.*, 2015).

Strigolactones (SLs), a new hormone discovered in the plant, regulates many growing lists of the process including secondary growth and is involved in auxin signalling pathway (Waldie *et al.*, 2014). *more axillary branches 1* (*max1*), as a SL biosynthesis mutant, shows an increase in shoot branching, while the mutant is fully rescued by SLs treatment (Bennett *et al.*, 2006; Crawford *et al.*, 2010). There are some studies indicating SLs play an important role in cambium activities, correlated with the auxin signalling pathway (Agusti *et al.*, 2011). Additionally, MAX1, MAX3, and MAX4 proteins are involved in the biosynthesis of carotenoids, a key precursor for SLs. In

Arabidopsis, *max1-1*, *max2-1*, *max3-9*, and *max4-1* mutants showed reduction on cambium activities and reduced secondary growth. In the *max1-1* mutant, auxin concentrates in the stems at all positions, indicating the cooperation between SLs and auxin. Interestingly, the functions of SLs on secondary growth with is conserved from species to species, like Eucalyptus trees and pea (Agusti *et al.*, 2011), indicating a long co-evolution between auxin and SLs in controlling vascular cambium proliferation.

Altogether, auxin with other phytohormones, regulates IAAs-ARFs modules. During secondary growth, auxin-centered regulatory networks are involved in vascular cambium establishment and promote vascular cambium differentiation, respectively. However, the following questions have no answers: the bilateral vascular cambium can differentiate into xylem or phloem, while it is unknown how respective differentiation is achieved; moreover, the correlation between xylem and phloem is unclear. My thesis will keep on following these questions.

3.2 Periderm, a key protective organ, contributes to secondary growth

Periderm, replacing the epidermis as an outer layer of a plant organ, is formed in the root and the stem of woody eudicotyledons and gymnosperms and is used as a protective barrier, which is efficient on pathogen infestation, gas exchange, and water loss (Groh *et al.*, 2002; Lendzian, 2006). Periderm has been studied in potato and cork oak due to its economic values, and cork is useful to produce wine-stoppers and insulating/building materials (Esau, 1977; Campilho *et al.*, 2020).

Recently, many studies of periderm have focused on the characteristics and functions but not the molecular mechanism. In many woody plants, periderm was forced to break due to biotic or abiotic stresses, it is replaced by a neo periderm formed underneath, and in turn is replaced by another periderm over the years (Esau, 1977). In some plant species, periderm has evolved different functions including storing starch in phelloderm and isolating salts in periderm (Esau, 1977; Junli *et al.*, 2020).

Periderm replaces the primary protective tissues such as the epidermis and works as the outer tissues on stems, roots and other plant organs/tissues, whereas the first phellogen is originated from different tissues depending on the plant organs and species. In the stems, the first phellogen is originated from the subepidermal layer, while in genus *Malus*, *Pyrus*, and *Oleander*, the first phellogen arises from the epidermis and in genus *Vitis*, *Pinus mugo*, *Alnus glutinosa* the first phellogen arises from the phloem (Esau., 1965; Evert, 2006; Schweingruber and Börner., 2018). In *Arabidopsis*, the first phellogen originates from the pericycle cells in the roots and hypocotyl and contributes to secondary growth (Fig 2). (Wunderling *et al.*, 2018; Ragni & Greb, 2018).

Based on our knowledges, periderm, similar to the vascular system, comprises three tissues (Fig 3) (Ragni & Greb, 2018). However, the number of periderm layer varies from species to species: cork oak contains many phellem layers whereas phelloderm is missing is some species (Esau, 1965; Roth, 1981; Evert *et al.*, 2006; Graça *et al.*,2015).

It is clear that we are short of knowledges on the molecular mechanism of periderm development. To achieve that, a functional model plant for periderm study is needed. In our lab, *Arabidopsis* is a model for periderm development. In *Arabidopsis*, the periderm is found in both hypocotyl and roots, and it is reminiscent of the periderm of woody plants, so we can use the *Arabidopsis* hypocotyl and roots as a model to study the mechanisms of periderm development (Ragni & Greb, 2018). Periderm development in *Arabidopsis* hypocotyl has been described into different stages which are as followed: 1), the pericycle started to divide; 2), a reduction on endodermal cells

caused by programmed cell death (PCD) and the establishment of phellogen began; 3), the one/two layers of periderm were established with one or two endodermal cells remained; 4), both inner cortex, outer cortex, and epidermal started to collapse and are detached from the periderm; 5), a mature periderm was established and becomes the new outer barrier of plant (Wunderling *et al.*, 2018).

In the more elaborated description on the root, periderm development is divided into serval developmental processes: 1), pericycle cells start anticlinal division with the expansion of endodermal cells; 2), pericycle cells start periclinal division and endodermal cells undergo PCD; 3), a three-layer periderm structure is formed and abscission occurs on the cortex and epidermal cells; 4), a ring of periderm is complete and works as a barrier to protect the plant organs/tissues (Wunderling *et al.*, 2018). Eventually, periderm, replacing epidermal cells and becoming the outer tissue of plant organs/tissues, protects it from abiotic or biotic pressure and offer a mechanical support (Campilho *et al.*, 2020). Phellem contains macromolecules, such as suberin and lignin, which are accumulated in phellem to enhance the capabilities of periderm to protect plants (Wunderling *et al.*, 2018). With a fully described developmental map, we can use the annual *Arabidopsis* plant as a model to deeply understand the molecular network in periderm development (Wunderling *et al.*, 2018). Interestingly, many genes like *MYB84*, *ANAC*78, *HORST*, *KCR1*, *DAISY*, and *RALPH* were expressed in the periderm and involved in suberin biosynthesis pathway, which may indicate their functions on periderm development (Wunderling *et al.*, 2018).

To sum it, we noticed the biological importance of periderm in plant and economical value of human being, However, it is unclear about the molecular mechanism of periderm development in *Arabidopsis*. Therefore, in my thesis, I will focus on how phellogen is established and fill the gaps of periderm study.

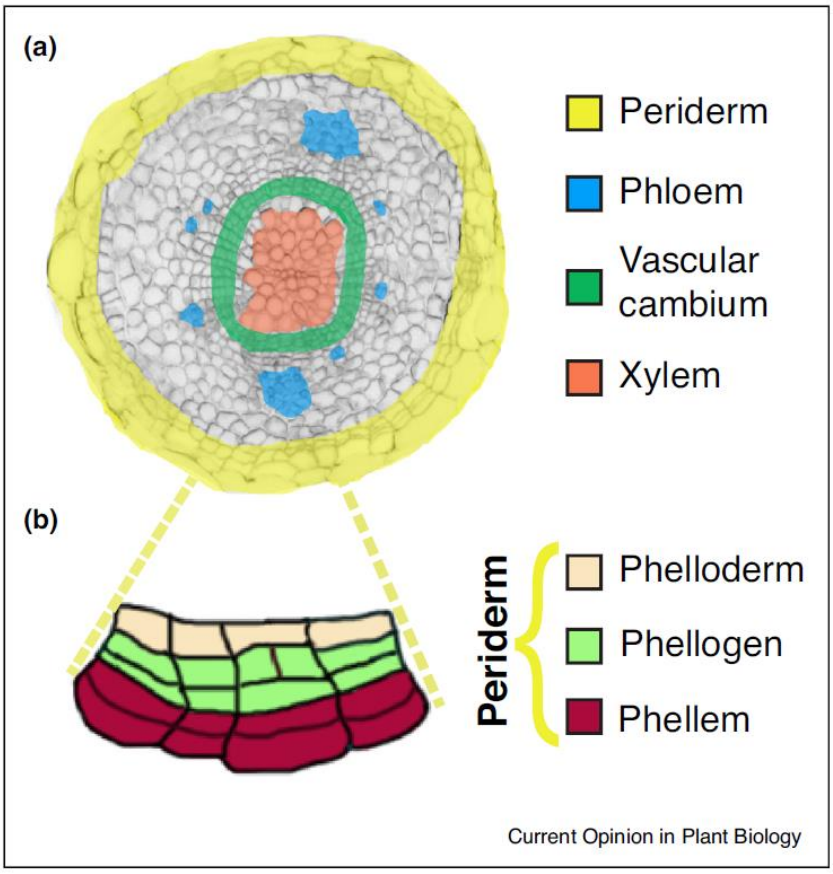

Figure 3. Anatomy of a tissue undergoing secondary growth (Campilho *et al.*, 2020).

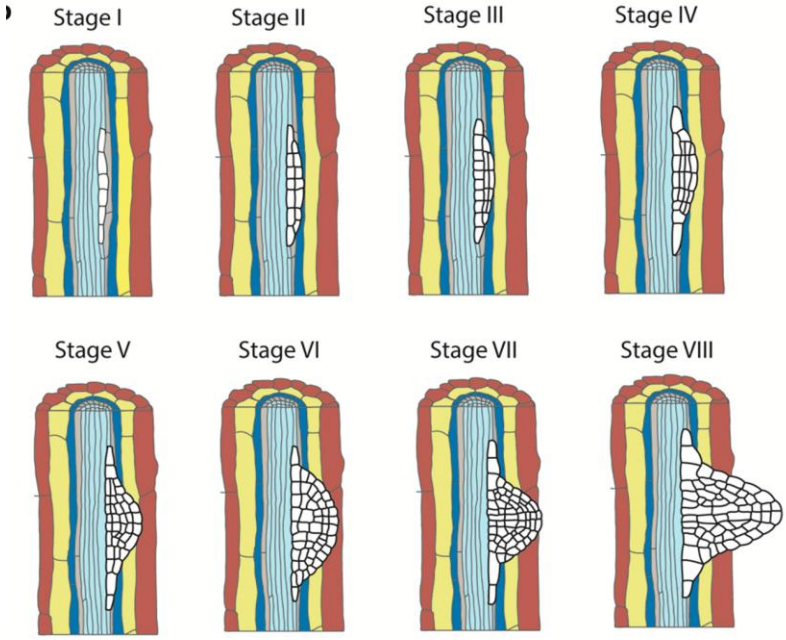

Figure 4. developmental processes of lateral roots formation (Jing & Strader, 2019).

3.3 Lateral roots formation is largely determined by IAA-ARF modules.

Lateral roots are important for increasing the surface area of root system architecture to explore heterogeneous soil environments, impacting the efficiency of water uptake and acquisition of nutrients. Understanding the lateral roots development is therefore of vital biological and agronomic importance. In *Arabidopsis*, lateral roots originate primarily from one side of XPP cells in an existent main root (Fig 1 and Fig 4); moreover, lateral roots can be divided into four main steps: (1) lateral root pre-branch site formation: XPP cells acquire founder cell (FC) identity, (2) lateral root initiation: an asymmetric cell division started, (3) lateral root primordium formation, and (4) lateral root emergence (Fig 4) (Lavenus *et al.*, 2013; Motte *et al.*, 2019).

Treated with auxin transport inhibitors (NPA) in *P. sativum* plants, lateral roots formation is lost which indicates the role of auxin in LR development (Hinchee and Rost, 1992; Casimiro *et al.*, 2001). Additionally, the phytohormone auxin functions in promoting anticlinal cell division, specifying the XPP cell identity and modulating lateral roots formation (De Smet *et al.*, 2007; Casimiro *et al.*, 2001) indication the role of auxin in lateral roots development.

In the processes of lateral roots formation, Aux/IAA and ARF proteins are expressed in LRP and deeply participate in lateral roots developmental processes (Rogg *et al.*, 2001; Fukaki *et al.*, 2002; Okushima *et al.*, 2005; Overvoorde *et al.*, 2005; Okushima *et al.*, 2007; De Rybel *et al.*, 2010; De Smet *et al.*, 2010; Goh *et al.*, 2012; Leyser, 2018). Many functional analyses on *iaas* or *arfs* mutants (overproducing or inhibiting lateral roots) allow us to understand how the plants coordinate between distinct IAAs-ARFs modules then control lateral roots formation, shaping root architecture. Many IAA-ARF modules promote lateral roots initiation: for example, 1) IAA28–ARFs module; 2) SOLITARY ROOT (SLR)/IAA14–ARF7–ARF19 module; 3) BDL-MP module; 4) SHY2–ARFs module. As the downstream targets of auxin, Aux/IAA-ARF module not only shapes many aspects of plant growth but also contributes to the architecture system. Furthermore, distinct IAAs-ARFs modules coordinated during lateral roots development.

IAA28 which is expressed the whole root, works as a transcriptional repressor targeting auxin-induced genes like ARF proteins (ARF5, ARF6, ARF7, ARF8, and ARF19) and repressing ARF's functions in the transition region of root and is degraded under high auxin level. Genetic data underlines IAA28-ARFs suppress the specification of lateral roots founder cell identity (LRFC) (Rogg *et al.*, 2001; De Rybel *et al.*, 2010). *GATA23*

transcription factor is expressed in XPP cells and acts as the downstream target of IAA28, regulating the LRFC identity in *Arabidopsis* (De Rybel *et al.*, 2010). After LRFC establishment, GATA23 is involved in lateral roots initiation, and after that, it decreases and finally disappears from primordia. IAA28-ARFs/GATA23 module plays a crucial in lateral roots priming and LRFC specification.

SLR-ARF7-ARF19 drives lateral roots initiation by activating several auxin-responsive genes (Fukaki *et al.*, 2002; Vanneste *et al.*, 2005; Wilmoth *et al.*, 2005; Lee *et al.*, 2009). Gain of function mutant *solitary root1-1* (*slr1-1*) reduces gravity sensing mechanisms and is devoid of the lateral roots. *slr1-1* inhibits XPP cell division blocking lateral roots initiation, showing the solitary phenotypes. SLR co-localizes with *ARF7* and *ARF19* including pericycle cells (Xiao *et al.*, 2020) and SLR protein interacts with ARF7 and ARF19 protein forming the complex to negatively regulate auxin downstream genes, repressing lateral roots initiation. Moreover, the SLR-ARF7-ARF19 module as an early auxin response module is crucial in the first XPP cell asymmetric divisions, succeeded by BDL-MP module, which positively regulates the lateral roots initiation and organogenesis (De Smet *et al.*, 2010). Furthermore, the SHY2-ARF module cooperates with the SLR-ARF7-ARF19 module, indirectly regulating developmental stages of the lateral roots development. In recent studies, *shy2-2*, a gain of function mutant in *Arabidopsis* showed a reduction in lateral roots numbers and strongly inhibited the processes of the lateral roots primordium and emergence (Tian & Reed, 1999; Swarup *et al.*, 2008; Goh *et al.*, 2012).

Except for four typical IAAs-ARFs modules, there are some other IAAs-ARFs modules participating in lateral roots formation such as CRANE/IAA18-ARF7-ARF19 module and MSG2/IAA19-ARF7 module (Tatematsu *et al.*, 2004; Uehara *et al.*, 2008). In *Arabidopsis*, the SLR-ARF7-ARF19 module works as a core on lateral roots development, and coordinates with other IAAs-ARFs modules (BDL-MP, SHY2-ARFs, MSG2-ARF19, and CRANE-ARF7-ARF19), playing the main role in positively regulating lateral roots formation.

Finally, in *Arabidopsis*, the lateral roots are regulated by auxin and more specifically, auxin modulates different IAAs-ARFs modules in order controls lateral roots developmental processes.

4. Objectives

In plant, root system architecture is largely determined by the balance of stem cell proliferation and differentiation during embryogenesis and post embryogenesis. Secondary growth, the increase in radial growth (girth) of a plant, represents a key structural novelty that characterizes the bulk of land plant diversity (Wunderling *et al.*, 2018; Ragni & Greb, 2018; Campilho *et al.*, 2020). The bilateral meristems (vascular cambium and phellogen) trigger secondary growth and shapes radical root system architecture.

Many studies have been shown on secondary growth, while there are some outstanding questions that remain to be addressed. First, it is clear that vascular cambium/phellogen are divided into xylem/phellem or phloem/phelloderm, while very little is known how the plants direct vascular cambium and phellogen differentiation. Second, the molecular networks on periderm establishment and development are still missing.

To answer the question, I used *Arabidopsis* root as the model. Our preliminary data suggested that auxin may also control phellogen initiation and proliferation, so I am interested in how auxin is involved in phellogen establishment and differentiation. To better understand the dynamics and which steps of periderm formation require auxin, I will use transgenic auxin concentration and activity reporter lines to discover the auxin distribution and accumulation. Next, I will obtain transgenic lines which I can manipulate auxin signalling in a tissue/temporal specific manner. Moreover, preliminary data in our lab suggested that several *IAAs* and *ARFs* are expressed in the phellogen. Therefore, I will complete the analyses of *IAAs* and *ARFs* expression patterns during secondary development in the root and I will study the gain of function or loss of function mutants of the *IAAs* and *ARFs* during secondary growth.

Furthermore, pericycle cells give/partially give rise to lateral roots, phellogen, and the vascular cambium, while it is unknown the correlation among these three plant organs/tissues. Therefore, I will focus on understanding the molecular mechanisms among these three plant organs/tissues.

I will complete the analyses of secondary growth some plants that lack of lateral roots. Next, I will obtain transgenic line that blocks auxin signalling in vascular cambium and another transgenic line that blocks auxin signalling in cork cambium, which allow me to separate auxin regulatory networks in these two cambia, so I will perform transcriptome analysis in these two transgenic lines. I will analyse the possible auxin

inducted candidates, which may give a clue on how plant direct vascular cambium and phellogen differentiation.

Altogether, our general interest is to better understand the genetic mechanism during secondary growth. This understanding includes the identification of key factors, which orchestrate secondary growth, how this important process is coordinated with other plant organs/tissues (i.e vascular cambium and phellogen), and the spatial-temporal regulators that regulate secondary growth. I aim to decipher the auxin-mediated regulatory hubs in the vascular cambium and phellogen, providing the basis for understanding stem cell specificity in different tissues and unveiling the correlating in different plant organs/tissues.

5. Manuscripts

5.1 Published manuscript 1:

Pluripotent Pericycle Cells Trigger Different Growth Outputs by Integrating Developmental Cues into Distinct Regulatory Modules

W.X. planned and conducted the majority of the experiments with input from L.R. L.R. and W.X. acquired the confocal images. A.W. conducted the initial experiments on the *arf* and *iaa* mutants. D.M., L.R., and W.X. did the molecular cloning and generated the plant lines. D.M. conducted the Fluorol Yellow (FY) experiments. W.X. and D.M. measured the number of periderm layers. A.W., W.X., and D.M. conducted the phellem ratio experiments. D.R. helped in generating the T3 lines and in the embedding of some experiments. J.E.M.V. provided the *PER15* promoter and significant input to the project. L.R. wrote the manuscript, with the help of W.X., D.M., A.W., and J.E.M

Article

Current Biology

Pluripotent Pericycle Cells Trigger Different Growth Outputs by Integrating Developmental Cues into Distinct Regulatory Modules

Highlights

- Auxin is required for phellogen establishment and maintenance
- Lateral root formation is the main auxin-induced program after plant greening
- The establishment of the vascular cambium is required for periderm initiation
- Different targets downstream of auxin control lateral root and periderm formation

Authors

Wei Xiao, David Molina, Anna Wunderling, Dagmar Ripper, Joop E.M. Vermeer, Laura Ragni

Correspondence

laura.ragni@zmbp.uni-tuebingen.de

In Brief

Xiao et al. describe how root pericycle output specificity is achieved. Auxin promotes LR and periderm formation through distinct transcription factors and via the integration of developmental cues.

Xiao et al., 2020, Current Biology *30*, 1–15
November 16, 2020
https://doi.org/10.1016/j.cub.2020.08.053

CellPress

Please cite this article in press as: Xiao et al., Pluripotent Pericycle Cells Trigger Different Growth Outputs by Integrating Developmental Cues into Distinct Regulatory Modules, Current Biology (2020), https://doi.org/10.1016/j.cub.2020.08.053

Current Biology

CellPress

Article

Pluripotent Pericycle Cells Trigger Different Growth Outputs by Integrating Developmental Cues into Distinct Regulatory Modules

Wei Xiao,[1] David Molina,[1,3] Anna Wunderling,[1,3] Dagmar Ripper,[1] Joop E.M. Vermeer,[2] and Laura Ragni[1,4,*]
[1]ZMBP-Center for Plant Molecular Biology, University of Tübingen, Auf der Morgenstelle 32, 72076 Tübingen, Germany
[2]Institute of Biology, University of Neuchâtel, Rue Emile-Argand 11, 2000 Neuchâtel, Switzerland
[3]These authors contributed equally
[4]Lead Contact
*Correspondence: laura.ragni@zmbp.uni-tuebingen.de
https://doi.org/10.1016/j.cub.2020.08.053

SUMMARY

During post-embryonic development, the pericycle specifies the stem cells that give rise to both lateral roots (LRs) and the periderm, a suberized barrier that protects the plant against biotic and abiotic stresses. Comparable auxin-mediated signaling hubs regulate meristem establishment in many developmental contexts; however, it is unknown how specific outputs are achieved. Using the *Arabidopsis* root as a model, we show that while LR formation is the main auxin-induced program after de-etiolation, plants with age become competent to form a periderm in response to auxin. The establishment of the vascular cambium acts as the developmental switch required to trigger auxin-mediated periderm initiation. Moreover, distinct auxin signaling components and targets control LR versus periderm formation. Among the periderm-specific-promoting transcription factors, *WUSCHEL-RELATED HOMEOBOX 4* (*WOX4*) and *KNAT1/BREVIPEDICELLUS* (*BP*) stand out as their specific overexpression in the periderm results in an increased number of periderm layers, a trait of agronomical importance in breeding programs targeting stress tolerance. These findings reveal that specificity in pericycle stem cell fate is achieved by the integration of developmental cues into distinct regulatory modules.

INTRODUCTION

The plant body consists of developmental units that are constantly produced by the stem cells located at the meristems. Primary meristems, such as the shoot and the root apical meristems, are formed during embryogenesis, while secondary meristems arise from differentiated cells or a mixture of differentiated and undifferentiated tissues that reacquire pluripotency during plant growth. Examples of secondary meristems are the vascular cambium and the phellogen/cork cambium, which are responsible for the increase in the girth of plant organs [1]. Both meristems divide bidirectionally, producing inward wood and phelloderm and outward phloem and phellem/cork, respectively [1, 2] (Figure 1A). While the vascular cambium in trees remains active throughout a tree's life, the phellogen may be replaced every year or after several years from the tissue underneath [3]. The phellogen, the phelloderm, and the phellem are usually referred to as the periderm. Phellem cells are highly suberized and lignified and act as a barrier, which restricts gas exchange, water loss, and pathogen attack [1, 3–5]. In most plant species, the stem phellogen originates from the subepidermal layer, whereas in roots, including *Arabidopsis*, root phellogen arises from the pericycle, an inner tissue that is surrounded by several cell layers (endodermis, cortex, and epidermis). If the first phellogen is superficial (as in stems), then only small amounts of primary tissues are shed during periderm growth, whereas deeper periderms slough away large amounts of primary tissues (as in roots). In the *Arabidopsis* root, periderm development can be dissected in 5 distinct stages in connection with the fate of the tissues surrounding the pericycle (Figures 1A and S1A).

Briefly, at stage 1, the pericycle cells located at the xylem poles start to proliferate, and then anticlinal cell divisions extend to the whole pericycle [3, 6]. At stage 2, the pericycle divides also periclinally, forming the meristematic ring comprising the phellogen, whereas the endodermis undergoes programmed cell death (PCD) [3, 6]. During stages 3 to 5, cork cells differentiate, and the epidermis and the cortex are sloughed away [3, 6]. Lateral roots (LRs), and to a lesser extent, the vascular cambium, also arise from xylem pole pericycle cells, highlighting the unique pluripotency capacity of this tissue [7, 8]. An auxin maxima specifies LRs in the region above the root apical meristem, and the first formative divisions occur before the onset of secondary growth; thus, LR formation precedes periderm initiation [9]. During LR emergence, similar to periderm development, the endodermis loses volume and can undergo PCD, whereas the epidermis and the cortex are pushed away to accommodate primordia outgrowth [10, 11].

It is known that conserved regulatory networks, including those triggered by auxin, play a major role in stem cell establishment and maintenance in the embryo, shoot and root apical

Please cite this article in press as: Xiao et al., Pluripotent Pericycle Cells Trigger Different Growth Outputs by Integrating Developmental Cues into Distinct Regulatory Modules, Current Biology (2020), https://doi.org/10.1016/j.cub.2020.08.053

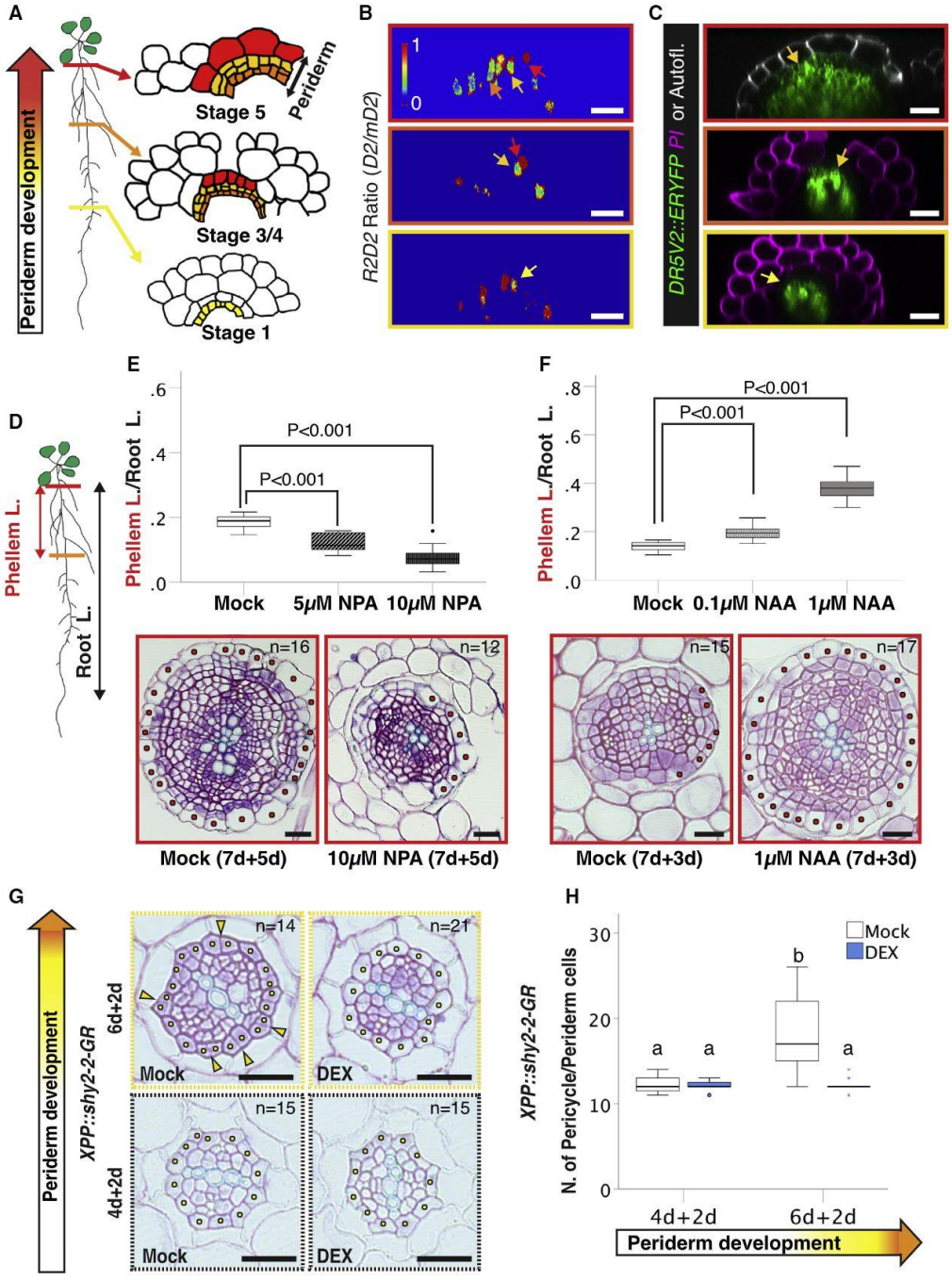

Figure 1. Auxin Promotes Phellogen Establishment from the Pericycle

(A) Periderm development in the *Arabidopsis* root can be followed along the root. Schematic of periderm development stages (pale yellow: pericycle; orange: phelloderm, dark yellow: phellogen, and red: phellem).

(B) Ratio of the relative intensities of D2-Venus/mD2-dTomato of the pictures shown in Figure S1B.

(C) Orthogonal view of z stacks of a *DR5v2::ER-YFP* root at the positions corresponding to stage 1 (bottom), stage 3/4 (center), and stage 5 (top) (12 days old).

(legend continued on next page)

Please cite this article in press as: Xiao et al., Pluripotent Pericycle Cells Trigger Different Growth Outputs by Integrating Developmental Cues into Distinct Regulatory Modules, Current Biology (2020), https://doi.org/10.1016/j.cub.2020.08.053

meristems, and the vascular cambium [12, 13]. Specific auxin-mediated signaling modules are active in different organs/tissues [8, 12, 14–17]; however, our understanding about how tissue output specificity is achieved is limited. Here, we investigated how two independent developmental programs, LR and periderm formation, are initiated from the same tissue.

RESULTS

Auxin Is Required for Periderm Establishment from the Pericycle

As the regulatory networks underlying periderm formation are largely unknown, we assessed whether auxin plays a role during phellogen establishment. Periderm development can be followed over space along the same root (which represents a developmental gradient) or over time in the same zone of the root (e.g., the most mature close to the hypocotyl) (Figures 1A and S1A) [6]. We mapped auxin distribution and activity at 3 representative stages of periderm formation, exploiting the genetically encoded biosensors *R2D2* and *DR5v2* [18]. *R2D2* is based on the auxin-induced degradation of a fluorophore (*RPS5A::D2-Venus*) coupled to a nondegradable internal control (*RPS5A::m-dTomato*). Hence, the ratio between the 2 fluorescent signals reports auxin cellular concentrations. We found that auxin accumulates in the xylem pole pericycle cells during periderm initiation (stage 1) and in the phellogen during periderm development (stage 3/4) (Figures 1B, S1B, and S1C). In a mature periderm, auxin levels peak in both phellogen and phelloderm. Consistently, an auxin minimum was detected in phellem cells (Figures 1B, S1B, and S1C). In line with this, auxin activity, as shown by *DR5v2::ER-YFP*, is high in the phellogen and phelloderm and low in the phellem (stages 3/4 and 5) (Figure 1C). Next, we blocked polar auxin transport by treating plants (7 days old), initiating periderm formation with N-1-naphthylphthalamic acid (NPA) for 5 days. In mock-treated plants, ¼ of the root (~2.5 cm), was covered by the phellem, whereas in NPA-treated plants, both phellem length and phellem ratio were significantly reduced (Figures 1D, 1E, and S1D). In addition, phellem (red dots) differentiation was incomplete in NPA-treated roots, indicating a delay in periderm development (Figure 1E). By contrast, treatment with auxin (1-Naphthaleneacetic acid [NAA], Indole-3-acetic acid [IAA], or 2,4-Dichlorophenoxyacetic acid [2,4-D]) promoted periderm formation as shown by an increased phellem length and phellem ratio (Figures 1F and S1E–S1G). Moreover, in cross-sections of NAA-treated plants, we observed that phellem cells were already differentiated and covered the whole root, whereas in the mock control, only a few phellem cells were present (Figure 1F). These results highlight the importance of auxin for periderm growth and initiation.

To further dissect the role of auxin during periderm development, we engineered plants to specifically block auxin signaling in the pericycle at the onset of periderm formation and in the phellogen at periderm maturity. This was achieved by using spatial and temporal controlled expression of stabilized Aux/IAA variants [19]. The *XYLEM POLE PERICYCLE* (*XPP*) promoter is active at the onset of periderm initiation in the xylem pole pericycle cells [20], whereas the *PEROXIDASE15* (*PER15*) promoter is expressed in the whole pericycle at stage 1 and in both phellem and phellogen at stage 5 of periderm development (Figures S1H and S1I). We observed that prolonged induction of *XPP::shy2-2-GR* and *PER15::slr-1-GR* (7–12 days) resulted in reduced phellem length, phellem ratio, and disorganized periderm (Figures S2A and S2B). Consistently, hindering the transcriptional auxin response precisely at the onset of periderm development abolished cell divisions in the pericycle and the expression of the periderm marker *MYB84* [6] (Figures 1G, 1H, and S2C–S2E), indicating that auxin signaling is required to trigger periderm initiation. Next, we investigated whether auxin is necessary to maintain stem cell activity in the phellogen, by inducing the *PER15::slr-1-GR* construct in a fully differentiated periderm (12 days old) (Figure S2F). A prolonged dexamethasone (DEX) induction (8 days) resulted in the loss of phellogen activity and *MYB84* expression (Figure S2F). As expected, cork cells were still suberized (Figure S2G), showing that stem cell activity can be stopped but cells cannot dedifferentiate. In summary, our results demonstrate that auxin-mediated transcriptional reprogramming is required for periderm establishment and development. Thus, auxin promotes both LR and periderm programs from the pericycle, raising the question of how auxin output specificity is achieved.

LR Formation Is the Main Auxin-Induced Program in the Pericycle after Plant Greening, whereas Plants with Aging Become Competent to Respond to Auxin to Form the Periderm

To investigate auxin specificity, we tested whether the dynamics of auxin responses differ during LR and periderm development. We studied the effect of a short auxin treatment (48 h) in plants before (4 day old), at (6 day old), and after the onset of periderm formation (8 day old) [6]. Auxin treatment resulted in roots with an

(D) Schematic representation of an *Arabidopsis* root showing how phellem length (phellem L. [cm]) and phellem ratio (phellem length [cm]/root length [cm]) are measured.
(E) Top: quantification of phellem length in 12-day-old WT roots. Seven-day-old plants were treated for 5 days with mock, 5 μM NPA, or 10 μM NPA; t test (n = 15). Lower panels: cross-sections (plastic embedding) of the uppermost part of 12-day-old WT roots. Seven-day-old plants were transferred for 5 days to mock or 10 μM NPA plates.
(F) Top: quantification of phellem ratio in 10-day-old WT roots. Seven-day-old plants were transferred to mock, 0.1 μM, or 1 μM NAA plates for 3 days; t test (n = 15). Bottom: cross-sections (plastic embedding) of the uppermost part of 10-day-old WT roots. Seven-day-old plants were transferred to mock or 1 μM NAA plates for 3 days.
(G) Cross-sections (plastic embedding) of the uppermost part of *XPP::shy2-2-GR* (in *MYB84::NLS-3xGFP W131Y;#1*) roots. Four- and 6-day-old plants were treated for 2 days with mock or 10 μM DEX.
(H) Quantification of number of pericycle/periderm cells of (G). One-way ANOVA (95% confidence interval [CI], post hoc: Tamhane, n = 15–21).
The pale yellow arrows indicate the pericycle, the dark yellow arrows indicate the phellogen, the red arrows indicate the phellem, and the orange arrows indicate the phelloderm. The red dots represent the phellem cells and the yellow dots represent the pericycle cells. Black and white scale bars: 20 μm.
See also Figures S1 and S2 and Data S2.

Please cite this article in press as: Xiao et al., Pluripotent Pericycle Cells Trigger Different Growth Outputs by Integrating Developmental Cues into Distinct Regulatory Modules, Current Biology (2020), https://doi.org/10.1016/j.cub.2020.08.053

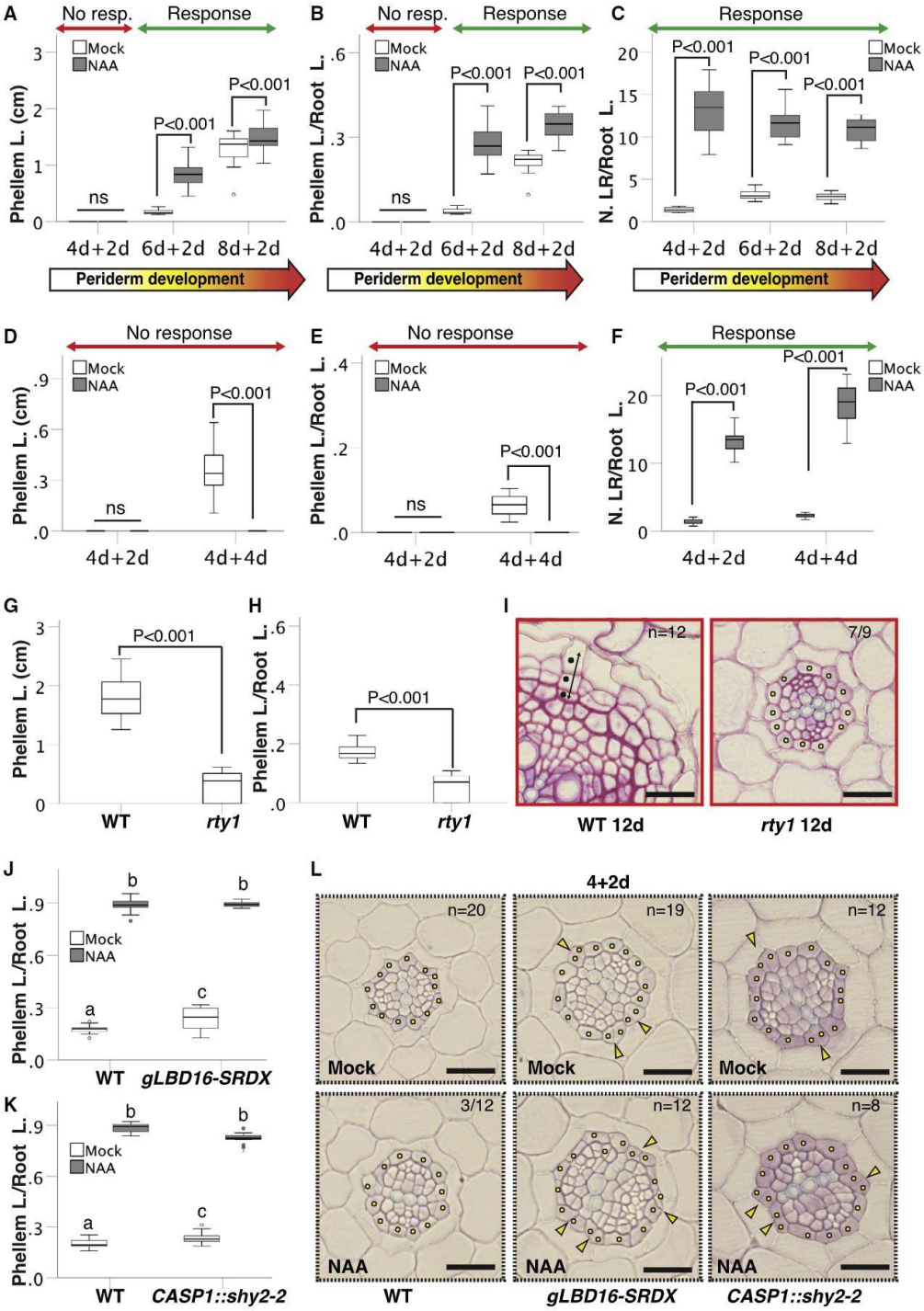

Figure 2. Auxin Is Not Sufficient to Induce Periderm Formation

(A and B) Quantification of phellem length (A) and phellem ratio (B) in WT (*MYB84::NLS-3xGFP W131Y*) roots. Four-, 6-, and 8-day-old plants were treated for 48 h with mock or 1 μM NAA; t test (ns, not significant; n = 14–15).

(legend continued on next page)

Please cite this article in press as: Xiao et al., Pluripotent Pericycle Cells Trigger Different Growth Outputs by Integrating Developmental Cues into Distinct Regulatory Modules, Current Biology (2020), https://doi.org/10.1016/j.cub.2020.08.053

increased phellem length and phellem ratio only when plants were treated upon periderm initiation time or later (Figures 2A and 2B). In contrast, auxin induced LR formation independent of the plant developmental stage after the body of the plant is established (after de-etiolation/greening occurred: hypocotyl has stopped elongation and the cotyledons are opened) (Figures 2C and S3A–S3C). Consistently, the periderm marker *MYB84* [6] is not expressed in 4-day-old auxin-treated plants, indicating that the periderm program is not triggered (Figure S3D). In line with this, we observed that a 20-h auxin treatment was sufficient to increase the number of pericycle divisions (quantified using the microtubule marker *35S::GFP-TUA6* [21]) at the onset of periderm formation (6-day-old plants) but not before (Figures S3E and S3F). Auxin did not induce periderm formation in 4-day-old plants, even when auxin treatment was prolonged to 4 days (Figures 2D and 2E). These plants kept producing LRs and no periderm was initiated, while mock roots had already started the periderm program (Figures 2F and S3G), pointing out that plants with age become competent to establish periderm in response to auxin.

To corroborate our results, we investigated periderm development in the auxin-overproducing mutant *superroot1/rooty1*(*rty1-1*) [22, 23]. In line with our auxin-feeding experiments, in *rty1* mutants periderm growth was almost blocked as seen by a drastic reduction in phellem length and phellem ratio and by the absence of pericycle divisions in the majority of the observed roots (Figures 2G–2I). These results suggest that LR formation is the main developmental program activated by auxin in the pericycle (after greening), and that periderm initiation requires the integration of additional developmental cues.

Blocking LR Initiation Has a Positive Effect on Periderm Growth

We next asked whether blocking LR formation in the zone of the root where periderm initiation occurs acts as a trigger for the periderm program. Thus, we quantified periderm growth in 2 independent genetic backgrounds, which lack LRs without altering auxin signaling in the periderm. In *CASP1::shy2-2* plants, LR initiation is arrested by blocking auxin signaling in the endodermis, whereas in *gLBD16-SRDX* lines, LATERAL ORGAN BOUNDARIES-DOMAIN 16 (LBD16), a transcription factor (TF) that acts downstream of auxin to promote LRs, is turned into a repressor [10, 24–26]. In both lines, we observed a mild increase in phellem length and phellem ratio when compared to wild type (WT), whereas upon auxin induction (7 days + 5 days), they were indistinguishable from WT, suggesting that the lack of LRs induces early periderm onset (Figures 2J, 2K, S3H, and S3I). To confirm it, we quantified the number of pericycle cells at the onset of periderm formation. In 6-day-old roots, the pericycle cell number was higher in both *CASP1::shy2-2* and *gLBD16-SRDX* compared to WT, and the effect was larger in 8-day-old plants (Figures 2L and S3K–S3M). However, the absence of LRs did not confer early competence to auxin to form a periderm, indicating that precocious periderm initiation in these lines may be indirectly triggered by other factors (Figures 2L and S3K-S3M). Supporting this, the number of vascular cells was also increased in *CASP1::shy2-2* and *gLBD16-SRDX* roots (Figure S3N).

The Establishment of the Vascular Cambium Acts as the Developmental Switch That Triggers the Auxin-Mediated Periderm Program

We noticed that in *CASP1::shy2-2* and *gLBD16-SRDX,* the establishment of the vascular cambium occurs earlier (Figure S3N), while in *rty1* mutants it is delayed (Figure 2I). We hypothesized that the formation of the vascular cambium may act as the developmental switch that is required to elicit periderm formation. In support of this hypothesis, a periderm is present only in species that undergo massive secondary growth [3, 4]. The onset of periderm development follows the first divisions in the pro-cambium, and the 2 meristems appear to develop simultaneously (Figure S4A). To validate this experimentally, we tested the effect of impaired cambium activity on periderm development. Loss of function of the master regulator of cambial activity *PHLOEM INTERCALATED WITH XYLEM/ TDIF RECEPTOR* (*PXY/TDR),* which is not expressed in the periderm (Figure S4B), results in altered cambium patterning and decreased cambium proliferation [27, 28]; thus, we inspected *pxy-3* mutants for periderm phenotypes. At 8 days, the whole pericycle is dividing in WT plants and the first periclinal divisions have already occurred, whereas in *pxy* mutants only a few divisions took place (Figures 3A and 3B). Moreover, phellem length, phellem ratio, and the periderm auxin response were highly reduced in *pxy* mutants (Figures 3C and S4C), suggesting that the vascular cambium is necessary for periderm formation. To further substantiate these findings, we exploited the fact that blocking auxin-mediated transcriptional responses in the *PXY* expression domain arrests cambium activity [14] without altering

(C) Quantification of LR density of WT (*MYB84::NLS-3xGFP W131Y*) roots. Four-, 6-, and 8-day-old plants were treated for 48 h with mock or 1 μM NAA; t test (n = 14–15).
(D–F) Quantification of phellem length (D), phellem ratio (E), and lateral root density (F) in WT roots. Four-day-old plants were treated for 96 h with mock or 1 μM NAA; t test (ns: not significant, n = 15).
(G and H) Quantification of phellem length (G) and phellem ratio (H) in 12-day-old WT and *rty* roots; t test (n = 15).
(I) Cross-sections (plastic embedding) of the uppermost part of 12-day-old WT and *rty1* roots.
(J) Quantification of phellem ratio in 12-day-old WT and *gLBD16-SRDX* roots. Seven-day-old plants were treated for 5 days with mock or 1 μM NAA. One-way ANOVA (95% CI, post hoc: Tamhane, n = 15).
(K) Quantification of phellem ratio in 12-day-old WT and *CASP1::shy2-2* roots. Seven-day-old plants were treated for 5 days with mock or 1 μM NAA. One-way ANOVA (95% CI, post hoc: Bonferroni, n = 14–15).
(L) Cross-sections (plastic embedding) of the uppermost part of 6-day-old WT, *gLBD16-SRDX*, and *CASP1::shy2-2* roots. Four-day-old plants were treated for 48 h with mock or 1 μM NAA. As WT roots when treated with NAA keep forming LRs, it is rare (3/12) to have sections without LRs.
The yellow dots represent pericycle cells, the black dots represent periderm cells, and the double-headed black arrows indicate periderm extension. The yellow arrowheads indicate pericycle cell divisions. Black scale bars: 20 μm.
See also Figure S3 and Data S2.

Please cite this article in press as: Xiao et al., Pluripotent Pericycle Cells Trigger Different Growth Outputs by Integrating Developmental Cues into Distinct Regulatory Modules, Current Biology (2020), https://doi.org/10.1016/j.cub.2020.08.053

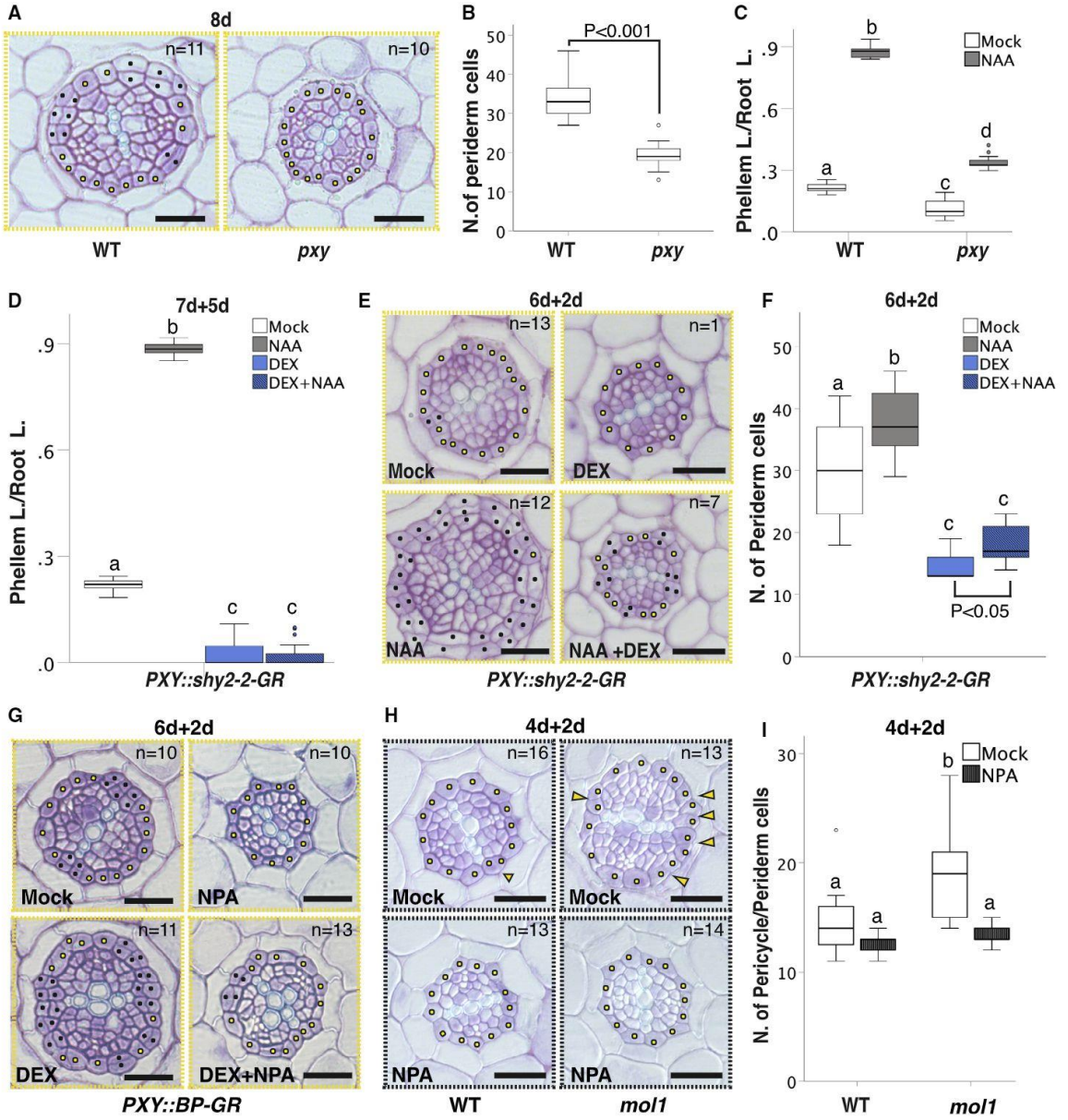

Figure 3. A Functional Vascular Cambium Is Required to Drive the Auxin-Induced Periderm Program

(A) Cross-sections (plastic embedding) of the uppermost part of 8-day-old WT and *pxy-3* roots.

(B) Quantification of number of pericycle/periderm cells in the experiment presented in (A); t test (n = 10–11).

(C) Quantification of phellem ratio in 12-day-old WT and *pxy-3* roots. Seven-day-old plants were treated for 5 days with mock or 1 μM NAA. One-way ANOVA (95% CI, post hoc: Tamhane, n = 14–15).

(D) Quantification of phellem ratio in 12-day-old roots of *PXY::shy2-2-GR* roots (in *MYB84::NLS-3xGFP W131Y*). Seven-day-old plants were treated for 5 days with mock, 1 μM NAA, 10 μM DEX, or 10 μM DEX + 1 μM NAA. One-way ANOVA (95% CI, post hoc: Tamhane, n = 15).

(E) Cross-sections (plastic embedding) of the uppermost part of *PXY::shy2-2-GR* (in *MYB84::NLS-3xGFP W131Y*) roots. Six-day-old plants were treated for 48 h with mock, 1 μM NAA, 10 μM DEX, or 10 μM DEX + 1 μM NAA.

(F) Quantification of number of pericycle/periderm cells in the experiment presented in (E). One-way ANOVA (95% CI, post hoc: Tamhane, n = 7–13) and t test.

(G) Cross-sections (plastic embedding) of the uppermost part of 6-day-old *PXY::BP-GR* roots. Four-day-old plants were treated for 48 h with mock, 10 μM DEX, 10 μM NPA, or 10 μM DEX + 10 μM NPA.

(H) Cross-sections (plastic embedding) of the uppermost part of 6-day-old WT and *mol1* roots. Four-day-old plants were treated for 48 h with mock or 10 μM NPA.

(legend continued on next page)

Please cite this article in press as: Xiao et al., Pluripotent Pericycle Cells Trigger Different Growth Outputs by Integrating Developmental Cues into Distinct Regulatory Modules, Current Biology (2020), https://doi.org/10.1016/j.cub.2020.08.053

the auxin response in the periderm. Prolonged induction (5 days) of *PXY::shy2-2-GR* from 7 days onward resulted in delayed periderm formation and abolished auxin responses in the periderm (Figures 3D, S4D, and S4F). Consistently, 2-day induction at the onset of periderm/cambium initiation arrested both cambium and periderm formation, even in the presence of auxin, indicating that the establishment of the vascular cambium is required for periderm development (Figures 3E and 3F).

Next, we assumed that if the initiation of the vascular cambium renders the pericycle competent to form the periderm, high vascular cambium activity should promote periderm growth. To test this, we specifically overexpressed a master cambial regulator [29, 30] in the vascular cambium with temporal control (*PXY::BP-GR*). Induction of BREVIPEDICELLUS/KNAT1 (BP) from day 7 onward resulted in an increase in phellem length and phellem ratio (Figures S4G and S4H). Consistently, a short induction in the vascular cambium at the onset of periderm development was sufficient to promote both programs and this effect was attenuated by blocking auxin polar transport (Figures 3G and S4I). We reinforced these findings by investigating *more lateral growth1* (*mol1-1*) mutants, which are characterized by enhanced vascular cambium activity [31]. *MOL1* is solely expressed in the phloem and pro-cambium before the initiation of periderm development [31] (Figure S4J). At 6 days, *mol1-1* mutants already showed many pericycle cell divisions, and the total number of pericycle cells was increased compared to WT, indicating that periderm initiation occurred earlier (Figures 3H and 3I). NPA treatment suppressed the *mol1-1* phenotypes, highlighting the importance of auxin for both programs (Figures 3H, 3I, and S4K).

In summary, our results demonstrate that the vascular cambium is required and sufficient to promote periderm initiation. Thus, it may act as the developmental cue that renders the xylem pole pericycle competent to initiate the periderm program.

Distinct Targets Downstream of Auxin Orchestrate Periderm and LR Formation

We hypothesized that output distinction among the 2 developmental programs is also mediated by specificity in the auxin responses. To test this, we investigated whether the key auxin signaling components that regulate LR formation act during periderm development. Different auxin signaling modules comprising Aux/IAAs and auxin response factors (ARFs) regulated LR formation [12,26 32–38]. By mean of fluorescent reporters, we observed the activity of *IAA3/SHORT HYPOCOTYL 2 (SHY2)*, *IAA12/BODENLOS (BDL)*, *IAA28*, and *IAA14/SOLITARY ROOT (SLR)* promoters at all stages of periderm development (Figures 4A–4D). Genetic analysis exploiting gain-of-function mutants (stabilized versions) of the expressed IAAs [32–36] confirmed their role during periderm development. All of the mutants displayed decreased phellem length, decreased phellem ratio, and an impaired auxin response (Figures 4E–4G and S5A–S5C), with *bdl-2* and *shy2-101* being the most affected (Figures 4E). Also, at the anatomical level, *bdl-2* and *shy2-101* roots showed the strongest phenotype, with only 1–2 formed periderm layers and reduced overall secondary growth (Figures 4H–4J). In, *slr-1*, which totally lacks LRs [33] (Figure S5M) and displays only a mild reduction in the number of periderm layers (Figure 4I), the positive effect on blocking LR initiation on the periderm growth is suppressed/masked by altered auxin signaling in the periderm and/or by the absence of enhanced cambial activity.

Next, we examined whether *ARF5/MONOPTEROS (MP)*, *ARF6*, *ARF7/NPH4*, *ARF8*, and *ARF19*, which regulate LR development [26, 32, 34, 37, 38], also contribute to periderm growth. We showed that all of these *ARFs* are expressed in the periderm, albeit not at all periderm developmental stages (Figures 5A–5E, S5D, and S5E). We detected the activity of *ARF5* and *ARF8* promoters in a few phellogen cells only during late (stage 5) periderm development (Figures 5D, 5E, S5D, and S5E), whereas *ARF6*, *ARF7*, and *ARF19* promoter activity was observed during all stages of periderm development, including the first divisions in the pericycle (Figures 5A–5C). The comparison of the expression levels of these ARFs in the pericycle in the root at the positions corresponding to LR initiations and periderm initiation points out that ARF19 acts predominantly during LR formation, whereas ARF6 and ARF7 act in both processes. As ARF5 and ARF8 are very weakly expressed [8, 37, 39] and were at the border of detection at both positions, no assumptions could be made.

To further study whether output specificity is encoded by different ARFs, we investigated periderm development in *ARF* loss-of-function mutants. Our genetic studies revealed that *ARF8* and *MP/ARF5* are the major ARFs contributing to periderm formation, despite their low abundance (Figures 5F–5I, S5B, and S5F–S5I). Both an induced *amiMP* line (*mp/arf5* mutant fails to form a root, so we used an inducible artificial microRNA [miRNA] targeting *MP/ARF5* [8]) and the *arf8-2* single mutant showed a reduction in phellem length, phellem ratio, and auxin response (Figures 5F, 5G, S5F, and S5G). In addition, the number of periderm layers was reduced in the induced *amiMP* roots, whereas LR formation was not altered (Figures 5H, 5I, S5J, and S5K). In line with this, prolonged induction of MP at the onset of periderm formation resulted in increased phellem length, phellem ratio, and periderm layers (Figures 5J–5L and S5L). ARF5/MP, which contributes the most to periderm development, is known to activate vascular cambium formation in the root and repress cambium activity in the stem [8, 14], highlighting regulatory conservation between the 2 meristems. By contrast, the *arf7-1 arf19-1* double mutant, which totally lacks LRs (Figure S5M), showed normal cambium [8] and periderm growth, except for a reduced auxin response (Figures 4F, 5M, 5N, and S5B), highlighting that distinct auxin signaling modules do not equally contribute to periderm, LR, and cambium formation. Considering that the analyzed ARF loss-of-function mutants show only mild periderm defects, compared to IAA gain-of-function mutants, it is reasonable to think that either the analyzed ARFs work redundantly and/or additional ARFs are involved. To conclude, pericycle output specificity is only partially resolved

(I) Quantification of number of pericycle cells in the experiment presented in (H). One-way ANOVA (95% CI, post hoc: Tamhane, n = 13–16).
The yellow dots represent the pericycle cells, the black dots represent the periderm cells, and the yellow arrowheads indicate the pericycle divisions. Black scale bars: 20 μm.
See also Figure S4 and Data S2.

Please cite this article in press as: Xiao et al., Pluripotent Pericycle Cells Trigger Different Growth Outputs by Integrating Developmental Cues into Distinct Regulatory Modules, Current Biology (2020), https://doi.org/10.1016/j.cub.2020.08.053

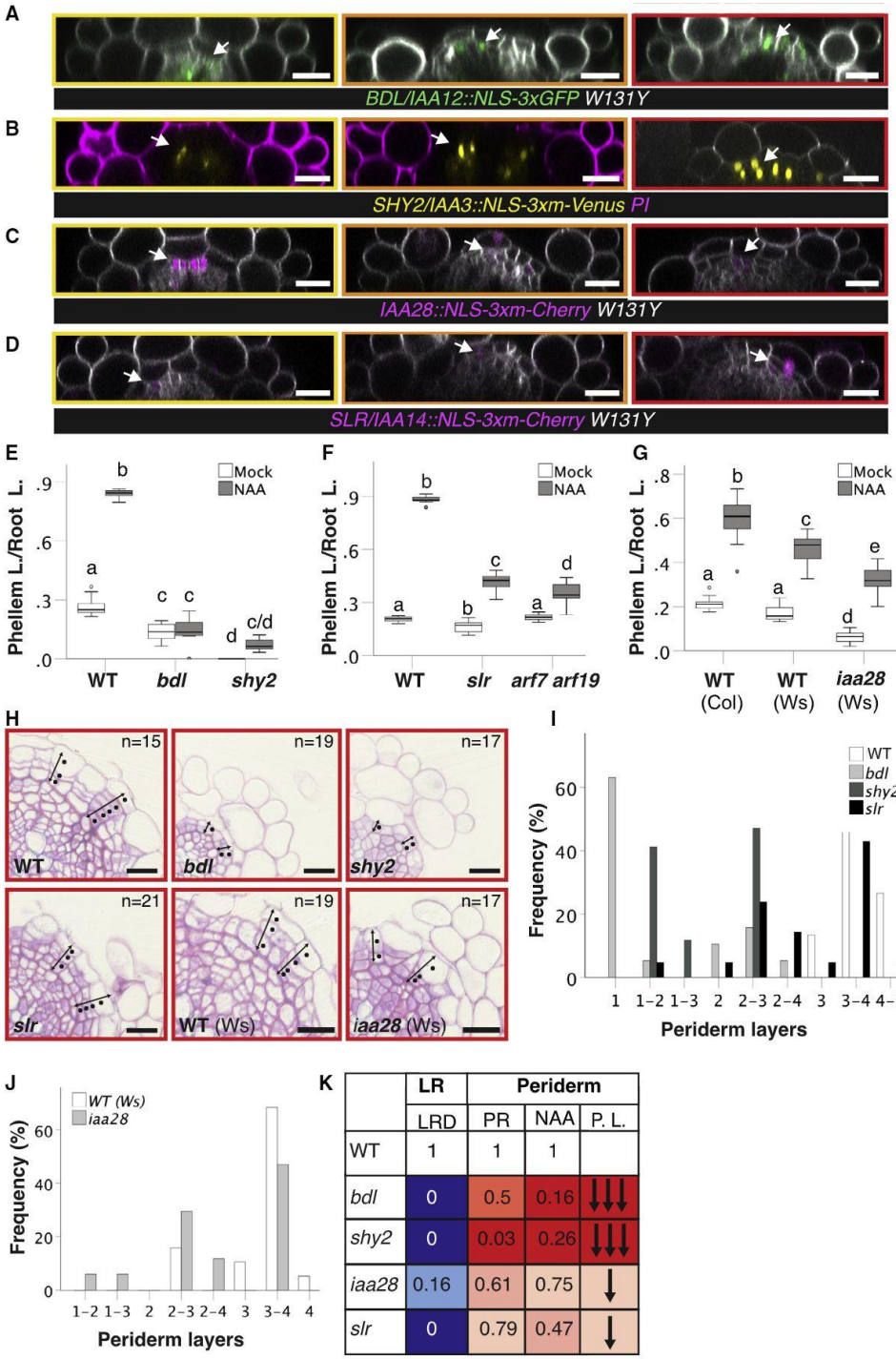

K

	LR	Periderm		
	LRD	PR	NAA	P. L.
WT	1	1	1	
bdl	0	0.5	0.16	↓↓↓
shy2	0	0.03	0.26	↓↓↓
iaa28	0.16	0.61	0.75	↓
slr	0	0.79	0.47	↓

(legend on next page)

Please cite this article in press as: Xiao et al., Pluripotent Pericycle Cells Trigger Different Growth Outputs by Integrating Developmental Cues into Distinct Regulatory Modules, Current Biology (2020), https://doi.org/10.1016/j.cub.2020.08.053

by differences in the auxin signaling machinery involved in the 2 processes (Figures 4K and 5O).

Furthermore, we tested whether auxin-induced LR regulators function during periderm formation. The GATA23 TF specifies LR founder cell identity in xylem pole pericycle cells [32], whereas LBD16 together with other auxin-induced-LBD TFs regulate LR initiation, primordium growth, and emergence [24–26]. We determined their expression pattern during periderm development. The activity of *GATA23* and *LBD16* promoters was observed in the pericycle during LR initiation (Figures 6A and S6A) [26, 32], whereas it was at the border of detection in the pericycle at the onset of periderm initiation (Figures 6A and S6A). Consistently, the expression of *GATA23* and *LBD16* was not reduced in the periderm of *XPP::shy-2-2-GR*-induced roots as expected for an auxin target gene, and *gLBD16-SRDX* roots do not show any defects in the periderm, indicating that they do not play a major role during periderm development (Figure 6B). In the quest for factors downstream of auxin that regulate periderm growth, we selected known and putative MP/ARF5 targets [14, 40], restricting the list to *WOX4* and *BP/KNAT1* based on their expression during secondary growth [29, 41, 42]. We confirmed that both *WOX4* and *BP* are expressed all through periderm development (Figures S6B and S6C) and their expression is reduced in the periderm of *XPP::shy2-2-GR*-induced roots (Figure 6B). *WOX4* expression is excluded from the pericycle during LR initiation, whereas *BP* could still be detected, albeit at lower levels (Figures 6C and S6D).

To further explore their role during periderm development, we analyzed *BP* and *WOX4* loss-of-function mutants. Both the *wox4-1* and *bp-9* mutants displayed a reduction in phellem length and phellem ratio and impaired auxin response when compared to WT (Figures 6D and S6E). At the anatomical level, the number of periderm layers was reduced (Figures S6F and S6G), indicating that *WOX4* and *BP* control phellogen activity. In line with their specific role during secondary growth, *wox4-1* and *bp-9* mutants do not display any obvious LR phenotype (Figures S6H and S6I). To further confirm the specific contribution of *WOX4* and *BP* during periderm development, we generated *PER15::BP-GR* and *PER15::WOX4-GR* plants. Inducing *WOX4* and *BP* expression in the periderm of WT plants from 7 days onward (at the onset of periderm formation) resulted in roots with an increased phellem length, phellem ratio, and periderm layers compared to mock controls, confirming that *WOX4* and *BP* are periderm-positive regulators (Figures 6E–6H, S6J, and S6K).

DISCUSSION

Our genetic and gene expression data demonstrate that auxin promotes both LR and periderm initiation from the same tissue: the pericycle. LRs and the periderm arise by the reactivation of cell divisions in the pericycle at distinct root zones, and their initiation displays different temporal dynamics. While auxin signaling is required for the first formative cell divisions at the xylem pole pericycle of both developmental programs, auxin is not sufficient to elicit periderm inception, indicating that LR production is the main auxin-induced program (after plant greening/plant body establishment), and additional developmental cues are needed to trigger periderm development. In fact, the establishment of the vascular cambium is a prerequisite for auxin-activated periderm initiation, and precocious activation of the vascular cambium is sufficient to trigger periderm initiation. Moreover, the positive effect of blocking LR formation on periderm initiation may be related to cambium establishment, as in plants that lack LRs; precocious periderm initiation was accompanied by enhanced cambial activity. We suggest that a non-cell-autonomous signal (hormone/peptide/small RNA/mobile TF) triggered by the cambium renders the xylem pole pericycle competent to form a periderm by either directly specifying periderm identity or by amplifying the endogenous cues required for periderm specification. Alternatively, the establishment of the vascular cambium and the consequence radial expansion may generate mechanical forces on the pericycle, which could drive periderm initiation (Figure 7).

Recently, clonal analyses experiments showed that the vascular cambium arises from cells that are adjacent to the xylem, including xylem pole pericycle cells. Thus, the portion of the cambium in correspondence with the original xylem poles derives from the pericycle, whereas the remaining part originates from pro-cambial cells, which are near the xylem [8]. Xylem proximity is a prerequisite only for vascular cambium formation and not for phellogen establishment, while auxin signaling is required in both processes, adding another level of complexity to the

Figure 4. Distinct IAAs Contribute to Periderm Development

(A–D) Orthogonal view of z stacks of *BDL/IAA12::NLS-3xGFP W131Y* (A), *SHY2/IAA3::NLS-3xm-Venus* (B), *IAA28::NLS-3xm-Cherry W131Y* (C), and *SLR/IAA14::NLS-3xm-Cherry W131Y* (D). Twelve-day-old roots at the positions corresponding to stage 1 (left panel), stages 3/4 (center panel), and stage 5 (right panel) of periderm development.

(E) Quantification of phellem ratio in 12-day-old WT, *bdl-2*, and *shy2-201* roots. Seven-day-old plants were treated for 5 days with mock or 1 μM NAA. One-way ANOVA (95% CI, post hoc: Tamhane, n = 8–14).

(F) Quantification of phellem ratio in 12-day-old WT, *slr-1*, and *arf7-1 arf19-1* roots. Seven-day-old plants were treated for 5 days with mock or 1 μM NAA. One-way ANOVA (95% CI, post hoc: Tamhane, n = 14–15).

(G) Quantification of phellem ratio in 10-day-old WT (Ws and Col) and *iaa28-1*(Ws) roots. Seven-day-old plants were treated for 3 days with mock or 1 μM NAA. One-way ANOVA (95% CI, post hoc: Tamhane, n = 14).

(H) Cross-sections (plastic embedding) of the uppermost part of 12-day-old WT, *bdl-2*, *shy2-201*, *slr-1*, WT (WS), and *iaa28-1* roots.

(I and J) Quantification of the number of periderm layers of (H).

(K) Table comparing *IAA* root phenotypes. Mutant phenotypes were normalized to WT, which was set to 1. LRD, lateral root density; PR, phellem ratio; NAA, auxin response (PR mock/PR NAA); and P.L., number of periderm layers.

The white arrows indicate the pericycle/phellogen, the double-headed black arrows indicate the periderm extension, and the black dots indicate the periderm layers. Black and white scale bars: 20 μm.

See also Figure S5 and Data S2.

Please cite this article in press as: Xiao et al., Pluripotent Pericycle Cells Trigger Different Growth Outputs by Integrating Developmental Cues into Distinct Regulatory Modules, Current Biology (2020), https://doi.org/10.1016/j.cub.2020.08.053

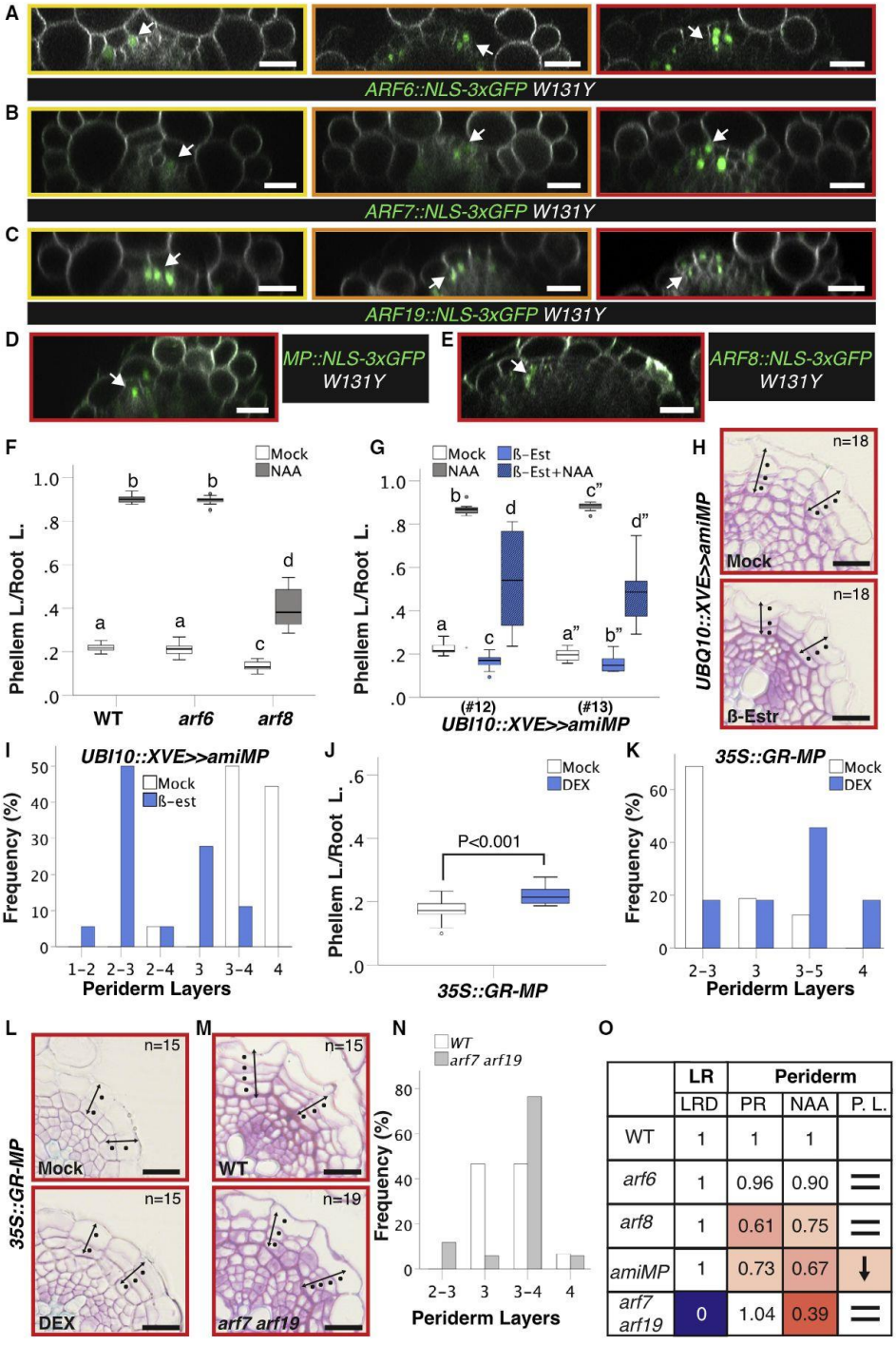

Figure 5. Distinct ARFs Contribute to Periderm Development

(A–C) Orthogonal view of z stacks of *ARF6::NLS-3xGFP W131Y* (A), *ARF7::NLS-3xGFP W131Y* (B), and *ARF19::NLS-3xGFP W131Y* (C) 12-day-old roots at the positions corresponding to stage 1 (left panels), stages 3/4 (center panels), and stage 5 (right panels) of periderm development.

(legend continued on next page)

Please cite this article in press as: Xiao et al., Pluripotent Pericycle Cells Trigger Different Growth Outputs by Integrating Developmental Cues into Distinct Regulatory Modules, Current Biology (2020), https://doi.org/10.1016/j.cub.2020.08.053

system [8]. Studies with single-cell resolution and temporal dynamics are necessary to further dissect how the 3 programs are connected, and, especially, whether LRs influence the establishment of the vascular cambium and how the phellogen and the vascular cambium are specified from xylem pole pericycle cells. In addition, LR initiation is strongly controlled by nutrient availability; therefore, it will be interesting to explore whether environmental stimuli influence pericycle developmental transitions.

We highlighted that distinct signaling pathways, downstream of auxin, orchestrate periderm and LR formation. We showed that MP, which also regulates cambium activity via WOX4 [8, 14], and ARF8 are the majors ARFs contributing to periderm formation, whereas the key LR module SLR-ARF7-ARF19 [26, 38] plays only a minor role during periderm growth. However, it is likely that other ARFs or other ARF combinations participate in periderm development, as the loss of function of ARF8 or conditionally knocking down MP only lead to mild periderm phenotypes. We found that downstream of ARFs during periderm development, WOX4 and BP play a prominent role in controlling meristem activity, highlighting distinction from the LR program and major overlaps between the vascular cambium and the phellogen networks (Figure 7). Periderm-specific overexpression of *WOX4* and *BP* provides a novel approach for increasing periderm layers, a trait that is known to contribute to stress tolerance [3, 43]. Another key aspect for breeding programs is that WOX4 and BP are sufficient to increase cambial activity [30], paving the way for programs targeting simultaneously biomass and resistance to abiotic stresses. In this regard, it would be interesting to further decipher the complex molecular mechanisms coordinating the activity of the phellogen and the vascular cambium.

STAR★METHODS

Detailed methods are provided in the online version of this paper and include the following:

- KEY RESOURCES TABLE
- RESOURCE AVAILABILITY
  - Lead Contact
  - Materials Availability
  - Data and Code Availability
- EXPERIMENTAL MODEL AND SUBJECT DETAILS
- METHOD DETAILS
  - Molecular Cloning
  - Histology and Fluorescent Stainings
  - Confocal Microscopy
  - Periderm Quantification and Image Analyses
  - Lateral Root Density
  - q-PCR
  - Gene List
- QUANTIFICATION AND STATISTICAL ANALYSES

SUPPLEMENTAL INFORMATION

Supplemental Information can be found online at https://doi.org/10.1016/j.cub.2020.08.053.

ACKNOWLEDGMENTS

We thank Stefan Mann for cloning the *PER15* promoter in GreenGate. We thank Marja Timmermans, Antia Rodriguez-Villalon, and Ari Pekka Mähönen for critical reading of the manuscript. We thank Andrea Boch for technical help. Work in the Vermeer lab is supported by grants from the Swiss National Science Foundation (Schweizerischer Nationalfonds zur Förderung der Wissenschaftlichen Forschung, PP00P3_157524 and 316030_164086) and the Netherlands Organisation for Scientific Research (Nederlandse Organisatie voor Wetenschappelijk Onderzoek, NWO 864.13.008). Work in the Ragni lab was supported by the Deutsche Forschungsgemeinschaft (DFG grant RA-2590/1-2).

AUTHOR CONTRIBUTIONS

W.X. planned and conducted the majority of the experiments with input from L.R. L.R. and W.X. acquired the confocal images. A.W. conducted the initial experiments on the *arf* and *iaa* mutants. D.M., L.R., and W.X. did the molecular cloning and generated the plant lines. D.M. conducted the Fluorol Yellow (FY) experiments. W.X. and D.M. measured the number of periderm layers. A.W., W.X., and D.M. conducted the phellem ratio experiments. D.R. helped in generating the T3 lines and in the embedding of some experiments. J.E.M.V. provided the PER15 promoter and significant input to the project. L.R. wrote the manuscript, with the help of W.X., D.M., A.W., and J.E.M.V.

(D and E), Orthogonal view of z stacks of *ARF5/MP::NLS-3xGFP W131Y* (D) and *ARF8::NLS-3xGFP W131Y* (E). Twelve-day-old roots at the position corresponding to stage 5 of periderm development.
(F) Quantification of phellem ratio in 12-day-old WT, *arf6-1*, and *arf8-2* roots. Seven-day-old plants were treated for 5 days with mock or 1 μM NAA. One-way ANOVA (95% CI, post hoc: Tamhane, n = 15–16).
(G) Quantification of phellem ratio in *UBI10::XVE>>amiMP* lines. Seven-day-old plants were treated for 5 days with mock, 1 μM NAA, 5 μM β-estradiol (β-Estr) or 5 μM β-Estr + 1 μM NAA. One-way ANOVA (95% CI, post hoc: Tamhane, n = 12–14).
(H) Cross-sections (plastic embedding) of the uppermost part of 12-day-old *amiMP* (#13) roots. Seven-day-old plants were treated for 5 days with mock or 5 μM β-Estr.
(I) Quantification of the number of periderm layers of the experiment shown in (H).
(J) Quantification of phellem ratio in *35S::GR-MP* roots. Seven-day-old plants were treated for 5 days with mock or 10 μM DEX; t test (n = 15).
(K) Quantification of the number of periderm layers of the experiment shown in (L).
(L) Cross-sections (plastic embedding) of the uppermost part of 12-day-old *35S::GR-MP* roots. Seven-day-old plants were treated for 5 days with mock or 10 μM DEX.
(M) Cross-sections roots (plastic embedding) of the uppermost part of WT and *arf7-1-arf19-1* 12-day-old roots.
(N) Quantification of the number of periderm layers of the experiment shown in (M).
(O) Table comparing *ARF* phenotypes in the root. Mutant phenotypes were normalized to WT, which was set to 1. LRD, lateral root density; PR, phellem ratio; NAA, auxin response (PR mock/PR NAA); and P.L., number of periderm layers.
The white arrows indicate the pericycle/phellogen, the double-headed black arrows indicate the periderm extension, and the black dots indicate the periderm layers. Black and white scale bars: 20 μm.
See also Figure S5 and Data S2.

Please cite this article in press as: Xiao et al., Pluripotent Pericycle Cells Trigger Different Growth Outputs by Integrating Developmental Cues into Distinct Regulatory Modules, Current Biology (2020), https://doi.org/10.1016/j.cub.2020.08.053

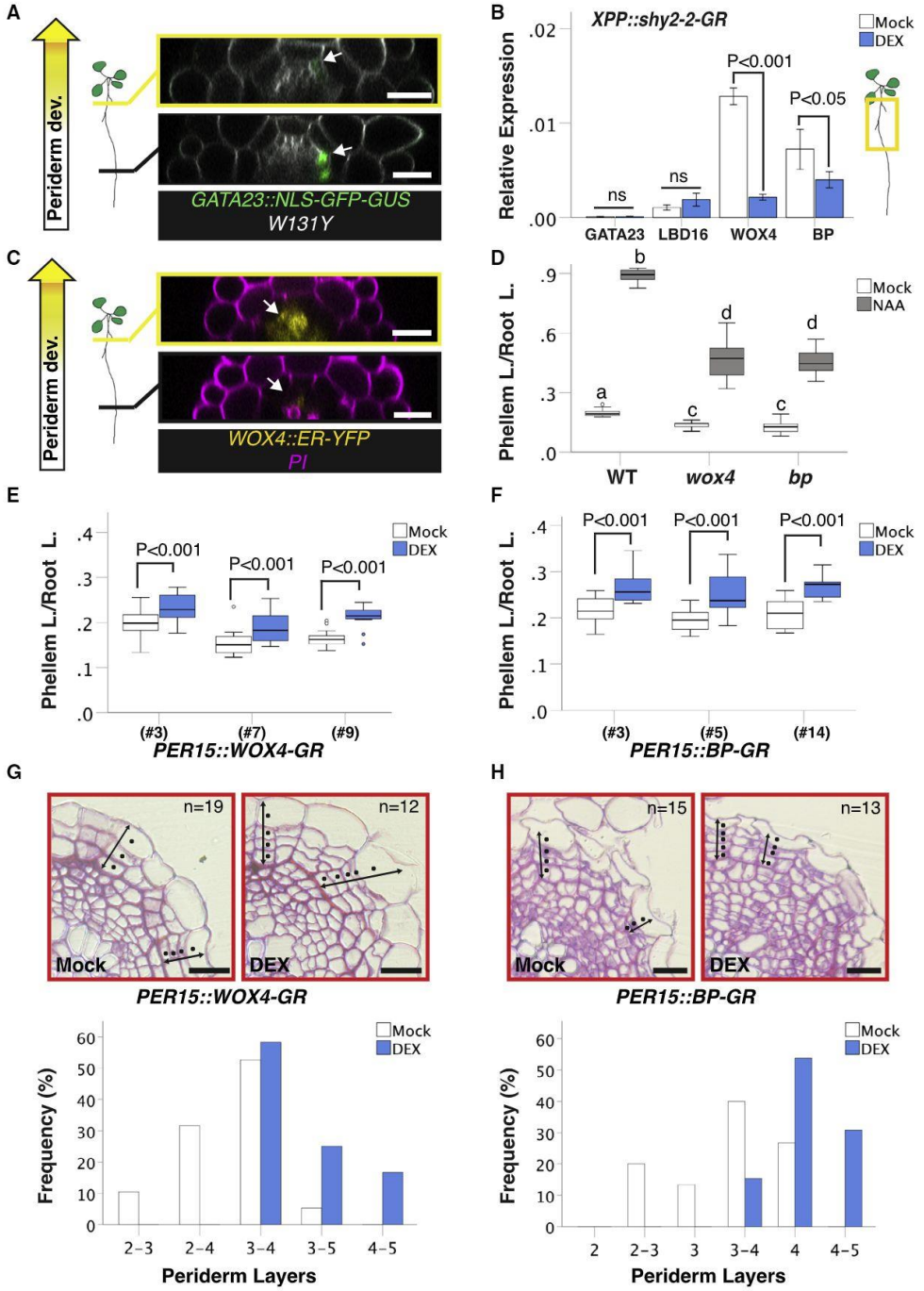

Figure 6. Distinct Targets Downstream of Auxin Orchestrate Periderm and LR Formation

(A) Orthogonal view of z stacks of a *GATA23::NLS-GFP-GUS W131Y* 7-day-old root at the positions corresponding to LR primordia (bottom) and stage 1 of periderm development (top).

(B) Relative expression of *LBD16*, *GATA23*, *WOX4*, and *BP/KNAT1* in the periderm of *XPP::shy2-2-GR* (in *MYB84::NLS-3xGFP W131Y*; #1) roots. Seven-day-old plants were treated for 2 days with mock or 10 μM DEX. The bars represent the means and the error bars represent ±2 SE; t test (ns, not significant; n = 3–4).

(C) Orthogonal view of z stacks of a *WOX4::ER-YFP* 7-day-old root at the positions corresponding to LR primordia (bottom) and stage 1 (top).

(legend continued on next page)

Please cite this article in press as: Xiao et al., Pluripotent Pericycle Cells Trigger Different Growth Outputs by Integrating Developmental Cues into Distinct Regulatory Modules, Current Biology (2020), https://doi.org/10.1016/j.cub.2020.08.053

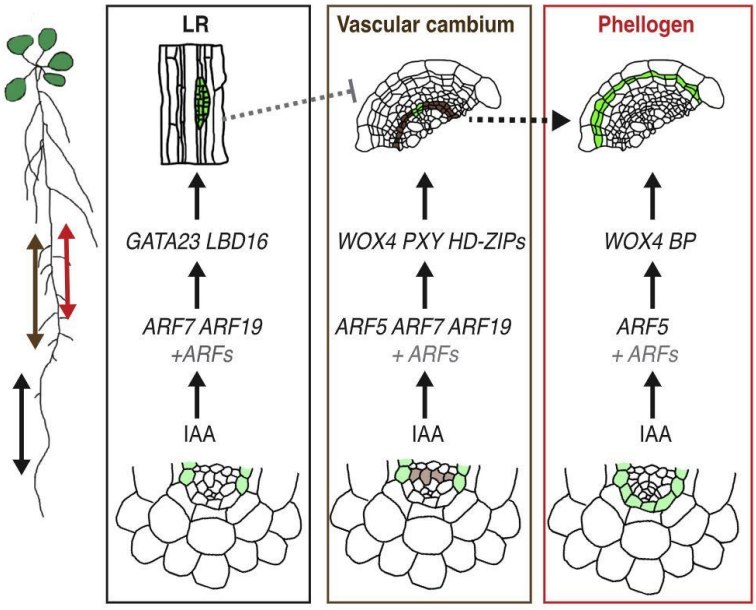

Figure 7. Model Explaining Pericycle Output Specificity

LRs, the phellogen, and part of the vascular cambium arise from reactivation of divisions in the pericycle. Auxin promotes these 3 programs. LR formation is the main auxin-induced program in the pericycle after the plant body is established. ARF7 and ARF19 are the main ARFs that activate GATA23 and LBDs, and thus the LR program. Auxin promotes phellogen formation via ARF5 and ARF8 (and probably other ARFs) and through the activation of WOX4 and BP. The establishment of the vascular cambium, which is also regulated by auxin via MP, WOX4, PXY, and HD-ZIPs, is required for periderm formation (the vascular cambium scheme is based on data in [8]).

The double-headed black arrow indicates the zone of the root where LR are specified and initiated, the double-headed red arrow indicates the zone of the root where periderm establishment occurs, and the double-headed brown arrow is where the vascular cambium is established. Gene names and arrows in gray indicate proposed interactions. The pericycle cells are depicted in pale green, the cells derived from the pericycle are depicted in green, the pro-cambial cells are in pale brown, and the cells derived from the pro-cambium are depicted in brown.

DECLARATION OF INTERESTS

The authors declare no competing interests.

Received: May 2, 2020
Revised: July 22, 2020
Accepted: August 14, 2020
Published: September 10, 2020

REFERENCES

1. Ragni, L., and Greb, T. (2018). Secondary growth as a determinant of plant shape and form. Semin. Cell Dev. Biol. *79*, 58–67.
2. Shi, D., Lebovka, I., López-Salmerón, V., Sanchez, P., and Greb, T. (2019). Bifacial cambium stem cells generate xylem and phloem during radial plant growth. Development *146*, dev171355.
3. Campilho, A., Nieminen, K., and Ragni, L. (2020). The development of the periderm: the final frontier between a plant and its environment. Curr. Opin. Plant Biol. *53*, 10–14.
4. Esau, K. (1965). Plant Anatomy (John Wiley & Sons).
5. Machado, A., Pereira, H., and Teixeira, R.T. (2013). Anatomy and development of the endodermis and phellem of Quercus suber L. roots. Microsc. Microanal. *19*, 525–534.
6. Wunderling, A., Ripper, D., Barra-Jimenez, A., Mahn, S., Sajak, K., Targem, M.B., and Ragni, L. (2018). A molecular framework to study periderm formation in Arabidopsis. New Phytol. *219*, 216–229.
7. Dolan, L., Janmaat, K., Willemsen, V., Linstead, P., Poethig, S., Roberts, K., and Scheres, B. (1993). Cellular organisation of the Arabidopsis thaliana root. Development *119*, 71–84.
8. Smetana, O., Mäkilä, R., Lyu, M., Amiryousefi, A., Sánchez Rodríguez, F., Wu, M.F., Solé-Gil, A., Leal Gavarrón, M., Siligato, R., Miyashima, S., et al. (2019). High levels of auxin signalling define the stem-cell organizer of the vascular cambium. Nature *565*, 485–489.
9. Du, Y., and Scheres, B. (2018). Lateral root formation and the multiple roles of auxin. J. Exp. Bot. *69*, 155–167.
10. Vermeer, J.E., von Wangenheim, D., Barberon, M., Lee, Y., Stelzer, E.H., Maizel, A., and Geldner, N. (2014). A spatial accommodation by neighboring cells is required for organ initiation in Arabidopsis. Science *343*, 178–183.
11. Escamez, S., André, D., Sztojka, B., Bollhöner, B., Hall, H., Berthet, B., Voß, U., Lers, A., Maizel, A., Andersson, M., et al. (2020). Cell Death in Cells Overlying Lateral Root Primordia Facilitates Organ Growth in Arabidopsis. Curr. Biol. *30*, 455–464.e7.
12. Leyser, O. (2018). Auxin Signaling. Plant Physiol. *176*, 465–479.

(D) Quantification of phellem ratio of 12-day-old WT, *wox4-1*, and *bp-9* roots. Seven-day-old plants were treated for 5 days with mock or 1 μM NAA. One-way ANOVA (95% CI, post hoc: Tamhane, n = 15–16).
(E) Quantification of phellem ratio in 3 independent *PER15::WOX4-GR* (in *W131Y*) T2 lines. Seven-day-old plants were treated for 5 days with mock or 10 μM DEX; t test (n = 14–16).
(F) Quantification of phellem ratio in 3 independent *PER15::BP-GR* lines. Seven-day-old plants were treated for 5 days with mock or 10 μM DEX; t test (n = 14–15).
(G) Top: cross-sections (plastic embedding) of the uppermost part of *PER15::WOX4-GR* (in *W131Y*; #3) roots: mock (left panel), 10 μM DEX induced (right panel). Seven-day-old plants were treated for 5 days with mock or 10 μM DEX. Bottom: quantification of the number of periderm layers in *PER15::WOX4-GR* (in *W131Y;* #3) of the experiment.
(H) Top: cross-sections of the uppermost part of *PER15::BP-GR* (#3) roots (plastic embedding): mock (left panel), 10 μM DEX induced (right panel). Seven-day-old plants were treated for 5 days with mock or 10 μM DEX. Bottom: quantification of the number of periderm layers in *PER15::BP-GR* (#3) of the experiment.
The white arrows indicate the pericycle, the double-headed black arrows indicate the periderm extension, and the black dots indicate the periderm cells. Black and white scale bars: 20 μm.
See also Figure S6 and Data S2.

Please cite this article in press as: Xiao et al., Pluripotent Pericycle Cells Trigger Different Growth Outputs by Integrating Developmental Cues into Distinct Regulatory Modules, Current Biology (2020), https://doi.org/10.1016/j.cub.2020.08.053

13. Yamaguchi, Y.L., Ishida, T., and Sawa, S. (2016). CLE peptides and their signaling pathways in plant development. J. Exp. Bot. *67*, 4813–4826.

14. Brackmann, K., Qi, J., Gebert, M., Jouannet, V., Schlamp, T., Grünwald, K., Wallner, E.-S., Novikova, D.D., Levitsky, V.G., Agustí, J., et al. (2018). Spatial specificity of auxin responses coordinates wood formation. Nat. Commun. *9*, 875.

15. Di Mambro, R., De Ruvo, M., Pacifici, E., Salvi, E., Sozzani, R., Benfey, P.N., Busch, W., Novak, O., Ljung, K., Di Paola, L., et al. (2017). Auxin minimum triggers the developmental switch from cell division to cell differentiation in the *Arabidopsis* root. Proc. Natl. Acad. Sci. USA *114*, E7641–E7649.

16. Motte, H., Vanneste, S., and Beeckman, T. (2019). Molecular and Environmental Regulation of Root Development. Annu. Rev. Plant Biol. *70*, 465–488.

17. Smit, M.E., and Weijers, D. (2015). The role of auxin signaling in early embryo pattern formation. Curr. Opin. Plant Biol. *28*, 99–105.

18. Liao, C.Y., Smet, W., Brunoud, G., Yoshida, S., Vernoux, T., and Weijers, D. (2015). Reporters for sensitive and quantitative measurement of auxin response. Nat. Methods *12*, 207–210.

19. Ramakrishna, P., Ruiz Duarte, P., Rance, G.A., Schubert, M., Vordermaier, V., Vu, L.D., Murphy, E., Vilches Barro, A., Swarup, K., Moirangthem, K., et al. (2019). EXPANSIN A1-mediated radial swelling of pericycle cells positions anticlinal cell divisions during lateral root initiation. Proc. Natl. Acad. Sci. USA *116*, 8597–8602.

20. Andersen, T.G., Naseer, S., Ursache, R., Wybouw, B., Smet, W., De Rybel, B., Vermeer, J.E.M., and Geldner, N. (2018). Diffusible repression of cytokinin signalling produces endodermal symmetry and passage cells. Nature *555*, 529–533.

21. Ueda, K., Matsuyama, T., and Hashimoto, T. (1999). Visualization of microtubules in living cells of transgenic Arabidopsis thaliana. Protoplasma *206*, 201–206.

22. Boerjan, W., Cervera, M.T., Delarue, M., Beeckman, T., Dewitte, W., Bellini, C., Caboche, M., Van Onckelen, H., Van Montagu, M., and Inzé, D. (1995). Superroot, a recessive mutation in Arabidopsis, confers auxin overproduction. Plant Cell *7*, 1405–1419.

23. Mikkelsen, M.D., Naur, P., and Halkier, B.A. (2004). Arabidopsis mutants in the C-S lyase of glucosinolate biosynthesis establish a critical role for indole-3-acetaldoxime in auxin homeostasis. Plant J. *37*, 770–777.

24. Goh, T., Joi, S., Mimura, T., and Fukaki, H. (2012). The establishment of asymmetry in Arabidopsis lateral root founder cells is regulated by LBD16/ASL18 and related LBD/ASL proteins. Development *139*, 883–893.

25. Lee, H.W., Kim, N.Y., Lee, D.J., and Kim, J. (2009). LBD18/ASL20 regulates lateral root formation in combination with LBD16/ASL18 downstream of ARF7 and ARF19 in Arabidopsis. Plant Physiol. *151*, 1377–1389.

26. Okushima, Y., Fukaki, H., Onoda, M., Theologis, A., and Tasaka, M. (2007). ARF7 and ARF19 regulate lateral root formation via direct activation of LBD/ASL genes in Arabidopsis. Plant Cell *19*, 118–130.

27. Fisher, K., and Turner, S. (2007). PXY, a receptor-like kinase essential for maintaining polarity during plant vascular-tissue development. Curr. Biol. *17*, 1061–1066.

28. Hirakawa, Y., Shinohara, H., Kondo, Y., Inoue, A., Nakanomyo, I., Ogawa, M., Sawa, S., Ohashi-Ito, K., Matsubayashi, Y., and Fukuda, H. (2008). Non-cell-autonomous control of vascular stem cell fate by a CLE peptide/receptor system. Proc. Natl. Acad. Sci. USA *105*, 15208–15213.

29. Liebsch, D., Sunaryo, W., Holmlund, M., Norberg, M., Zhang, J., Hall, H.C., Helizon, H., Jin, X., Helariutta, Y., Nilsson, O., et al. (2014). Class I KNOX transcription factors promote differentiation of cambial derivatives into xylem fibers in the Arabidopsis hypocotyl. Development *141*, 4311–4319.

30. Zhang, J., Eswaran, G., Alonso-Serra, J., Kucukoglu, M., Xiang, J., Yang, W., Elo, A., Nieminen, K., Damén, T., Joung, J.G., et al. (2019). Transcriptional regulatory framework for vascular cambium development in Arabidopsis roots. Nat. Plants *5*, 1033–1042.

31. Agusti, J., Lichtenberger, R., Schwarz, M., Nehlin, L., and Greb, T. (2011). Characterization of transcriptome remodeling during cambium formation identifies MOL1 and RUL1 as opposing regulators of secondary growth. PLOS Genet. *7*, e1001312.

32. De Rybel, B., Vassileva, V., Parizot, B., Demeulenaere, M., Grunewald, W., Audenaert, D., Van Campenhout, J., Overvoorde, P., Jansen, L., Vanneste, S., et al. (2010). A novel aux/IAA28 signaling cascade activates GATA23-dependent specification of lateral root founder cell identity. Curr. Biol. *20*, 1697–1706.

33. Fukaki, H., Tameda, S., Masuda, H., and Tasaka, M. (2002). Lateral root formation is blocked by a gain-of-function mutation in the SOLITARY-ROOT/IAA14 gene of Arabidopsis. Plant J. *29*, 153–168.

34. Goh, T., Kasahara, H., Mimura, T., Kamiya, Y., and Fukaki, H. (2012). Multiple AUX/IAA-ARF modules regulate lateral root formation: the role of Arabidopsis SHY2/IAA3-mediated auxin signalling. Philos. Trans. R. Soc. Lond. B Biol. Sci. *367*, 1461–1468.

35. Hayward, A., Stirnberg, P., Beveridge, C., and Leyser, O. (2009). Interactions between auxin and strigolactone in shoot branching control. Plant Physiol. *151*, 400–412.

36. Rogg, L.E., Lasswell, J., and Bartel, B. (2001). A gain-of-function mutation in IAA28 suppresses lateral root development. Plant Cell *13*, 465–480.

37. De Smet, I., Lau, S., Voss, U., Vanneste, S., Benjamins, R., Rademacher, E.H., Schlereth, A., De Rybel, B., Vassileva, V., Grunewald, W., et al. (2010). Bimodular auxin response controls organogenesis in Arabidopsis. Proc. Natl. Acad. Sci. USA *107*, 2705–2710.

38. Okushima, Y., Overvoorde, P.J., Arima, K., Alonso, J.M., Chan, A., Chang, C., Ecker, J.R., Hughes, B., Lui, A., Nguyen, D., et al. (2005). Functional genomic analysis of the AUXIN RESPONSE FACTOR gene family members in Arabidopsis thaliana: unique and overlapping functions of ARF7 and ARF19. Plant Cell *17*, 444–463.

39. Hardtke, C.S., Ckurshumova, W., Vidaurre, D.P., Singh, S.A., Stamatiou, G., Tiwari, S.B., Hagen, G., Guilfoyle, T.J., and Berleth, T. (2004). Overlapping and non-redundant functions of the Arabidopsis auxin response factors MONOPTEROS and NONPHOTOTROPIC HYPOCOTYL 4. Development *131*, 1089–1100.

40. O'Malley, R.C., Huang, S.C., Song, L., Lewsey, M.G., Bartlett, A., Nery, J.R., Galli, M., Gallavotti, A., and Ecker, J.R. (2016). Cistrome and Epicistrome Features Shape the Regulatory DNA Landscape. Cell *165*, 1280–1292.

41. Hirakawa, Y., Kondo, Y., and Fukuda, H. (2010). TDIF peptide signaling regulates vascular stem cell proliferation via the WOX4 homeobox gene in Arabidopsis. Plant Cell *22*, 2618–2629.

42. Suer, S., Agusti, J., Sanchez, P., Schwarz, M., and Greb, T. (2011). WOX4 imparts auxin responsiveness to cambium cells in Arabidopsis. Plant Cell *23*, 3247–3259.

43. Thangavel, T., Tegg, R.S., and Wilson, C.R. (2016). Toughing It Out–Disease-Resistant Potato Mutants Have Enhanced Tuber Skin Defenses. Phytopathology *106*, 474–483.

44. Geldner, Niko, Dénervaud-Tendon, Valerie, Hyman, D.L., Mayer, U., Stierhof, Y.-D., and Chory, J. (2009). Rapid, combinatorial analysis of membrane compartments in intact plants with a multicolor marker set. Plant J *59*, 169–178.

45. Rademacher, E.H., Moller, B., Lokerse, A.S., Llavata-Peris, C.I., van den Berg, W., and Weijers, D. (2011). A cellular expression map of the Arabidopsis AUXIN RESPONSE FACTOR gene family. Plant J *68*, 597–606.

46. Ito, J., Fukaki, H., Onoda, M., Li, L., Li, C., Tasaka, M., et al. (2016). Auxin-dependent compositional change in Mediator in ARF7- and ARF19-mediated transcription. Proc. Nat. Acad. Sci. U.S.A. *113*, 6562–6567.

Please cite this article in press as: Xiao et al., Pluripotent Pericycle Cells Trigger Different Growth Outputs by Integrating Developmental Cues into Distinct Regulatory Modules, Current Biology (2020), https://doi.org/10.1016/j.cub.2020.08.053

47. Smith, H.M., and Hake, S. (2003). The interaction of two homeobox genes, BREVIPEDICELLUS and PENNYWISE, regulates internode patterning in the Arabidopsis inflorescence. Plant Cell *15*, 1717–1727.

48. Agusti, J., Herold, S., Schwarz, M., Sanchez, P., Ljung, K., Dun, E.A., et al. (2011). Strigolactone signaling is required for auxin-dependent stimulation of secondary growth in plants. Proc. Natl. Acad. Sci. U.S.A. *108*, 20242–20247.

49. Gursanscky, N.R., Jouannet, V., Grunwald, K., Sanchez, P., Laaber-Schwarz, M., and Greb, T. (2016). MOL1 is required for cambium homeostasis in Arabidopsis. Plant J *86*, 210–220.

50. Vilches Barro, A., Stockle, D., Thellmann, M., Ruiz-Duarte, P., Bald, L., Louveaux, M., et al. (2019). Cytoskeleton Dynamics Are Necessary for Early Events of Lateral Root Initiation in Arabidopsis. Curr. Biol. *29*, 2443–2454.

51. Ulmasov, T., Murfett, J., Hagen, G., and Guilfoyle, T.J. (1997). Aux/IAA proteins repress expression of reporter genes containing natural and highly active synthetic auxin response elements. Plant Cell *9*, 1963–1971.

52. Schindelin, J., Arganda-Carreras, I., Frise, E., Kaynig, V., Longair, M., Pietzsch, T., Preibisch, S., Rueden, C., Saalfeld, S., Schmid, B., et al. (2012). Fiji: an open-source platform for biological-image analysis. Nat. Methods *9*, 676–682.

53. Lampropoulos, A., Sutikovic, Z., Wenzl, C., Maegele, I., Lohmann, J.U., and Forner, J. (2013). GreenGate—a novel, versatile, and efficient cloning system for plant transgenesis. PLOS ONE *8*, e83043.

54. Schürholz, A.K., López-Salmerón, V., Li, Z., Forner, J., Wenzl, C., Gaillochet, C., Augustin, S., Barro, A.V., Fuchs, M., Gebert, M., et al. (2018). A Comprehensive Toolkit for Inducible, Cell Type-Specific Gene Expression in Arabidopsis. Plant Physiol. *178*, 40–53.

55. de Reuille, P.B., and Ragni, L. (2017). Vascular Morphodynamics During Secondary Growth. Methods Mol. Biol. *1544*, 103–125.

56. Naseer, S., Lee, Y., Lapierre, C., Franke, R., Nawrath, C., and Geldner, N. (2012). Casparian strip diffusion barrier in Arabidopsis is made of a lignin polymer without suberin. Proc. Natl. Acad. Sci. USA *109*, 10101–10106.

Please cite this article in press as: Xiao et al., Pluripotent Pericycle Cells Trigger Different Growth Outputs by Integrating Developmental Cues into Distinct Regulatory Modules, Current Biology (2020), https://doi.org/10.1016/j.cub.2020.08.053

STAR★METHODS

KEY RESOURCES TABLE

REAGENT or RESOURCE	SOURCE	IDENTIFIER
Bacterial and Virus Strains		
Escherichia coli DH5alfa	Widely distributed	N/A
Agrobacterium tumefaciens GV3101	Widely distributed	N/A
Chemicals, Peptides, and Recombinant Proteins		
Indole-3-acetic acid (IAA)	Duchefa	Cat# I0901
1-Naphthaleneacetic acid (NAA)	Duchefa	Cat# N0903
N-1-naphthylphthalamic acid (NPA)	Duchefa	Cat# N0926
Dexamethasone (DEX)	Sigma	Cat# D1756
β-Estradiol (β-Estr.)	Sigma	Cat# E8875
Propidium Iodide (PI)	Sigma	Cat# P4864
Murashige and Skoog Basal Medium (MS)	Duchefa	Cat# M0255
Plant Agar	Duchefa	Cat# P1001.1000
2,4-Dichlorophenoxyacetic acid (2,4 D)	Sigma	Cat# D-7299
Technovit 7100	Heraeus Kulzer	Cat# 64709003
Fluorol yellow (FY)	Santa Cruz	Cat# sc-215052
X-Glux	Duchefa	Cat# X-1405
Toluidine blue	Sigma	Cat# T3260
Chloral hydrate	Merck	Cat# 1.02425.1000
Glycerol	Roth	Cat# 6962.1
Critical Commercial Assays		
The Universal RNA Purification Kit	Roboklon	Cat# E3598-02
AMV Reverse Transcriptase Native	Roboklon	Cat# E1372-01
MESA blue	Eurogentec	Cat# RT-SYS2X-03+NRWOUB
Experimental Models: Organisms/Strains		
Arabidopsis: Col-0	Widely distributed	N/A
Arabidopsis: Ws	Widely distributed	N/A
Arabidopsis: *MYB84::NLS-3xGFP* in W131Y	[6]	N/A
Arabidopsis: *UBQ10::eYFP-NPSN12 (W131Y)*	[44]	N/A
Arabidopsis: *R2D2 (RPS5A::m-D2-dTomato>> RPS5A::D2VENUS)* in Col-0	[18]	N/A
Arabidopsis: *ARF7::NLS-3xGFP* in Col-0	[45]	NASC: N67080
Arabidopsis: *ARF19::NLS-3xGFP* in Col-0	[45]	NASC: N67104
Arabidopsis: *ARF8::NLS-3xGFP* in Col-0	[45]	NASC: N67082

(*Continued on next page*)

Please cite this article in press as: Xiao et al., Pluripotent Pericycle Cells Trigger Different Growth Outputs by Integrating Developmental Cues into Distinct Regulatory Modules, Current Biology (2020), https://doi.org/10.1016/j.cub.2020.08.053

Continued

REAGENT or RESOURCE	SOURCE	IDENTIFIER
Arabidopsis: *ARF6::NLS-3xGFP* in Col-0	[45]	NASC: N67078
Arabidopsis: *ARF5::NLS-3xGFP* in Col-0	[45]	NASC: N67076
Arabidopsis: *IAA28::NLS-3xm-Cherry* in *MYB84::NLS-3xGFP* W131Y	This manuscript	N/A
Arabidopsis: *SLR/IAA14::NLS-3xm-Cherry* in *MYB84::NLS-3xGFP* in W131Y	This manuscript	N/A
Arabidopsis: *BDL/IAA12::NLS-3xGFP*	[37]	N/A
Arabidopsis: *SHY2/IAA2::NLS-3xm-Venus*	[10]	N/A
Arabidopsis: *LBD16::GUS* in Col-0	[46]	N/A
Arabidopsis: *DR5v2::ER-YFP* in Col-0	[14]	N/A
Arabidopsis: *shy2-101* in Col-0	[34]	N/A
Arabidopsis: *bdl-2* in Col-0	[35]	N/A
Arabidopsis: *GATA23::NLS-GFP-GUS*	[32]	N/A
Arabidopsis: *iaa28-1* in Ws	[36]	N/A
Arabidopsis: *arf7-1 arf19-1*	[38]	NASC: N24629
Arabidopsis: *slr-1* in Col-0	[33]	N/A
Arabidopsis: *arf8-3* in Col-0	[38]	N/A
Arabidopsis: *arf6-2* in Col-0	[38]	NASC: N24606
Arabidopsis: *UBI10::XVE>>amiR-MP* in Col-0	[8]	N/A
Arabidopsis: *PER15::H2B-3xm-Cherry* in *MYB84::NLS-3xGFP* in W131Y	This manuscript	N/A
Arabidopsis: *CASP1::shy2-2* in Col-0	[10]	N/A
Arabidopsis: *35S::TUA6-GFP* in Col-0	[21]	NASC: N6551
Arabidopsis: *PER15::slr-1-GR* in *MYB84::NLS-3xGFP* in W131Y	This manuscript	N/A
Arabidopsis: *XPP::shy2-2-GR* in *MYB84::NLS-3xGFP* in W131Y	This manuscript	N/A
Arabidopsis: *bp-9* in Col-0	[47]	N/A
Arabidopsis: *wox4-1* in Col-0	[42]	N/A
Arabidopsis: *WOX4::ER-YFP* in Col-0	[42]	N/A
Arabidopsis: *BP/KNAT1::NLS-3xm-Cherry* in *MYB84::NLS-3xGFP* in W131Y	This manuscript	N/A

(*Continued on next page*)

Please cite this article in press as: Xiao et al., Pluripotent Pericycle Cells Trigger Different Growth Outputs by Integrating Developmental Cues into Distinct Regulatory Modules, Current Biology (2020), https://doi.org/10.1016/j.cub.2020.08.053

Continued

REAGENT or RESOURCE	SOURCE	IDENTIFIER
Arabidopsis: *XPP::m-Citrine-SYP122* in Col-0	[20]	N/A
Arabidopsis: *PER15::WOX4-GR* in W131Y	This manuscript	N/A
Arabidopsis: *PER15::BP-GR* in Col-0	This manuscript	N/A
Arabidopsis: *PXY::shy2-2-GR* in W131Y	This manuscript	N/A
Arabidopsis: *pxy-3* in Col-0	[20]	NASC: N9871
Arabidopsis: *PXY::ER-CFP* in Col-0	[48]	N/A
Arabidopsis: *mol1-1* in Col-0	[31]	N/A
Arabidopsis: *pMOL1::ER-YFP* in *PXY::ER-CFP*	[49]	N/A
Arabidopsis: *PXY::BP-GR* in W131Y	This manuscript	N/A
Arabidopsis: *35S::GR-MP* in Col-0	[14]	N/A
Arabidopsis: *gLBD16-SRDX* in Col-0	[50]	N/A
Arabidopsis: *rty1-1/+* in *DR5::GUS*	[22]	NASC: N16708
Arabidopsis: *DR5::GUS* in Col-0	[51]	from segregation of N16708
Oligonucleotides		
See Table S1	Sigma	N/A
Recombinant DNA		
PER15::slr-1-GR	This manuscript	See Data S1
XPP::shy2-2-GR	This manuscript	See Data S1
IAA28::NLS-3xm-Cherry	This manuscript	See Data S1
IAA14/SLR::NLS-3xm-Cherry	This manuscript	See Data S1
BP::NLS-3xm-Cherry	This manuscript	See Data S1
PER15::BP-GR	This manuscript	See Data S1
PER15::WOX4-GR	This manuscript	See Data S1
PER15::H2B-3xm-Cherry	This manuscript	See Data S1
PXY::shy2-2-GR	This manuscript	See Data S1
PXY::BP-GR	This manuscript	See Data S1
Software and Algorithms		
ZEN Black (Zen 2.3 SP1)	Zeiss	https://www.zeiss.de
Fiji	[52]	https://fiji.sc/
IBM SPSS Statistics version 24-25-26	IBM	https://www.ibm.com/products/spss-statistics
CFX Maestro	BIO-RAD	www.bio-rad.com

RESOURCE AVAILABILITY

Lead Contact

Further information and requests for resources should be directed to and will be fulfilled by the Lead Contact, Laura Ragni (laura.ragni@zmbp.uni-tuebingen.de).

Please cite this article in press as: Xiao et al., Pluripotent Pericycle Cells Trigger Different Growth Outputs by Integrating Developmental Cues into Distinct Regulatory Modules, Current Biology (2020), https://doi.org/10.1016/j.cub.2020.08.053

Materials Availability

There are no restrictions to the availability of the newly generated resources.

Data and Code Availability

This study did not generate any unique code. This study did not produce any unique NGS sequencing/ protein structure/microarray data.

EXPERIMENTAL MODEL AND SUBJECT DETAILS

Arabidopsis thaliana transgenic and mutant lines were used to performed experiments. The ecotype and the background of each line/ mutant is specified in the Key Resources Table. GFP-based fluorescent reporters were crossed to the W131Y line to outline the cells and experiments were performed with F2 segregating and/or F3 homozygous populations. Plants were grown in continuous light condition *in vitro* on ½ MS plates supplemented with 1% sugar and 0.8% plant agar. For long auxin and NPA treatments, plants were grown on ½ MS and transferred after 7 days (unless it is specified otherwise in the text or figures) on ½ MS supplemented with 1μM NAA or 1μM IAA or 1μM 2,4D or 10μM NPA respectively. For β-Estradiol induction, plants were grown on ½ MS and transferred after 7 days on plates supplemented with 5μM β-Estradiol. For DEX induction, plants were grown on ½ MS and after 7days transferred (unless it is specified otherwise in the text or figures on plates supplemented with 10 μM DEX.

METHOD DETAILS

Molecular Cloning

All constructs have been obtained using the modular green gate technology [53]. Promoters were amplified from genomic DNA and the BP/KNAT1 coding sequence from root c-DNA with the primers listed in Data S1. If a BSAI site was present in the sequence, it was replaced as previously described in [54]. All modules and vectors used in this study are described in Data S1. The module assembly strategy is described in Data S1. All final plasmids were transformed into Agrobacterium tumefaciens GV3101. *Arabidopsis thaliana* plants were transformed via floral dipping. Homozygous T3 lines were used unless specified otherwise.

Histology and Fluorescent Stainings

Root samples for plastic embedding were taken 0.5mm from the root junction unless stated otherwise. Thin plastic cross-sections were obtained as described in [55], using Technovit 7100. 5-7 μm plastic sections were stained with 0.1% toluidine blue and imaged with a Zeiss Axio M2 imager microscope or a Zeiss Axiophot microscope. Fluorol yellow (FY) staining for suberin deposition was performed as described in [56] using Fluorol yellow. Propidium Iodide (PI) staining was achieved by directly mounting the root in a 10-20 μg/ml solution. GUS staining was performed as described in [6] using X-Glux. Roots were mounted in chloral hydrate solution (8:3:1; Chloral hydrate: Water: Glycerol).

Confocal Microscopy

Confocal images were acquired from whole-mount samples using a Zeiss LSM880 with the following settings. For Cyan fluorescent protein (CFP): excitation wavelength (ex.) 458 nm; emission (em.) 464–499 nm; For green fluorescent protein (GFP): ex. 488 nm; em 490–510 nm. For yellow fluorescent protein (YFP), mCitrine and Venus: ex. 514 nm; em. 520–540 nm. For mCherry, d-Tomato and PI: ex. 561 nm; em. 570–630 nm. For FY: ex. 488nm; em 490-540nm. For phellem autofluorescence: ex. 405 nm; em. 420–460 nm. 3D reconstructions, Orthogonal views of a Z stack and the ratio images of R2D2 were obtained using the ZEN Black software (Zen 2.3 SP1).

Periderm Quantification and Image Analyses

No statistical methods were used to predetermine sample size. The experiments were not randomized. Only few experiments were performed and analyzed blindly. Phellem length and Phellem ratio were measured as described in [6] using Fiji (https://fiji.sc/) [52]. At least 2-3 independent experiments were performed and the graphs of one representative experiment each are presented. The number of periderm layers was calculated as follow: the minimum and the maximum number of periderm layers per cross-section/sample was measured. For every genotype 9-20 cross-sections, coming from independent plants, were analyzed. According to the min and max number of layers, a sample was assigned to a certain class. For instance, if a sample has minimum 3 layers and maximum 4 layers, it was assigned to class 3-4. The frequency for each class was calculated and displayed as percentage. At least 2-3 independent experiments were performed and the graphs of one representative experiment is presented. The number of pericycle divisions upon auxin induction, was calculates using the *35S::TUA6-GFP* marker. Confocal Z stack images of two regions of the uppermost part of the root were acquired using the tile function (with 5% overlap). 8-9 roots per conditions were analyzed. The number of pericycle cells divisions per region of interest (ROI:(3x1 tiles: ≈600 μm) was quantified using the cell counter plugin of Fiji. The experiment was repeated twice and one representative is presented. The number of pericycle/periderm cells was quantified, measuring the number of pericycle/periderm cells in a cross-section using the cell counter plug in of FiJi for 10-12 roots.

Please cite this article in press as: Xiao et al., Pluripotent Pericycle Cells Trigger Different Growth Outputs by Integrating Developmental Cues into Distinct Regulatory Modules, Current Biology (2020), https://doi.org/10.1016/j.cub.2020.08.053

Lateral Root Density

Lateral root density was measured counting the number of lateral root primordia present in 7-day-old roots and dividing it by the root length in cm or by counting the number of emerged lateral root in present in 12-day-old roots and dividing it by the root length in cm.

q-PCR

RNA was extracted from upper most 3cm of at least 30 roots for each genotype/treatment using the Universal RNA Purification Kit (Roboklon, E3598-02) according to the manufacturer protocol. C-DNA was synthetized using AMV Reverse Transcriptase Native (Roboklon, E1372-01) according to manufacturer protocol. qPCR was performed using MESA blue (Eurogentec, RT-SYS2X-03+NRWOUB) in a CFX96 Real-Time System machine (BIO-RAD). Primers used for qPCR are listed in Table S1. The relative expression was calculated using *CFX Maestro software (*BIO-RAD) and the sample were normalized against EF1. qPCR experiments were repeated at least 3 times and one experiment is shown.

Gene List

The gene number and the full name of all genes mention in this study is presented in Data S1.

QUANTIFICATION AND STATISTICAL ANALYSES

We performed statistical analyses using IBM SPSS Statistics version 24-25-26 (IBM). The datasets were at first tested for homogeneity of variances using the Levene's Test. Then the significant differences between two datasets were calculated using a Welch's t test in case of a non-homogeneous variance or a Student's t test if the variance was homogeneous. The threshold for significance is indicated with P in the graphs. For multiple sample comparison, we calculated the significant differences between each dataset using One-way ANOVA with Tamhane's post hoc (equal variance not assumed) or a Bonferroni correction (equal variance assumed). The statistical analyses of the root length relative to phellem ratio and lateral root density measurement can be found in Data S2.

Current Biology, Volume *30*

Supplemental Information

Pluripotent Pericycle Cells Trigger Different Growth Outputs by Integrating Developmental Cues into Distinct Regulatory Modules

Wei Xiao, David Molina, Anna Wunderling, Dagmar Ripper, Joop E.M. Vermeer, and Laura Ragni

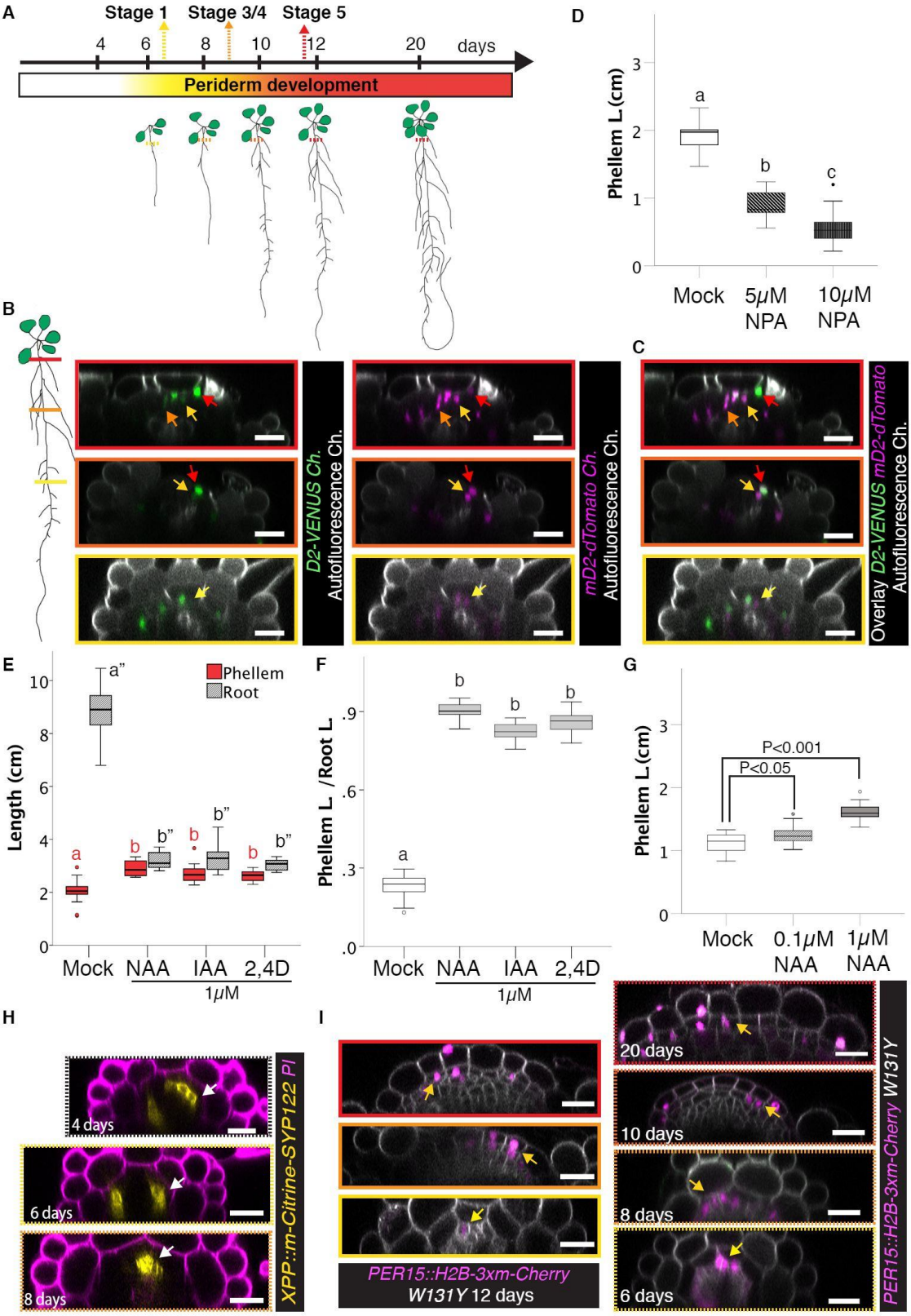
A
Stage 1
Stage 3/4
Stage 5
4
6
8
10
12
20
days
Periderm development
D
Phellem L (cm)
a
b
c
Mock
5μM NPA
10μM NPA
B
C
D2-VENUS Ch.
Autofluorescence Ch.
mD2-dTomato Ch.
Autofluorescence Ch.
Overlay D2-VENUS mD2-dTomato
Autofluorescence Ch.
E
Length (cm)
Phellem
Root
a"
a
b
b"
Mock
NAA
IAA
2,4D
1μM
F
Phellem L /Root L
a
b
Mock
NAA
IAA
2,4D
1μM
G
Phellem L (cm)
P<0.001
P<0.05
Mock
0.1μM NAA
1μM NAA
H
4 days
6 days
8 days
XPP::m-Citrine-SYP122 PI
I
PER15::H2B-3xm-Cherry
W131Y 12 days
20 days
10 days
8 days
6 days
PER15::H2B-3xm-Cherry W131Y

Figure S1. The phellogen is a site of auxin accumulation and auxin promotes periderm development. Related to Figure 1. (A) Periderm development in the Arabidopsis root can be followed over time. Distinct periderm development stages in the uppermost part of roots at different ages. Periderm development starts at around 6 days (d) and a fully developed periderm is present in the uppermost part of 12-d-old roots or older roots. (B) Auxin accumulates in the phellogen. Orthogonal view of Z-stacks of a R2D2 root showing *RPS5A::D2VENUS* (*D2-VENUS*) channel (left panels) and *RPS5A::m-D2-dTomato* (*mD2-dTomato*) channel (right panels) at the positions corresponding to stage 1 (lower panels), stage 3/4 (middle panels) and stage 5 (upper panels) (12-d-old; White signal that outline the cells: autofluorescence) relative to Figure 1B. (C) Overlay of *D2-VENUS* and *mD2-dTomato* channels of (B). (D) Quantification of phellem length in 12-d-old mock, 5μM NPA and 10μM NPA treated roots. 7-d-old plants were treated for 5-d with mock, 5μM NPA or 10μM NPA. One-way ANOVA (CI95%, Post-Hoc: Bonferroni, n =15). (E-F) Quantification of phellem length, root length and phellem ratio in 12-d-old mock, 1μM NAA, 1μM IAA and 1μM 2,4D treated roots. 7-d-old plants were treated for 5-d with mock, NAA, IAA or 2,4D. One-way ANOVA (CI95%, Post-Hoc: Bonferroni, n =10-15). (G) Quantification of phellem length in 10-d-old mock, 0.1μM NAA and 1μM NAA treated roots. T-test (n =15). (H) Orthogonal view of Z-stacks of *XPP::m-Citrine-SYP122* roots at 4, 6 and 8 days (uppermost part of the root). (I) Left panels: orthogonal view of Z-stacks of *PER15::H2B-3xm-Cherry W131Y* roots at the positions corresponding to stage 1 (lower panel), stage 3/4 (middle panel) and stage 5 (upper panel) (12-d-old). Right panels: orthogonal view of Z-stacks of *PER15:: H2B-3xm-Cherry W131Y* roots at 6,8,10 and 20 days (uppermost part of the root). White arrows indicate fluorescence signal of the *XPP::m-Citrine-SYP122* marker at the xylem pole pericycle. Pale yellow arrows indicate the pericycle, dark yellow the phellogen, red arrows the phellem and orange arrows the phelloderm. White scale bars: 20μm.

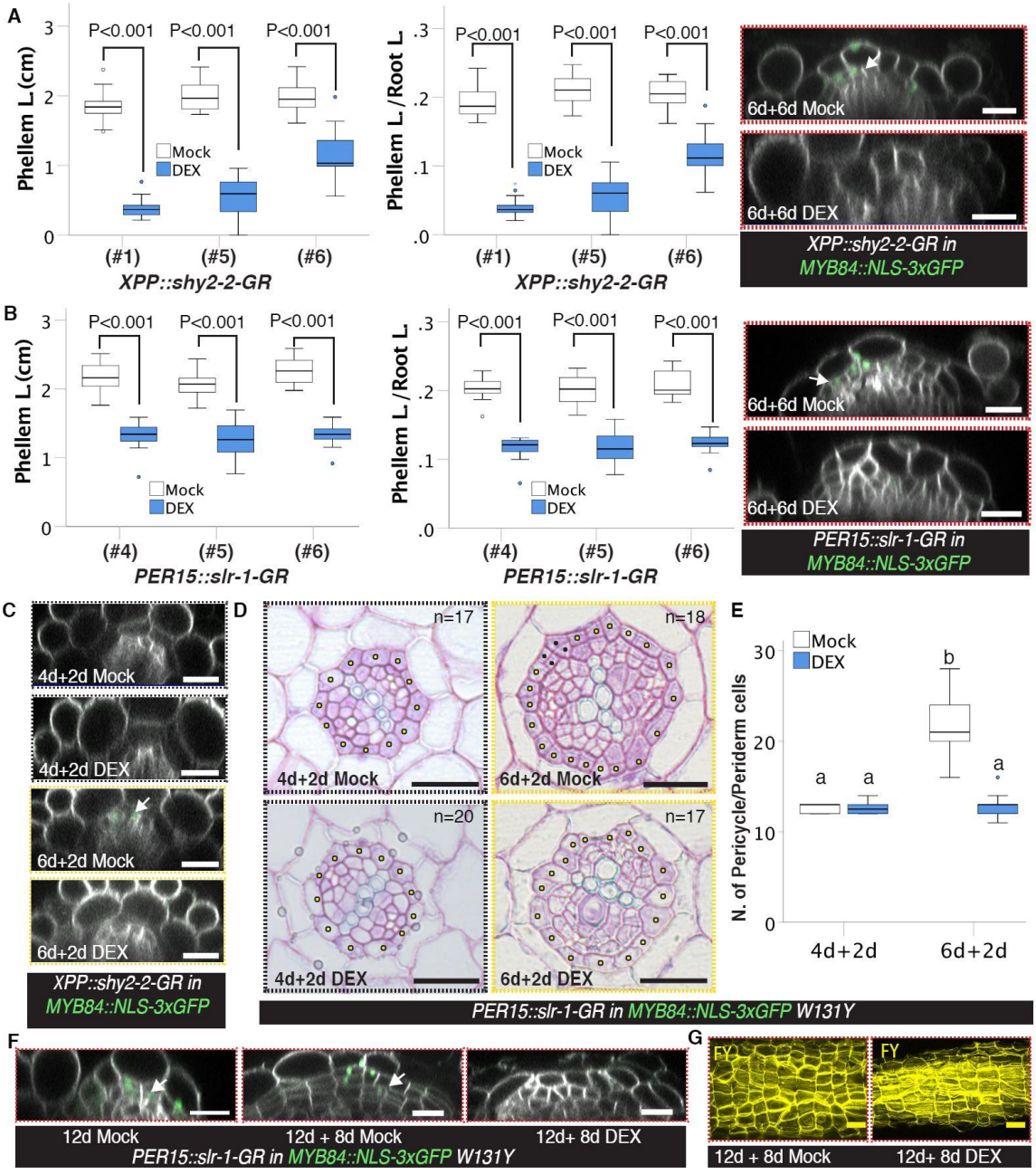
A
Phellem L (cm)
P<0.001
Mock
DEX
(#1)
(#5)
(#6)
XPP::shy2-2-GR
Phellem L /Root L
6d+6d Mock
6d+6d DEX
XPP::shy2-2-GR in
MYB84::NLS-3xGFP
B
(#4)
PER15::slr-1-GR
PER15::slr-1-GR in
MYB84::NLS-3xGFP
C
4d+2d Mock
4d+2d DEX
6d+2d Mock
6d+2d DEX
XPP::shy2-2-GR in
MYB84::NLS-3xGFP
D
n=17
n=18
n=20
n=17
4d+2d Mock
6d+2d Mock
4d+2d DEX
6d+2d DEX
PER15::slr-1-GR in MYB84::NLS-3xGFP W131Y
E
N. of Pericycle/Periderm cells
a
b
4d+2d
6d+2d
F
12d Mock
12d + 8d Mock
12d+ 8d DEX
PER15::slr-1-GR in MYB84::NLS-3xGFP W131Y
G
FY
12d + 8d Mock
12d+ 8d DEX

Figure S2. Auxin signaling is required for phellogen establishment and maintenance. Related to Figure 1. (A) Quantification of phellem length (left panel) and phellem ratio (middle panel) in 3 independent *XPP::shy2-2-GR (in MYB84::NLS-3xGFP W131Y)* lines. 7-day-old (d-old) plants were treated for 5-d with mock or 10μM DEX. T-test (n =15). Right panels: orthogonal view of Z-stacks of *XPP::shy2-2-GR MYB84::NLS-3xGFP W131Y* (#1) 12-d-old roots (uppermost part of the root). 6-d-old plants were treated for 6-d with mock or 10μM DEX. (B) Quantification of phellem length (left panel) and phellem ratio (middle panel) in 3 independent *PER15::slr-1-GR* (in *MYB84::NLS-3xGFP W131Y*) lines. 7-d-old plants were treated for 5-d with mock or 10μM DEX. T-test (n =15). Right panels: orthogonal view of Z-stacks of *PER15::slr-1-GR MYB84::NLS-3xGFP W131Y* (#4) 12-old roots (uppermost part of the root). 6-d-old plants were treated for 6-d with mock or 10μM DEX. (C) Orthogonal view of Z-stacks of *XPP::shy2-2-GR MYB84::NLS-3xGFP W131Y* (#1) roots at 6 and 8 days (uppermost part of the root). 4-d-old and 6-d-old plants were treated for 48h with mock or 10μM DEX. (D) Cross-sections (plastic embedding) of the upper most part of *PER15::slr-1-GR* (in *MYB84::NLS-3xGFP W131Y*; #1) roots. 4-d-old and 6-d-old were treated for 48h with mock or 10μM DEX. (E) Quantification of the number of pericycle/periderm cells in (D). One-way ANOVA (CI95%, Post-Hoc: Tamhane, n =17-20). (F) Orthogonal view of Z-stacks of *PER15::slr-1-GR MYB84:NLS-3xGFP W131Y* (#4) roots at 12 days (left panel) and 20 days (middle and right panels) (uppermost part of the root). 12-d-old plants were treated for 8-d with mock (middle panel) or 10μM DEX (right panel). (G) 3D reconstruction of Z-stacks of 20-d-old *PER15::slr-1-GR MYB84::NLS-3xGFP W131Y* (#4) roots stained with Fluorol yellow (FY). 12-d-old plants were treated for 8-d with mock (left panel) or 10μM DEX (right panel). White arrows indicate *MYB84* expression in the pericycle/phellogen, yellow dots indicate pericycle cells and black dots periderm cells. Black and white scale bars: 20μm and yellow scale bars: 50μm.

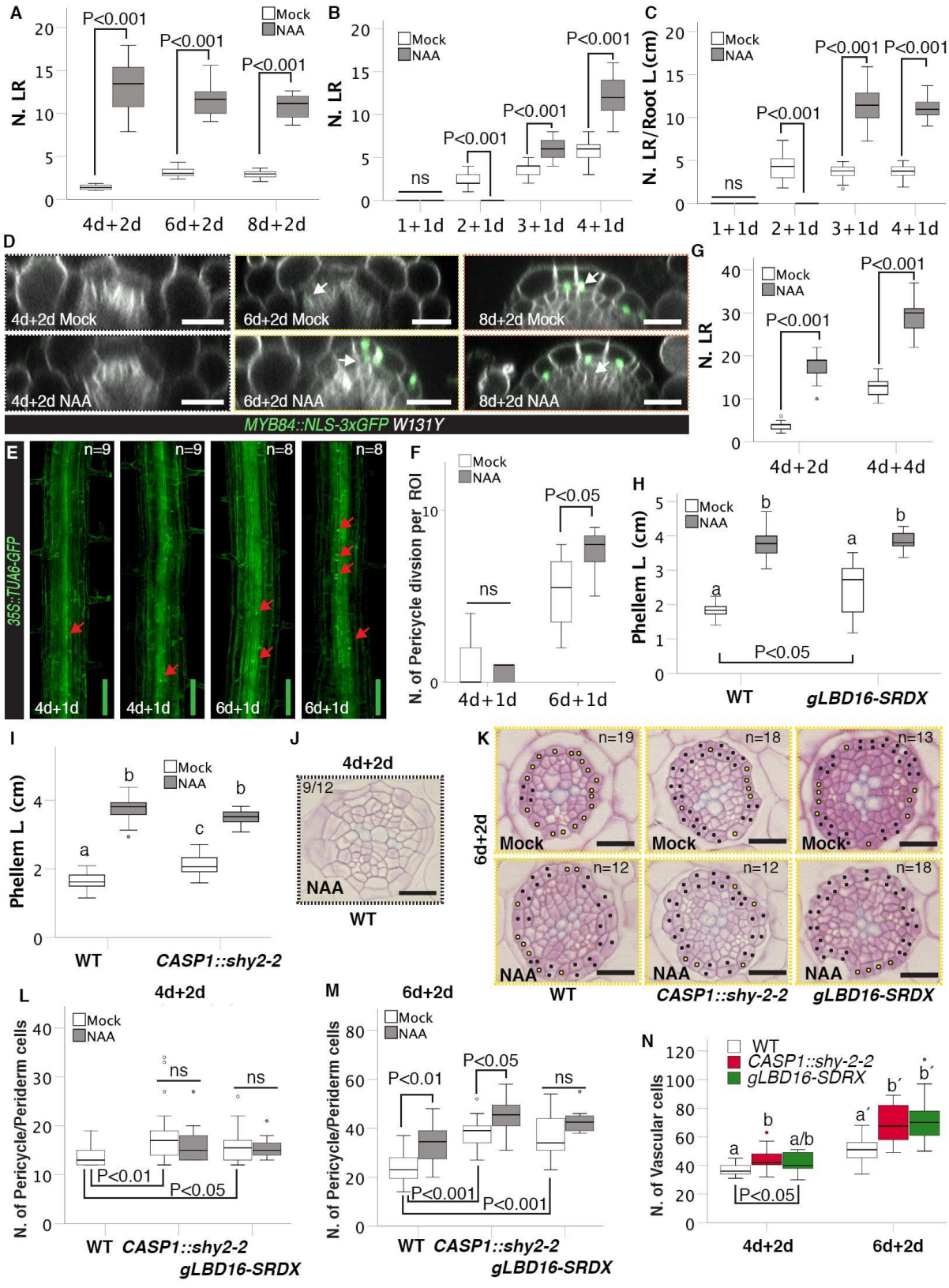
A
N. LR
Mock
NAA
P<0.001
4d+2d
6d+2d
8d+2d
B
N. LR
ns
P<0.001
1+1d
2+1d
3+1d
4+1d
C
N. LR/Root L (cm)
D
4d+2d Mock
6d+2d Mock
8d+2d Mock
4d+2d NAA
6d+2d NAA
8d+2d NAA
MYB84::NLS-3xGFP W131Y
G
N. LR
4d+4d
E
35S::TUA6-GFP
n=9
n=8
4d+1d
6d+1d
F
N. of Pericycle divsion per ROI
P<0.05
H
Phellem L (cm)
WT
gLBD16-SRDX
I
CASP1::shy2-2
J
4d+2d
9/12
K
6d+2d
n=19
n=18
n=13
n=12
CASP1::shy-2-2
L
N. of Pericycle/Periderm cells
M
6d+2d
N
N. of Vascular cells
CASP1::shy2-2
gLBD16-SRDX

Figure S3. Auxin is not sufficient to trigger periderm formation. Related to Figure 2. (A) Quantification of lateral root numbers in WT (*MYB84::NLS-3xGFP W131Y*) roots. 4-day-old (d-old), 6-d-old and 8d-old plants were treated for 48h with mock or 1μM NAA. T-test (n =14-15). (B-C) Quantification of lateral root number and lateral root density in WT roots. 1-d-old, 2-d-old, 3-d-old and 4-d-old plants were treated for 24h with mock or 1μM NAA. T-test (ns: not significant, n =15). (D) Orthogonal view of Z-stacks of *MYB84::NLS-3xGFP W131Y* roots (uppermost part of the root). 4-d-old, 6-d-old and 8d-old plants were treated for 48h with mock or 1μM NAA. (E) 3D reconstructions of Z-stacks of *35S::TUA6-GFP* roots. 4-d-old, 6-d-old plants were treated for 24h with mock or 1μM NAA. Red arrows indicate cell divisions in the pericycle. (F) Quantification of number of pericycle cell divisions in the experiment presented in (E) T -test (ns: not significant, n =8-9). (G) Quantification of lateral root number in WT roots. 4-d-old plants were treated for 96h with mock or 1μM NAA. T-test (n =15). (H) Quantification of phellem length in WT and *gLBD16-SRDX* roots. 7-d-old plants were treated for 5-d with mock or 1μM NAA. One-way ANOVA (CI95%, Post-Hoc: Tamhane, n =15). (I) Quantification of phellem length in WT and *CASP1::shy2-2* roots. 7-d-old plants were treated for 5-d with mock or 1μM NAA. One-way ANOVA (CI95%, Post-Hoc: Bonferroni, n =14-15). (J) Panel relative to Figure 2L**.** cross-section of a 4-d-old WT root treated for 48h with NAA, showing that in the majority of the sections LR primordia are formed. (K) Cross-sections (plastic embedding) of the upper most part of 8-d-old WT, *CASP1::shy2-2* and *gLBD16-SRDX* roots. 6-d-old plants were treated for 2-d with mock or 1μM NAA. (L) Quantification of number of pericycle/periderm cells in the experiment presented in Figure 2L. T-test (ns: not significant, n =8-20). As WT roots when treated with IAA keep forming LR, it is rare (3/12) to have sections without LRs, thus we did not quantify pericycle cells for the WT auxin treated sample. (M) Quantification of number of pericycle/periderm cells in the experiment presented in (K). T-test (ns: not significant, n =12-19). (N) Quantification of vascular cells in the experiment presented in Figure 2L and 2K. One-way ANOVA (CI95%, Post-Hoc: Tamhane, n = 12-20) and T-Test. Black and white scale bars: 20μm. Green scale bars: 100μm. White arrows indicate *MYB84* expression in the pericycle/phellogen, yellow dots indicate pericycle cells and black dots periderm cells.

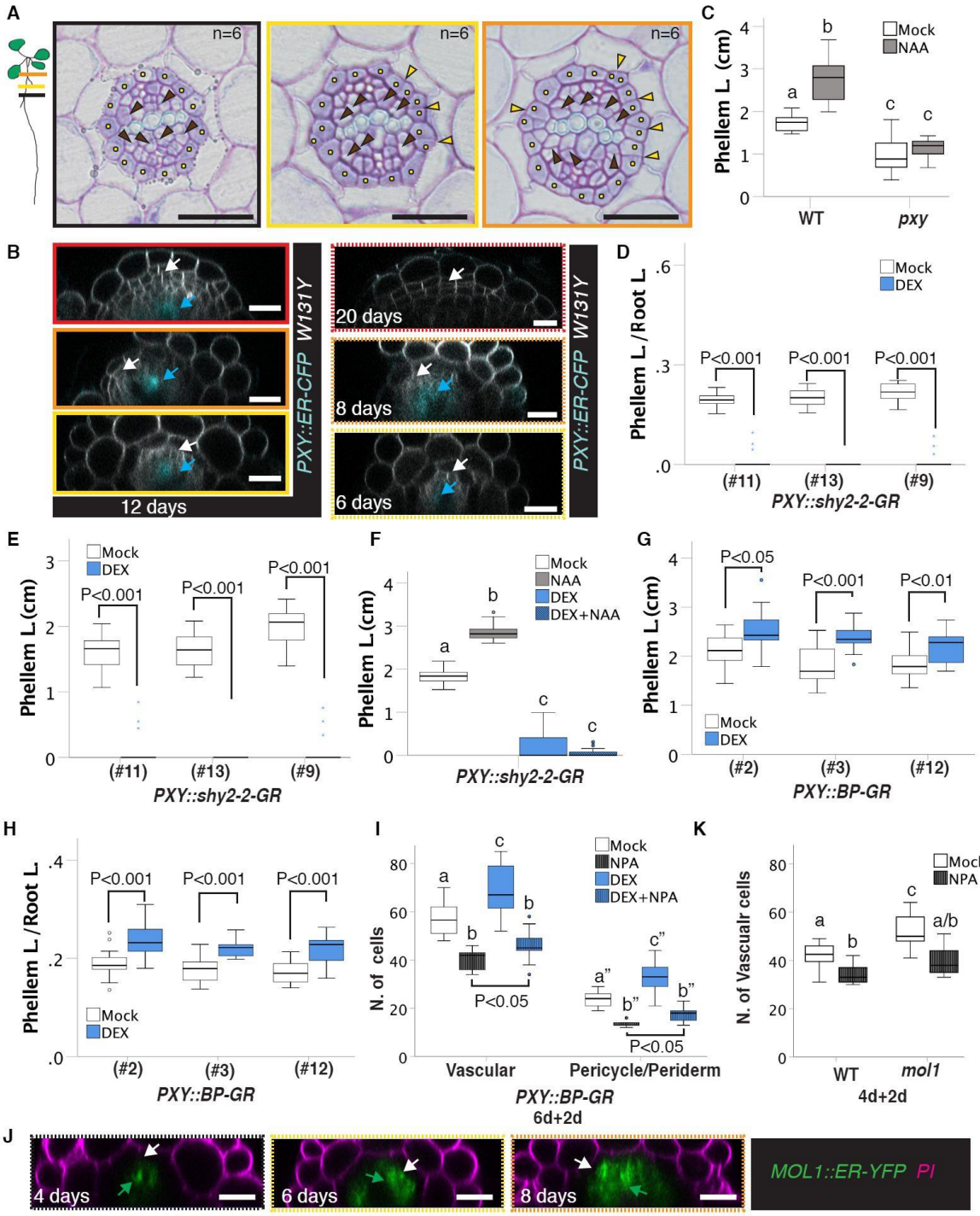
A
n=6
n=6
n=6
C
Phellem L (cm)
Mock
NAA
a
b
c
c
WT
pxy
B
PXY::ER-CFP W131Y
12 days
20 days
8 days
6 days
D
Phellem L /Root L
Mock
DEX
P<0.001
P<0.001
P<0.001
(#11)
(#13)
(#9)
PXY::shy2-2-GR
E
Phellem L (cm)
Mock
DEX
P<0.001
P<0.001
P<0.001
(#11)
(#13)
(#9)
PXY::shy2-2-GR
F
Phellem L (cm)
Mock
NAA
DEX
DEX+NAA
PXY::shy2-2-GR
G
Phellem L (cm)
P<0.05
P<0.001
P<0.01
Mock
DEX
(#2)
(#3)
(#12)
PXY::BP-GR
H
Phellem L /Root L
P<0.001
P<0.001
P<0.001
Mock
DEX
(#2)
(#3)
(#12)
PXY::BP-GR
I
N. of cells
Mock
NPA
DEX
DEX+NPA
P<0.05
P<0.05
Vascular
Pericycle/Periderm
PXY::BP-GR
6d+2d
K
N. of Vascualr cells
Mock
NPA
a/b
WT
mol1
4d+2d
J
4 days
6 days
8 days
MOL1::ER-YFP PI

Figure S4. A functional vascular cambium is required for periderm development. Related to Figure 3. (A) Secondary growth progression. Cross-sections of an 8-day-old (d-old) WT root at the positions indicated in the sketch (plastic embedding). (B) Left panels: orthogonal views of Z-stacks of *PXY::ER-CFP W131Y* 12-d-old roots at the positions corresponding to stage 1 (lower panel), stage 3/4 (middle panel) and stage 5 (upper panel) of periderm development. Right panels: orthogonal view of Z-stacks of *PXY::ER-CFP W131Y* roots at 6, 8 and 20 days (uppermost part of the root). Blue arrows indicate *PXY* expression in the pro-cambium/cambium, white arrows indicate the pericycle/periderm. (C) Quantification of phellem length in 12-d-old WT and *pxy* roots. 7-d-old plants were treated for 5-d with mock or 1μM NAA. One-way ANOVA (CI95%, Post-Hoc: Tamhane, n =15). (D-E) Quantification of phellem length and phellem ratio in 3 independent *PXY::shy2-2-GR* lines. 7-d-old plants were treated for 5-d with mock or 10μM DEX. T-test (n =15). (F) Quantification of phellem length in 12-d-old *PXY::shy2-2-GR* (#9*)* roots. 7-d-old plants were treated for 5-d with mock, 1μM NAA, 10μM DEX or 10μM DEX+1μM NAA. One-way ANOVA (CI95%, Post-Hoc: Tamhane, n =15). (G-H) Quantification of phellem length and phellem ratio in 3 independent *PXY::BP-GR* lines. 7-d-old plants were treated for 5-d with mock or 10μM DEX. T-test (n =15). (I) Quantification of number of vascular and pericycle/periderm cells in the experiment presented in Figure 3G. One-way ANOVA (CI95%, Post-Hoc: Tamhane, n =10-12) and T-test. (J) Orthogonal view of Z-stacks of *MOL1::ER-YFP* roots at 4, 6, and 8 days (uppermost part of the root). Green arrows indicate *MOL1* expression in the phloem, white arrows indicate the pericycle/periderm. (K) Quantification of number of vascular cells in the experiment presented in Figure 3H**.** One-way ANOVA (CI95%, Post-Hoc: Bonferroni, n =13-16). Brown arrowheads indicate pro-cambium divisions and yellow arrowheads indicate pericycle cell divisions. Yellow dots indicate pericycle cells. Black and white scale bars: 20μm.

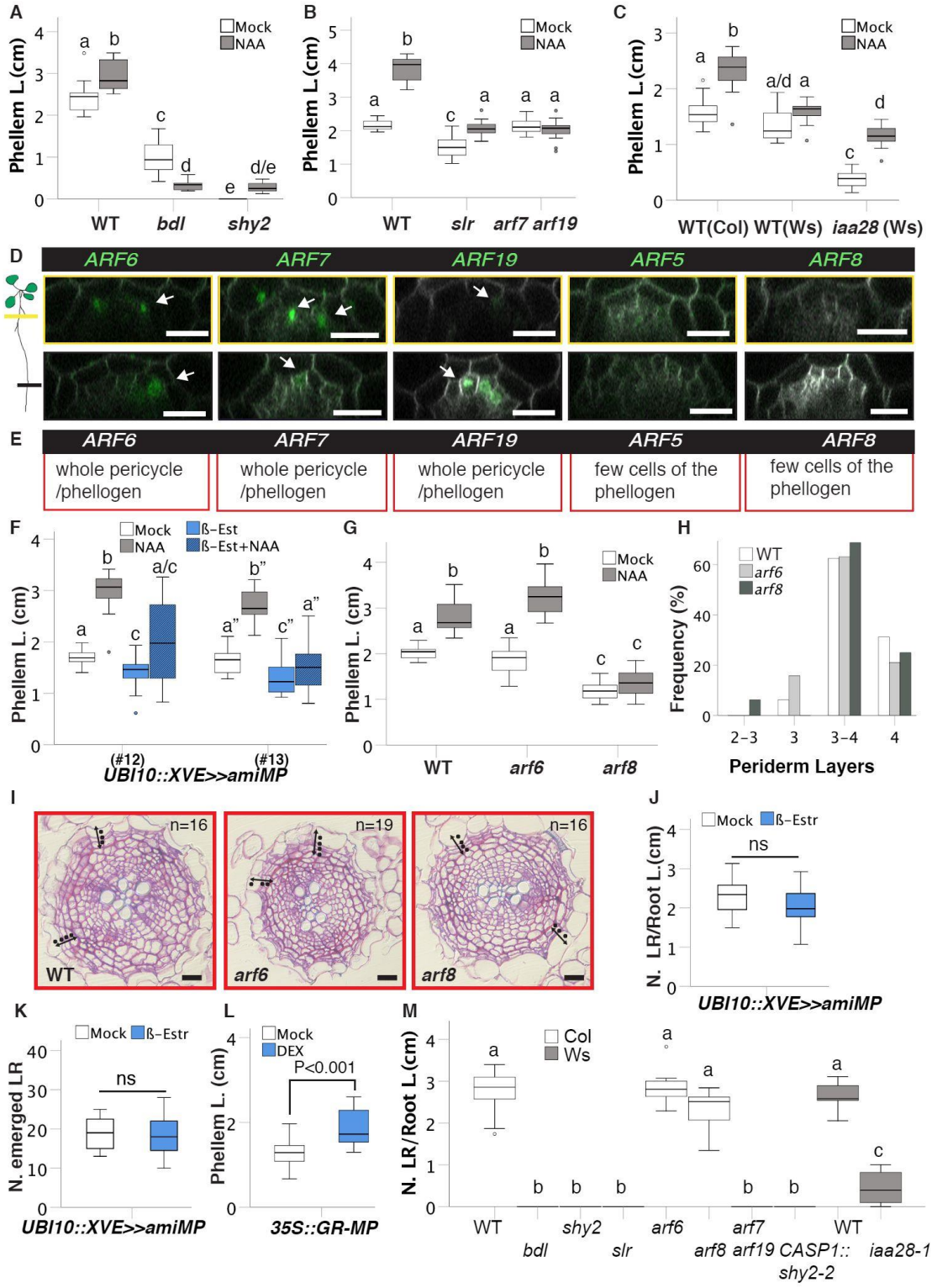
A
Phellem L.(cm)
Mock
NAA
WT
bdl
shy2
B
WT
slr
arf7 arf19
C
WT(Col) WT(Ws)
iaa28 (Ws)
D
ARF6
ARF7
ARF19
ARF5
ARF8
E
whole pericycle /phellogen
few cells of the phellogen
F
ß-Est
ß-Est+NAA
(#12)
(#13)
UBI10::XVE>>amiMP
G
WT
arf6
arf8
H
Frequency (%)
Periderm Layers
I
n=16
n=19
J
N. LR/Root L.(cm)
ns
K
N. emerged LR
L
DEX
P<0.001
35S::GR-MP
M
Col
Ws
N. LR/Root L.(cm)
bdl
shy2
slr
arf6
arf7
arf8
arf19
CASP1:: shy2-2
iaa28-1

Figure S5. Distinct auxin signaling components regulate periderm and LR development. Related to Figure 4 and Figure 5. (A-B) Quantification of phellem length in 12-d-old (d-old) WT, *bdl-2*, *shy2-201, slr-1* and *arf7-1 arf19-1* roots. 7-d-old plants were treated for 5-d with mock or 1μM NAA. One-way ANOVA (CI95%, Post-Hoc: Tamhane, n =8-15). (C) Quantification of phellem length in 10-d-old WT (Ws and Col) and *iaa28-1*(Ws) roots. 7-d-old plants were treated for 3-d with mock or 1μM NAA. One-way ANOVA (CI95%, Post-Hoc: Tamhane, n =14). (D) Orthogonal view of Z-stacks of *ARFs::NLS-3xGFP W131Y* 7d-old root at the positions corresponding to lateral root primordia (black lower panels) and periderm stage 1 (yellow upper panels). (E) Table summarizing ARFs expression pattern. (F) Quantification of phellem length in *UBI10::XVE>>amiMP* lines. 7-d-old plants were treated for 5-d with mock, 1μM NAA, 5μM β-Estradiol (β-Estr) or 5μM β-Estradiol+1μM NAA. One-way ANOVA (CI95%, Post-Hoc: Tamhane, n =12-14). (G) Quantification of phellem ratio in 12-d-old WT, *arf6-1* and *arf8-2* roots. 7-d-old plants were treated for 5-d with mock or 1μM NAA. One-way ANOVA (CI95%, Post-Hoc: Tamhane, n = 15-16). (H) Quantification of the number of periderm layers of the experiment showed in (I). (I) Cross-sections of the upper most part of 12-d-old roots (plastic embedding): WT (left panel), *arf6-1* (middle panel) and *arf8-2* (right panel). (J-K) Quantification of lateral root density and emerged lateral root number in 12-day-old *UBI10::XVE>>amiMP* roots. 7-d-old plants were treated for 5-d with mock or 5μM β-Estradiol (β-Estr). T-test (ns: not significant, n =15). (L) Quantification of phellem ratio in 12-d-old *35S::GR-MP* roots. 7-d-old plants were treated for 5-d with mock or 10μM DEX. T-test (n =15). (M) Quantification of lateral root density in 12-d-old WT (Col), *bdl-2*, *shy2-201*, *slr-1, arf6-2,arf8-2,arf7-1arf19-1, CASP1:shy2-2,* WT (Ws) and *iaa28-1* roots. One-way ANOVA (CI95%, Post-Hoc: Tamhane, n =14-15). White arrows indicate the pericycle, double black arrows indicate periderm extension and black dots periderm layers. Black and white scale bars: 20μm.

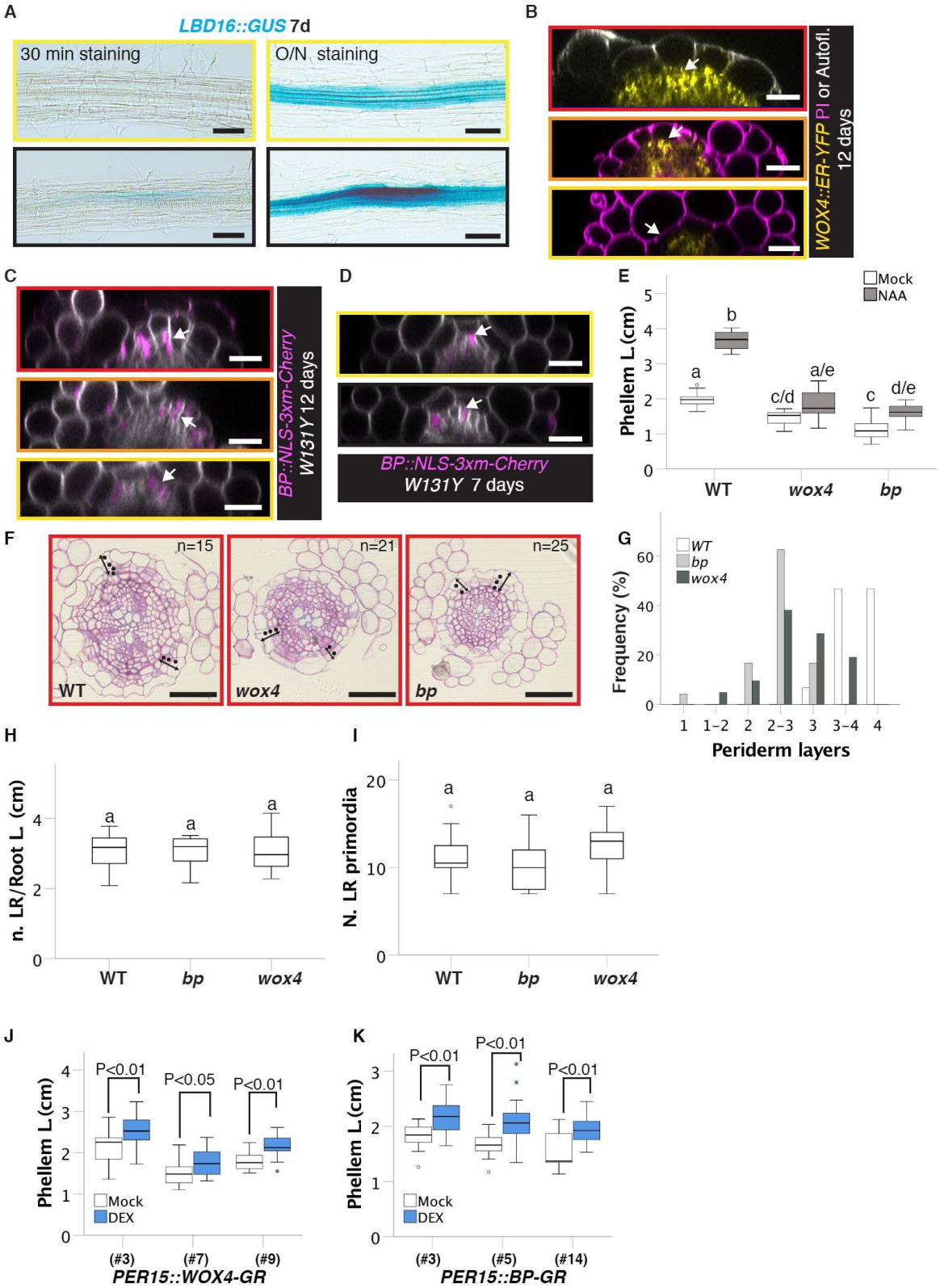
A
LBD16::GUS 7d
30 min staining
O/N staining
B
WOX4::ER-YFP PI or Autofl.
12 days
C
BP::NLS-3xm-Cherry
W131Y 12 days
D
BP::NLS-3xm-Cherry
W131Y 7 days
E
Mock
NAA
Phellem L.(cm)
a
b
c/d
a/e
c
d/e
WT
wox4
bp
F
n=15
n=21
n=25
WT
wox4
bp
G
WT
bp
wox4
Frequency (%)
Periderm layers
H
n. LR/Root L. (cm)
I
N. LR primordia
J
P<0.01
P<0.05
P<0.01
Phellem L.(cm)
Mock
DEX
(#3)
(#7)
(#9)
PER15::WOX4-GR
K
P<0.01
P<0.01
P<0.01
Phellem L.(cm)
Mock
DEX
(#3)
(#5)
(#14)
PER15::BP-GR

Figure S6. WOX4 and BP promote periderm development downstream auxin. Related to Figure 6. (A) Images of GUS staining of 7-day-old (d-old) *LBD16::GUS* roots at the positions corresponding to lateral root primordia (black lower panels) and periderm stage 1 (yellow upper panels). (B) Orthogonal view of Z-stacks of *WOX4::ER-YFP* 12-d-old roots at the positions corresponding to stage 1 (lower panel), stage 3/4 (middle panel) and stage 5 (upper panel) of periderm development. (C) Orthogonal view of Z-stacks of *BP/KNAT1::NLS-3xm-Cherry W131Y* 12-d-old roots the at the positions corresponding to stage 1 (lower panel), stage 3/4 (middle panel) and stage 5 (upper panel) of periderm development. (D) Orthogonal view of Z-stacks of a *BP/KNAT1::NLS-3xm-Cherry W131Y* 7d-old root at the positions corresponding to lateral root primordia (black lower panel) and periderm stage 1 (yellow upper panel). (E) Quantification of phellem length in 12-d-old WT, *wox4-1* and *bp-9* roots. 7-d-old plants were treated for 5-d with mock or 1μM NAA. One-way ANOVA (CI95%, Post-Hoc: Bonferroni, n =15-16). (F) Cross-sections of the upper most part of 12-d-old roots (plastic embedding): WT (left panel), *wox4-1* (middle panel), *bp-9* (right panel). (G) Quantification of the number of periderm layers in WT, *wox4-1* and *bp-9* of the experiment showed in (F). (H-I) Quantification of lateral root density and lateral root primordium number in 7-d-old roots of WT, *wox4-1* and *bp-9*. One-way ANOVA (CI95%, Post-Hoc: Bonferroni, n =16). (J) Quantification of phellem length in 3 independent *PER15::WOX4-GR* (in *W131Y*) *T2* lines. 7-d-old plants were treated for 5-d with mock or 10μM DEX. T-test (n =14-16). (K) Quantification of phellem length in 3 independent *PER15::BP-GR* lines. 7-d-old plants were treated for 5-d with mock or 10μM DEX. T-test (n =14-15). Double black arrows indicate periderm extension and black dots periderm layers. White arrows indicate the phellogen/ pericycle. Black scale bars: 50μm and white scale bars: 20μm.

Supplemental References.

S1. Lampropoulos, A., Sutikovic, Z., Wenzl, C., Maegele, I., Lohmann, J.U., and Forner, J. (2013). GreenGate - A Novel, Versatile, and Efficient Cloning System for Plant Transgenesis. PLoS ONE *8*, e83043.

S2. Suer, S., Agusti, J., Sanchez, P., Schwarz, M., and Greb, T. (2011). WOX4 Imparts Auxin Responsiveness to Cambium Cells in Arabidopsis. Plant Cell *23*, 3247-3259.

S3. Schurholz, A.K., Lopez-Salmeron, V., Li, Z., Forner, J., Wenzl, C., Gaillochet, C., Augustin, S., Barro, A.V., Fuchs, M., Gebert, M., et al. (2018). A Comprehensive Toolkit for Inducible, Cell Type-Specific Gene Expression in Arabidopsis. Plant Physiol. *178*, 40-53.

S4. Ramakrishna, P., Ruiz Duarte, P., Rance, G.A., Schubert, M., Vordermaier, V., Vu, L.D., Murphy, E., Vilches Barro, A., Swarup, K., Moirangthem, K., et al. (2019). EXPANSIN A1-mediated radial swelling of pericycle cells positions anticlinal cell divisions during lateral root initiation. Proc. Natl. Acad. Sci. U.S.A. *116*, 8597-8602.

S5. Vilches Barro, A., Stockle, D., Thellmann, M., Ruiz-Duarte, P., Bald, L., Louveaux, M., von Born, P., Denninger, P., Goh, T., Fukaki, H., et al. (2019). Cytoskeleton Dynamics Are Necessary for Early Events of Lateral Root Initiation in Arabidopsis. Curr. Biol. *29*, 2443-2454.e2445.

5.2 Draft manuscript 2:

ERECTA-AINTEGUMENTA Module Directs Secondary Meristems Differentiation in *Arabidopsis*

W.X. and L.R. planned and conducted the majority of the experiments. W.X. acquired the confocal images. W.X. did the molecular cloning and generated the plant lines. D.M. and W.X. conducted the Fluorol Yellow (FY) experiments. W.X., and X.D. conduct the plant embedding. W.X. measured root area. W.X. conducted the phellem ratio experiments. W.X. generated the library for RNA sequencing/qPCR experiments with the help of D.M. W.X. and L.R. analysed the sequencing data. D.R. helped in generating the T3 lines and embedding the roots. W.X. and L.R. wrote the paper.

Title: ERECTA-AINTEGUMENTA module directs secondary meristems differentiation in *Arabidopsis*

Running title: How auxin output specificity is achieved in the vascular cambium and cork cambium cell fate

Authors: Wei Xiao[1, *], David Molina[1], Xudong Zhang[1], Dagmar Ripper[1], Laura Ragni[1,2, *]

[1] ZMBP-Center for Plant Molecular Biology, University of Tübingen, Auf der Morgenstelle 32, D-72076 Tübingen, Germany.

[2] Lead Contact

[*] Corresponding author: laura.ragni@zmbp.uni.tuebingen.de, wei.xiao@zmbp.uni.tuebingen.de

Wei Xiao: 0000-0002-6392-5866; wei.xiao@zmbp.uni-tuebingen.de
David Molina: 0000-0001-5858-3331; david.molina@zmbp.uni-tuebingen.de
Xudong Zhang: xudong.zhang@zmbp.uni-tuebingen.de
Dagmar Ripper: dagmar.ripper@zmbp.uni-tuebingen.de
Laura Ragni: 0000-0002-3651-8966; laura.ragni@zmbp.uni-tuebngen.de

Keywords: vascular cambium, cork cambium, auxin, phloem, xylem.

Highlights:

- Auxin maintains cork cambium identity and directs cork cambium differentiation.
- A compensation mechanism exists between secondary meristems against unsatisfactory environment.
- ERECTA-ANT module promotes vascular cambium proliferation and phloem differentiation.
- The balances of the phloem and xylem proportion is required for secondary thickening.

Summary

Secondary growth, the increase in radial growth (girth) of a plant, represents a key structural novelty that characterizes the bulk of land plant diversity and shapes the world as we know today. The secondary meristems (cork cambium and vascular cambium) are divided bilaterally and contributes to secondary growth. However, how secondary meristems coordinate their activity and how these bilateral meristems direct differentiation are still unknown. Here, using the *Arabidopsis* root as a model, we show that auxin plays an essential role in maintaining cork cambium identity and direct cork cambium differentiation. Interestingly, specifically hindering auxin signalling in the cork cambium, ectopically enhances also the activity of the vascular cambium, suggesting a compensation mechanism balancing secondary growth output. We further show that *ER* (*ERECTA*) receptor kinase and *ANT* (*AINTEGUMENTA*) transcriptional factor that act as auxin-mediated downstream signalling regulators, promote vascular cambium proliferation and direct differentiation from vascular cambium to phloem. Cork cambium and vascular cambium specific induction of *ER*, *ANT* and *ANT-SRDX* expression revealed overlapping and distinct downstream targets paving the way for understanding stem cell specificity in secondary growth. Altogether, our results decipher the auxin-mediated regulatory hubs in the vascular cambium and cork cambium, providing the basis for understanding how auxin directs differentiation of bilateral meristems.

Introduction

Secondary growth, the increase in girth of plant organs contributed to the large success of seed plants, providing efficient long-distance transportation of water, nutrient, salts, and photo-assimilates. Secondary growth is largely determined by the phytohormones induced proliferation or differentiation of stem cells/meristems, which are the vascular cambium and the cork cambium (phellogen). Particularly, the first cork cambium is initiated and differentiated from pericycle cells whereas the first vascular cambium generates from vascular cambium and pro-cambia (Wunderling *et al.*, 2018; Smetana *et al.*, 2019; Zhang *et al.*, 2019). These two bilateral meristems produce inward xylem and phelloderm and outward phloem and phellem/cork, respectively. Secondary vascular (consists of secondary xylem, vascular cambium, and phloem) facilitates the transportation of organic and/or inorganic nutrients throughout the plant vasculature,

while periderm (consists of phelloderm, cork cambium and cork) as a barrier protects plants from abiotic and biotic stresses (Barra-Jimenez & Ragni, 2017; Wunderling *et al.*, 2018; Ragni & Greb, 2018; Zhang *et al.*, 2019; Campilho *et al.*, 2020).

Briefly, an elaborate corelation between vascular cambium and the cork cambium has been demonstrated: the establishment of the vascular cambium is a required for auxin-activated periderm initiation, and precocious initiation of the vascular cambium is sufficient to trigger periderm development (Xiao *et al.*, 2020). In *Arabidopsis*, auxin-induced regulators MONOPTEROS (MP) is repressed by BDL (BODENLOS), and activates in secondary growth in plant. Moreover, MP works as a center to activate *BREVIPEDICELLUS* (*BP*), *WUSCHEL-RELATED HOMEOBOX 4* (*WOX4*), *WOX14*, *HD-ZIPs*, and *PHLOEM INTERCALATED WITH XYLEM*/*TDIF RECEPTOR* (*PXY*/*TDR*), promote proliferation on vascular cambium and xylem development (Etchells *et al.*, 2013; Barra-Jimenez & Ragni, 2017; Wunderling *et al.*, 2018; Ragni & Greb, 2018; Smetana *et al.*, 2019; Zhang *et al.*, 2019; Campilho *et al.*, 2020; Xiao *et al.*, 2020).

Intriguingly, ER (*ERECTA* receptor kinases) and *ANT* (*AINTEGUMENTA*) are the downstream of cytokinin and involved in vascular cambium proliferation or phloem regulation. In *Arabidopsis*, the *ER* gene family contains three paralogues: *ER*, *ER-LIKE1* (*ERL1*), and *ERL2* (Shpak *et al.*, 2004). In the stem, *ER*, *ERL1*, and *ERL2* are involved in cytokinin signalling and regulate phloem expansion (Ragni *et al.*, 2011; Ikematsu *et al.*, 2017; Wang *et al.*, 2019). Interestingly, *ANT* coupled with *CYCD3;1* promotes secondary thickening in roots (Randall *et al.*, 2015). Both *ER* and *ANT* are involved in secondary thickening and phloem regulation; moreover, previous studies mentioned that *ER* and *ANT* are expressed in vascular cambium (Uchida & Tasaka, 2013; Wang *et al.*, 2019; Zhang *et al.*, 2019; Xiao *et al.*, 2020). It is known that conserved phytohormones-centered regulatory networks play a major role in two cambia establishment and maintenance; whereas how phytohormones direct the differentiation of these two cambia is still missing.

In this study, using the *Arabidopsis* root as a model, we showed that auxin activating *BP*, *WOX4*, *ER*, and *ANT*, played an essential role in vascular cambium and cork cambium establishment and maintenance (Zhang *et al.*, 2019; Xiao *et al.*, 2020). We compared auxin responses in both vascular cambium and cork cambium and we found that auxin is the key to maintain cork cambium identity and direct differentiation from cork cambium into phelloderm. Interestingly, specifically hindering auxin signalling in

the cork cambium, had a positive effect on the activity of the vascular cambium, suggesting a compensation mechanism balancing secondary growth output. We further showed that *ER* acted as auxin-mediated downstream signalling regulators activating vascular cambium/cork cambium proliferation and direct its differentiation into phloem/phelloderm. Moreover, we found both *ER* and *ANT* regulate vascular cambium output specificity and influence vascular cambium division. Vascular cambium specific induction of *ANT* repressed xylem cell formation whereas *ANT-SRDX* had a positive effect. Altogether, our results deciphered the auxin-mediated regulatory hubs in the vascular cambium and cork cambium, providing the basis for understanding bilateral meristems specificity in differentiating into different cell types.

Results

Auxin promotes vascular cambium and cork cambium proliferation and directs cork cambium differentiation.

As auxin is involved in many aspects of plant development, including secondary growth in roots, we assessed auxin signalling has a tissue/temporal specific manner in between vascular cambium and cork cambium. To further dissect the role of auxin in non-meristematic tissues (cork and endodermis), and meristematic tissues (cork cambium and vascular cambium), we engineered plants to specifically block auxin signalling in the endodermis and cork with stabilized Aux/IAA variants (Ramakrishna *et al.*, 2019). The *GLYCEROL-3-PHOSPHATE SN-2-ACYLTRANSFERASE 5* (*GPAT5*) promoter is active in the endodermis and cork (Figure S1A-B), *PEROXIDASE15* (*PER15*) promoter is expressed in both cork and cork cambium, and *PXY*/*TDR* is localized in vascular cambium (Xiao *et al.*, 2020). We observed that prolonged induction of *GPAT5::shy2-2-GR*, *XPP::shy2-2-GR* and *PER15::slr-1-GR* resulted to further understand the function of auxin in non-meristematic tissues and meristematic tissues during secondary growth. First, we used *GPAT5::shy2-2-GR* plants to understand auxin's function in non-meristem tissues during secondary growth. In the initiation of secondary growth, blocking transcriptional auxin response at endodermis in *GPAT5::shy2-2-GR* plants doesn't abolish pericycle and pro-cambium division (Figure S2A-B). Next, we observed that the prolonged induction (7-12d or 12-8d dexamethasone (DEX) treatment) in *GPAT5::shy2-2-GR* line shows no affection on root length, phellem length, phellem ratio, secondary growth, and suberin deposition (Figure S1C and Figure S2C-E). It indicates auxin doesn't accumulate in the cork and

endodermis.

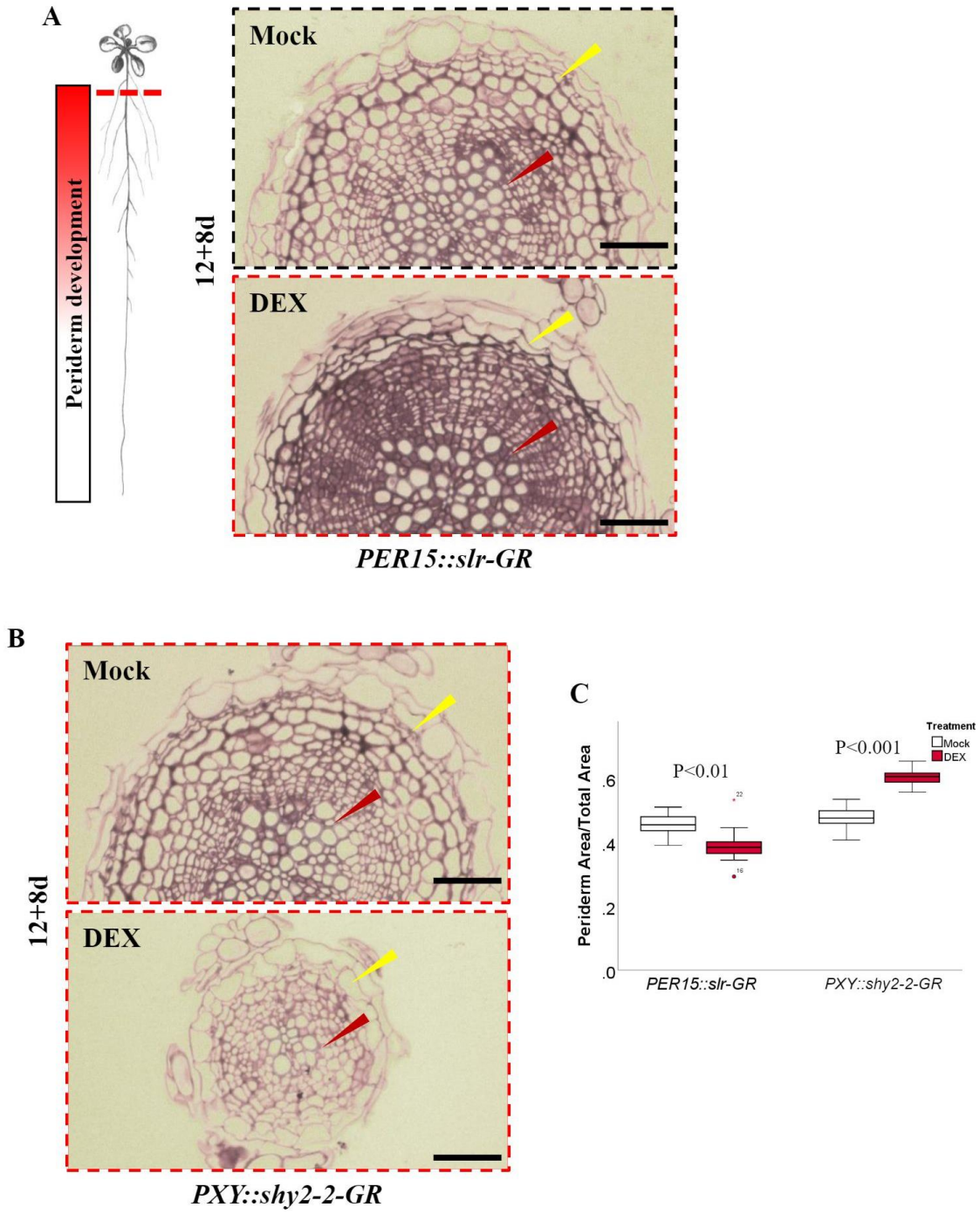

Figure 1. Blocking auxin signalling impairs secondary growth in root.

A, Cross-sections (plastic embedding) of the uppermost part of *PER15::slr-1-GR* (in *MYB84::NLS-3xGFP W131Y*; #1) roots. 12-d-old plants were transferred for 8-d on Mock (upper panels) or 10µM DEX (lower panels) plates. **B,** Cross-sections (plastic embedding) of the uppermost part of *PXY::shy2-2-GR* (in *MYB84::NLS-3xGFP W131Y*) roots. 12-d-old plants were transferred for 8-d on Mock (upper panels) or 10µM DEX (lower panels) plates. **C,**

Quantification of periderm area/total area of the experiment shown in (A-B). T-test (n =12-13). Yellow triangular arrow indicates cork cambium. Red triangular arrow indicates vascular cambium. Black scale bars: 50µm.

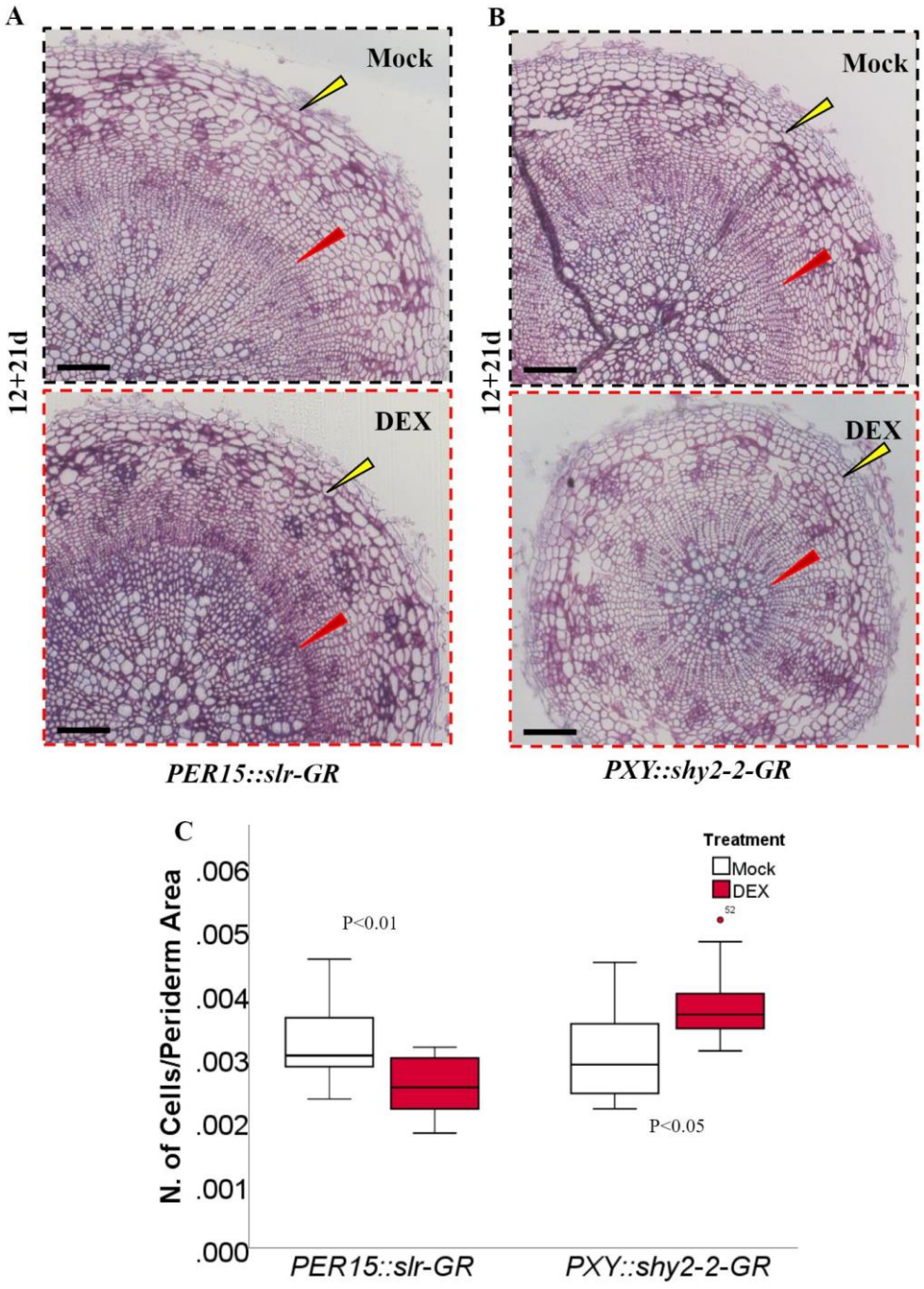

Figure 2. A compensate mechanism on secondary growth between periderm and vascular.

A, Cross-sections (plastic embedding) of the uppermost part of *PER15::slr-1-GR* (in *MYB84::NLS-3xGFP W131Y*; #1) roots. 12-d-old plants were transferred for 21-d on soil, watering with Mock (upper panels) or 10µM DEX (lower panels) water. **B,** Cross-sections

(plastic embedding) of the uppermost part of *PXY::shy2-2-GR* (in *MYB84::NLS-3xGFP W131Y*) roots. 12-d-old plants were transferred for 21-d on soil, watering with Mock (upper panels) or 10μM DEX (lower panels) water. **C,** Quantification of peridermal cell number/periderm area of the experiment shown in (A-B). T-test (n =10-13). Yellow triangular arrow indicates cork cambium. Red triangular arrow indicates vascular cambium. Black scale bars: 100μm.

To further validate how the auxin regulates cork cambium and vascular cambium proliferation and differentiation, we designed experiments with prolonged induction (7+5d and 12+8 DEX treatment) in *PER15::slr-GR* and *PXY::shy2-2-GR* plants. Blocking auxin signalling in cork cambium shows an abolishment on periderm development (Figure 1A and S3B); while impairing auxin signalling in vascular cambium shows a strong reduction in the girth of the roots, leading a delay on secondary growth (Figure 1B and S3C) (Xiao *et al.*, 2020). Furthermore, a prolonged DEX induction (8 days) in the *PER15::slr-GR* resulted in a blenching on cork cambium (Figure S3D). Consistently, blocking auxin signalling in cork cambium enlarged the cork cambium cell size and cork cambium was differentiated into the cork-like cells with suberin deposition. Interestingly, blocking auxin signalling in vascular cambium only delayed the progression of secondary growth, while blocking auxin signalling in cork cambium destroyed the cork cambium, which indicated different functions in auxin between these two cambia. These results highlighted the importance of auxin for secondary growth and maintaining cork cambium identity in meristematic tissues.

To further dissect secondary growth in roots, we quantify total area, vascular area, xylem area, phloem area (consists of phloem and vascular cambium), and periderm area on root plastic cross-section (Figure S3A). With this measurement approach, we deeply dissected the contribution of vascular cambium and cork cambium during secondary growth. A prolonged DEX induction (8 days) in the *PER15::slr-GR* line shows no difference in total area and periderm area compared with Mock, while a strong reduction on both total area, vascular area, and periderm area compared with Mock in *PXY::shy2-2-GR* plants (Figure S4A). Hindering the transcriptional auxin response in vascular cambium increases the percentage of periderm area in total area (Figure 1C), showing a rescue strategy was occurring when the plant is under stress. We analysed whether secondary growth is influenced by auxin and understand the interconnection between vascular cambium and cork cambium after premature bolting. To understand the functions of auxin in a long-treated period, we designed to transfer the plants into

the soil. First of all, we sowed the seeds on plates, and we transferred the seedling from plates to soils on 12-d. Before plants were transferred to soil, we collected the samples of *PER15::slr-GR* and *PXY::shy2-2-GR* root, shown a well-established cork cambium and vascular cambium (Figure S4B). After the transferring process, we performed a prolonged DEX water induction (21 days) on *PER15::slr-GR* and *PXY::shy2-2-GR* plants. Compared with Mock treatment, hindering auxin signalling shows a strong reduction on secondary growth in both *PER15::slr-GR* and *PXY::shy2-2-GR* root cross-section (Figure 2A-B). In *PER15::slr-GR* plants, blocking auxin signalling on cork cambium caused the xylem fiber deposition on vascular cambium (Figure 2A). It indicated the unexpected stresses on the root, causing the plant to reinforce the root structure by xylem fiber deposition. Furthermore, the plant sensed a malfunction in one of the cambia and activated another cambium to recover from unsatisfactory growth condition, while it can't fully rescue the plant, causing a reduction in secondary growth in the root (Figure 2C and S4C). Moreover, blocking the transcriptional auxin response in cork cambium shows an inhibition on peridermal cell proliferation, while blocking the transcriptional auxin response in vascular cambium increases peridermal cell numbers (Figure 2C). Altogether, these results indicate a possible compensation mechanism upon these two cambia, which means plants reinforce and are against the unsatisfactory situation. Moreover, auxin direct cork cambium cell fate, differentiating into phelloderm.

Auxin signalling within the vascular cambium and cork cambium shares a similar regulatory network.

To identify the potential cambial regulators involved in the regulation of the secondary growth in both cambia, we performed RNA sequencing (RNA-seq) of 24 h Mock/DEX-treated on *PER15::slr-GR* and *PXY::shy2-2-GR* roots. In RNA-seq data, we identified 371 genes were downregulated in both *PER15::slr-GR* and *PXY::shy2-2-GR* roots ($log2FC > 0.5$; $padj < 0.05$), while 292 genes upregulated ($log2FC > 0.5$; $padj < 0.05$) (Figure 3A). Anthocyanin-containing compound biosynthesis process, syncytium formation, and cell cycle process were the most enriched pathways among the genes expressed in the *PER15::slr-GR* plants; however, cell cycle process, microtubule-based process and nuclear division were the most enriched pathways among the genes expressed in the *PXY::shy2-2-GR* roots, supporting their distinct cellular activities (Figure S5C-D). Next, we identified some regulators which have been found to be

required for cambial meristematic activity in our dataset (Figure 3B) (Zhang *et al.*, 2019; Xiao *et al.*, 2020). Interestingly, among these candidates, we selected interested candidates like *BP*, *WOX4*, *ER* and, *ANT* for the next step in our RNA-seq datasets (Figure 3B). Therefore, we decided to understand how these 4 auxin-induced regulators work and corporate in secondary growth, unveiling the correlation between vascular cambium and cork cambium.

A

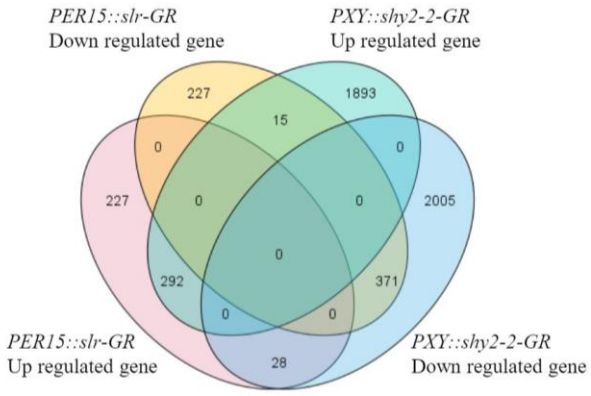

B

Gene	*PER15::slr-GR* Log_2FC	*PXY::shy2-2-GR* LOG_2FC
BP	-0.65	-0.8
WOX4	-1.39	-1.48
ANT	-1.16	-3.49
ER	-1.3	-1.21
PLT2	-0.96484	-0.86221
PIN4	-1.05117	-0.53448
WOX14	-0.57546	-0.51691

Figure 3. Differentially expressed genes among different treatment.

A, Venn diagram shows the overlap of genes up regulated or genes down regulated in *PER15::slr-1-GR* and *PXY::shy2-2-GR* in Mock or 10μM DEX treatment. **B,** Expression heatmap showing expression patterns.

***ERECTA* receptor kinase promotes secondary growth and xylem formation.**

Based on RNA seq data, we hypothesized that ER positively regulates cork cambium and vascular cambium activities, especially on differentiation and proliferation. To answer this, we first determined the expression pattern of *ER* during secondary growth. By mean of fluorescent reporters, we observed the activity of *ER* promoters at all stages of secondary growth (Wang *et al.*, 2019; Uchida & Tasaka, 2013) (Figure 4A). To further discover the role of *ER* in secondary growth, thus, we inspected *ER* loss of function mutant for secondary growth phenotypes. Moreover, we noticed that *ER* is involved in auxin signalling during periderm and vascular development (Ben-Targem *et al.*, 2021; Dalby, 2021); thus, we inspected *er-105* mutants for periderm and vascular phenotypes under NAA treatment. At 8 days, *er-105* mutants already showed many pericycle cell divisions and the vascular cell divisions was similar compared to *Col0*, and both *Col0* and *er-105* mutants are activated by NAA treatment (Figure S6A-B). In *Arabidopsis*, former study showed that *er erl1 erl2* triple mutant has stronger repression on plant growth, lacking of secondary growth, thus we used *er erl2* double mutant instead (Shpak *et al.*, 2004). At 8 days, *er erl2* double mutant started normal secondary growth compared to *Col0*, while *er erl2* double mutant show less response compared with *Col0* under NAA treatment (Figure S6C-D). To further dissect the specific contribution of ER during secondary growth, we obtain *BIR-ER* complex that the extracellular LRR domain of BIR3 (BAK1-INTERACTING RECEPTOR-LIKE KINASE3) is fused to the cytoplasmic kinase domains of the SERK-dependent LRR-RKs ERECTA to form tight complexes, independently from ligand stimulus (Hohmann *et al.*, 2020). Using this module, we generated *PER15::BIR-ER* and *PXY::BIR-ER* plants with permanent receptor activation of ER. In 12-d plants, *PER15::BIR-ER* showed a reduction in total area, vascular area, and periderm area compared with *Col0*, which indicated the plants decreased the girth of root; while *PXY:: BIR-ER* plants showed an amazing phenotype, and largely increase the girth of the root and proportion of vascular cambium; moreover, we observed an increase on xylem cell formation and ectopic xylem formation in the phloem region, indicating *ER* had affection on vascular cambium cell fate (Figure 4B-C, S7A-F, S7H-I). Interestingly, both *PER15::BIR-ER* and *PXY::BIR-ER* plants increase cork cell numbers (Figure S7G). Altogether, these results indicate that *ER* is a downstream regulator of auxin signalling, promotes secondary growth, and partially controls vascular cambium cell fate.

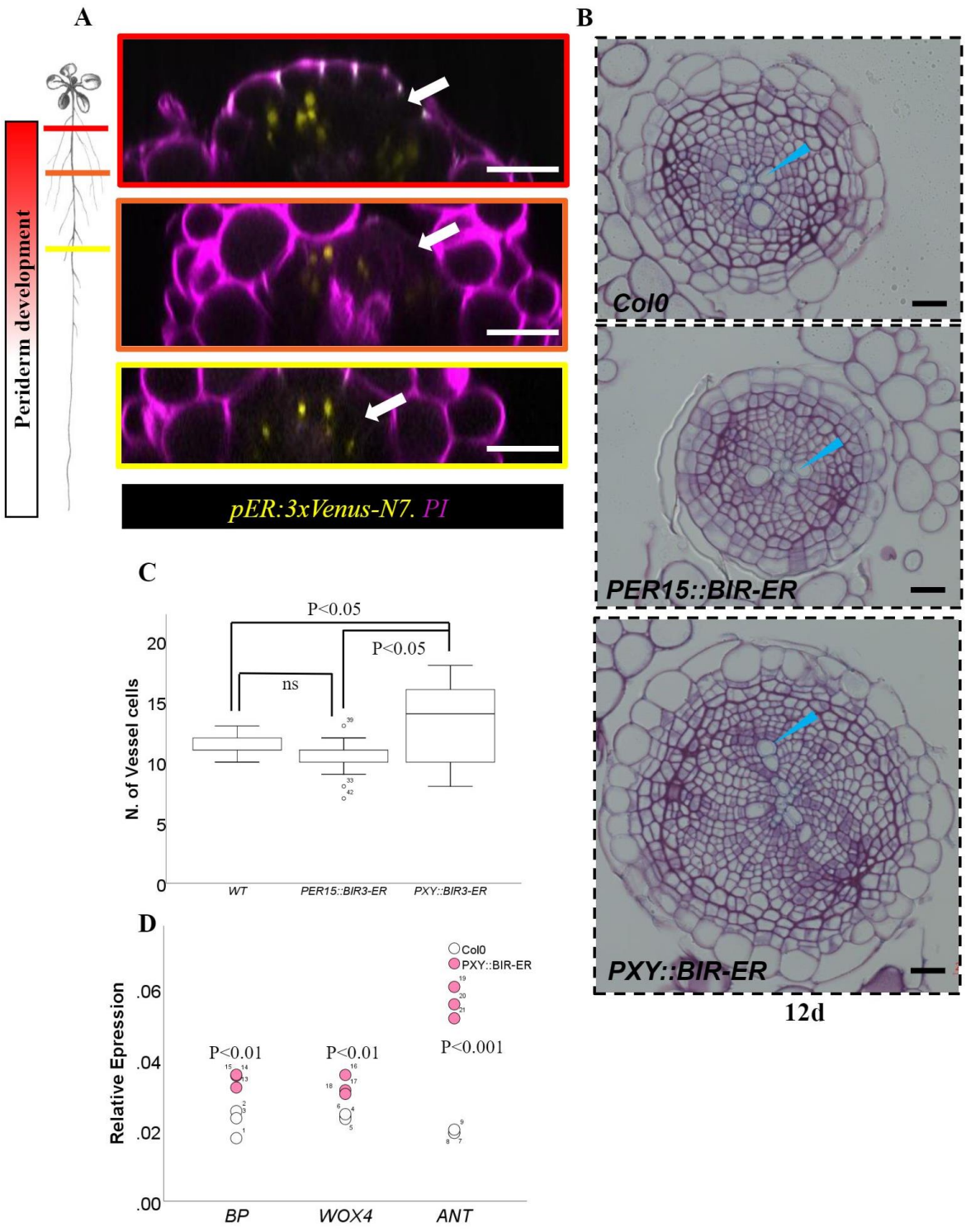

Figure 4. ERECTA promotes secondary growth in root.

A, Orthogonal view of z stacks of *pER::3xVenus-N7*. 12-day-old roots at the positions corresponding to stage 1 (lower panel), stages 3/4 (center panel), and stage 5 (up panel) of periderm development. **B,** Cross-sections (plastic embedding) of the uppermost part of 12-d-old *Col0* (up panel), *PER15::BIR-ER* (center panel), and *PXY::BIR-ER* (lower panel) roots. **C,** Quantification of xylem cell number of the experiment shown in (A-B). T-test (n =10-15). Blue

triangular arrow indicates xylem cells. Black scale bars: 20μm. **D,** Relative expression of *BP*, *WOX4*, and *ANT* in the Col0 and *PXY::BIR-ER* roots. 14-d-old roots for collection. T-test (n =3)

ANT (_AINTEGUMENTA_) specific overexpression in the vascular cambium promotes xylem formation.

To further understand the functions of *WOX4* and *BP* during secondary growth, we generated transgenic lines: transcriptional factor fused with EAR-repression domain (SRDX) to generate a chimeric repressor line (*PER15::BP-SRDX-GR*, *PXY::BP-SRDX-GR*, *PER15::WOX4-SRDX-GR*, and *PXY::WOX4-SRDX-GR* plants) (Mahfouz *et al.*, 2012). Inducing *BP-SRDX* expression in the cork cambium of WT plants resulted in root with an increase in total area and periderm area, while in *WOX4-SRDX* expression in the cork cambium showed a promotion in total area, vascular area, phloem area, and periderm area (Figure S8A, S8C, S9A, and S9C). Both *WOX4-SRDX* and *BP-SRDX* promote periderm development, but in vascular cambium, *PXY::BP-SRDX-GR* and *PXY::WOX4-SRDX-GR* plants showed no affection on secondary growth compared with Mock (Figure S8A-C and S9A-C). It indicates a bi-function of *WOX4* and *BP* during periderm development in all 5 areas measurement. (However, we haven't proved that the lines are really functional and working as a chimeric repressor, and we will prove it in the future.)

We further hypothesized that *ANT* plays a crucial role during secondary growth. To test this, we first investigated expression pattern of *ANT* during secondary growth. By mean of fluorescent reporters, we observed the activity of *ANT* promoters at all stages of secondary growth (Zhang *et al.*, 2019) (Figure 5A) and its expression is reduced in the secondary growth of *PER15::slr-GR* and *PXY::shy2-2-GR* induced roots (Figure 3B). To uncover the functions of *ANT*, we obtained transgenic lines (*PER15::ANT-GR*, *PXY::ANT-GR*, *PER15::ANT-SRDX-GR*, and *PXY::ANT-SRDX-GR* plants). Inducing *ANT* or *ANT-SRDX* in the cork cambium of WT plants resulted in root with an increase in periderm development (Figure S10A-B and S11A-B). It may indicate *ANT* contains multiple roles during periderm development and promotes periderm layer formation. Interestingly, inducing *ANT* or *ANT-SRDX* in the vascular cambium of WT plants, affects the balancing of vascular cambium differentiation, repressing xylem cell formation but increasing the vascular cambium (Figure 5B-D). Moreover, the overexpression of *ANT* or *ANT-SRDX* in vascular cambium disturbed the balance of

xylem and phloem cell formation, causing a reduction on secondary growth (Figure S11A-B). Altogether, these results indicate *ANT* is involved in secondary growth and determines vascular cambium cell fate, repressing xylem cell differentiation.

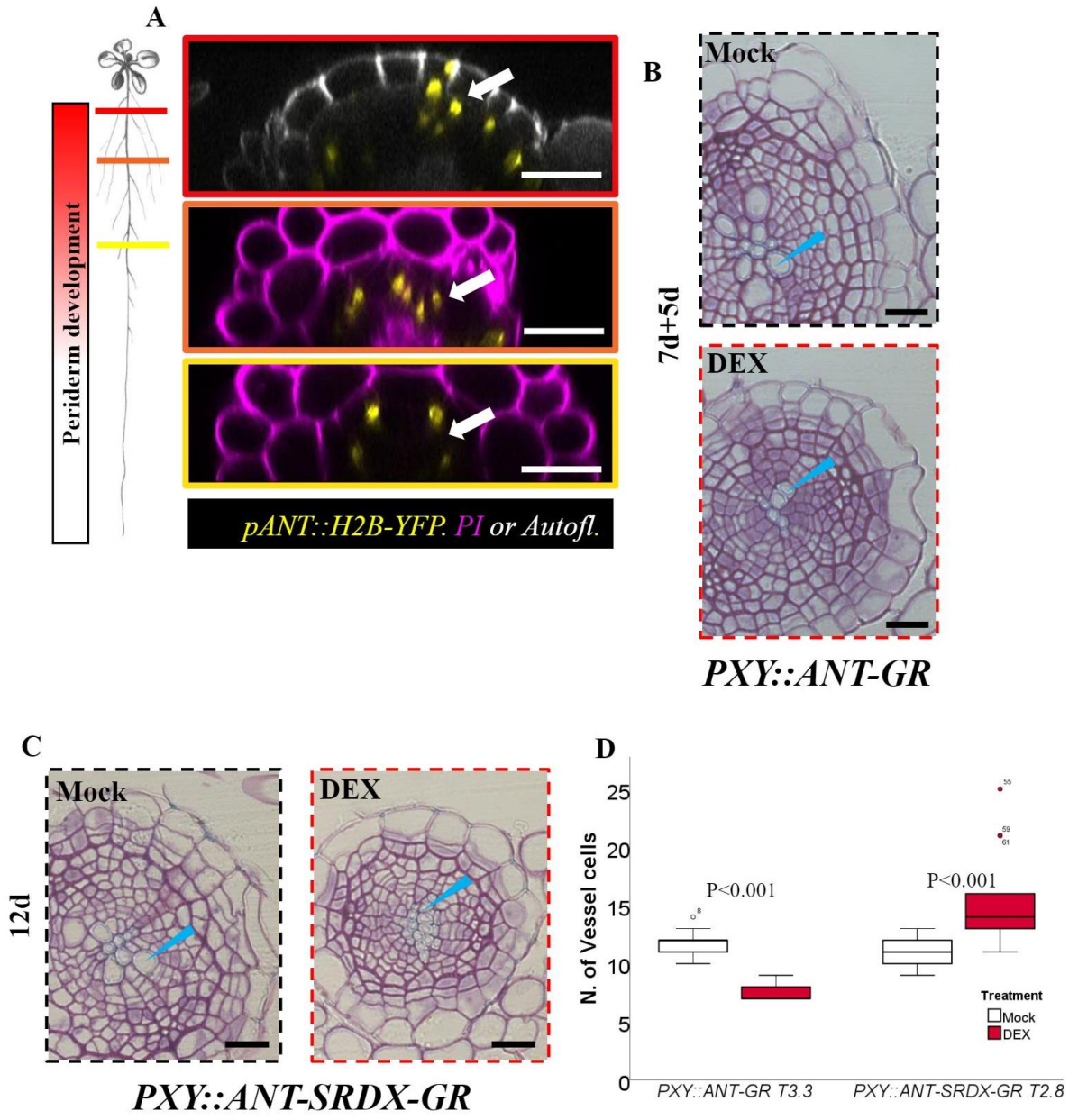

Figure 5. ANT promotes xylem differentiation in vascular cambium.

A, Orthogonal view of z stacks of *pANT::ANT-H2B-YFP*. 12-day-old roots at the positions corresponding to stage 1 (lower panel), stages 3/4 (center panel), and stage 5 (up panel) of periderm development. **B,** Cross-sections (plastic embedding) of the uppermost part of *PXY::ANT-GR* (in *MYB84::NLS-3xGFP W131Y*) roots. 7-d-old plants were transferred for 5-d on Mock (left panels) or 10µM DEX (right panels) plates. **C,** Cross-sections (plastic embedding)

of the uppermost part of *PXY::ANT-SRDX-GR* (in *W131Y*) roots. 12-d-old plants were grown on Mock (left panels) or 10μM DEX (right panels) plates. **D,** Quantification of xylem cell number of the experiment shown in (A-B). T-test (n =11-15). Blue triangular arrow indicates xylem cells. Black scale bars: 20μm.

Discussion

Our genetic and gene expression data demonstrate that auxin as one of the key phytohormones is involved in both vascular cambium and cork cambium establishment and maintenance by activating distinct regulators (Zhang *et al.*, 2019; Xiao *et al.*, 2020) (Figure 6). Interestingly, in the root, auxin signalling is required for cork cambium proliferation and maintenance, promoting its differentiation into the phelloderm cells, while auxin is required for vascular cambium proliferation and xylem differentiation. It indicates auxin has a different affection on vascular cambium and cork cambium. Moreover, we suggested a compensation mechanism for vascular cambium and cork cambium: a stress on one of the cambia, the plants tried to recover from the unsatisfactory situation by activating another cambium.

We highlighted that auxin signalling pathways, orchestrate secondary growth by promoting *BP*, *WOX4*, *ER*, and *ANT*, then manipulate proliferation and cell fate in vascular cambium and cork cambium (Zhang *et al.*, 2019; Xiao *et al.*, 2020) (Figure 6). In our auxin responsive networks, *ER* and *ANT* serve as the core nodes that shape the patterns of secondary growth (Figure 6). We confirmed that vascular cambium specific overexpression of *BIR-ER* and *ANT* decrease xylem formation, which indicates that ER-ANT module has an effect on vascular cambium proliferation and direct cambia differentiation in the *Arabidopsis* root (Figure 4B, 5B, 6). These findings allowed us to generate a model where auxin signalling in root activates *ER* and *ANT*, promotes vascular cambium proliferation and finally determines vascular cadmium cell fate (Figure 6).

However, induction of *ANT* or *ANT-SRDX* in the vascular cambium represses or accelerates xylem cell divisions, while the girth of the root is strongly reduced (Figure 5B-D, S11A-B). It indicates plant needs to keep a balance of these two distinct cell types. Interestingly, plants need to sense the various surroundings and decide the correct ratio of phloem and the xylem in a changeable environment, like drought or dry. It is very crucial to understand how plants keep dynamic balance of the phloem and the xylem to against unsuitable environment. In this regard, it would be interesting to

further decipher the complex molecular mechanisms coordinating the best ratio of the phloem and the xylem under distinct environment.

In plants, it remains to be determined whether other plant hormones or other regulators are involved in this balancing of the phloem and the xylem. Thus, the downstream regulators of *ANT* and *ER* with hormonal pathways appear complex and warrants further investigation. Thus, the ER-ANT module is regulated by auxin signalling and may be a potentially universal molecular toolkit for xylem cell formation. Furthermore, cytokinin signalling is also critical player in activating regulators like *BP*, *WOX4*, *ER*, and *ANT* during secondary growth (Randall *et al.*, 2015; Zhang *et al.*, 2019) (Figure 6), which provides an idea to further investigate how the plants shape their own root structure by controlling different phytohormones.

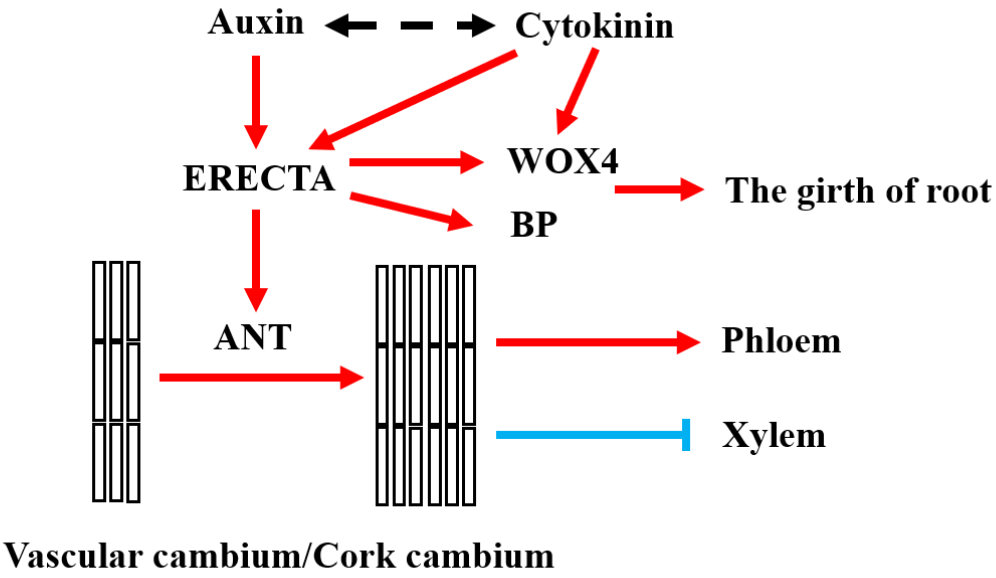

Figure 6. Model explaining vascular cambium output specificity.

Author contributions

W.X. and L.R. planned and conducted the majority of the experiments. W.X. acquired the confocal images. W.X. did the molecular cloning and generated the plant lines. D.M. and W.X. conducted the Fluorol Yellow (FY) experiments. W.X., and X.D. conduct the plant embedding. W.X. measured root area. W.X. conducted the phellem ratio experiments. W.X. generated the library for RNA sequencing/qPCR experiments with the help of D.M. W.X. and L.R. analysed the sequencing data. D.R. helped in generating the T3 lines and embedding the roots. W.X. and L.R. wrote the paper.

Acknowledgement

We thank Martin Bayer and Peter Etchells for sharing the seeds. We thank Andrea Boch for technical help. Work was supported by the Deutsche Forschungsgemeinschaft (DFG grant RA-2590/1-2).

Conflict of Interest

The authors declare no conflict of interest.

Method details

Plant material and growth

The mutants and transgenic lines (F2 segregating and/or F3 homozygous populations) used in this study are described in Supplementary Table 1. The plants were grown on 1/2MS with 1% sugar plates (0.8% plant agar), DEX plates (10µM, Sigma, D1756), or NAA plates (1µM, Duchefa, N0903). The plants were grown on 1/2MS with 1% sugar plates under continuous light until sampling, or in soil with long day conditions (16 hours light versus 8 hours dark). For DEX or NAA treatment, the plates were grown on 1/2MS with 1% sugar plates, transferred on DEX plates or NAA plates.

Molecular cloning

Promoters were cloned from *Arabidopsis thaliana* DNA and proteins coding sequence from *Arabidopsis thaliana* root cDNA with the primers in Supplementary Table 2. All transgenic constructs were assembled with the modular green gate technology (Lampropoulos *et al.*, 2013). If promoters or protein coding sequences contain BSA sites, it need to be replaced as followed in (Schurholz *et al.*, 2018). In Supplementary Table 3, it contains all the modulars and constructs in this study. In Supplementary Table 4, it contains all the module assembly strategies. Agrobacterium tumefaciens GV3101 was used for transformation and *Arabidopsis* thaliana plants were transformed via floral dipping. Heterozygous T2 or Homozygous T3 line were used in this study.

Histology and fluorescent staining

The root samples have been collected from root junction (0.5-1 cm) for plastic embedding. The plastic cross-sections were followed instruction on (de Reuille &

Ragni, 2017), using Technovit 7100 (Heraeus Kulzer; 64709003). The plastic sections (5-8 μm) were stained with 0.1 % toluidine blue (Sigma; T3260). The pictures were imaged with a Zeiss Axio M2 imager microscope or a Zeiss Axiophot microscope, modified by ZEN Blue software (version 3.4). Suberin deposition were stained by Fluorol yellow (FY), followed the instruction in (Naseer *et al.*, 2012) using Fluorol yellow (Santa Cruz, sc-215052). Propidium Iodide (PI) staining was achieved by directly mounting the root in a 10-30 μg/ml solution (Sigma, P4864).

Confocal Microscopy

Zeiss confocal (LSM880) was used for acquiring the confocal images with sepcific settings. For GFP (green fluorescent protein): ex. 488 nm; em. 485–505 nm. For YFP (yellow fluorescent protein), mCitrine and Venus: ex. 514 nm; em. 515–545 nm. For mCherry, mCherry and PI: ex. 561 nm; em. 570–630 nm. For FY: ex. 488nm; em 480-550nm. Orthogonal views of a Z stack were modified by ZEN Black software (Zen 2.3 SP1).

RNA sequence

RNA was extract from 14-day old plants, up most 1.5 cm- 2cm for each sample with Mock or DEX treatment (Approximately 100 plants for each sample), using Universal RNA Purification Kit (Roboklon, E3598-02) for RNA extraction. RNA samples were qualified by Agilent RNA Bioanalyzer chip traces and quantified by Nanodrop 2000. The enrichment of mRNA by oligo-dT pull-down was used the NEBNext Poly(A) mRNA Magnetic Isolation Module (NEB #E7490L), and the construction of RNA libraries were used NEBNext Ultra II RNA Library Prep Kit for Illumina (NEB #E7530L) with NEBNext Multiplex Oligos for Illumina (Index Primers Set 1 to Set 4). Finally, the RNA library size and quality were measured on DNA High Sensitivity Bioanalyzer chip (Agilent), and RNA libraries were quantified by the NEBNext Library Quant Kit for Illumina (NEB #E7630S).

qPCR

RNA was extracted from upper most 1.5cm of at least 60 roots for each genotype/treatment using the Universal RNA Purification Kit (Roboklon, E3598-02) according to the manufacturer protocol. C-DNA was synthetized using AMV Reverse

Transcriptase Native (Roboklon, E1372-01) according to manufacturer protocol. qPCR was performed using MESA blue (Eurogentec, RT-SYS2X-03-+NRWOUB) in a CFX96 Real-Time System machine (BIO-RAD). Primers used for qPCR are listed in Table S2A. The relative expression was calculated using CFX Maestro software (BIO-RAD) and the sample were normalized against EF1. qPCR experiments were repeated at least 3 times and one experiment is shown.

Statistical analyses

IBM SPSS Statistics version 25-26 (IBM) was used for statistical analyses. The Levene's Test was used for homogeneity of variances testing. The significant differences between two datasets were calculated by a student's t-test (homogeneous) and Welch's t-test (non-homogenous). One-way ANOVA with a Bonferroni correction (equal variance assumed) or Tamhane's post (equal variance not assumed) hoc was used for multiple datasets.

Periderm quantification, area quantification and image analyses

The quantification of phellem length and phellem ratio was described on (Wunderling *et al.*, 2018), measured by Fiji (https://fiji.sc/) (Schindelin *et al.*, 2012). 3 independent experiments were performed and only one results has been presented. The area quantification was performed by Fiji. For every genotype, 10-25 cross-sections from independent plants were analysed. 2 independent experiments were performed and only one results were presented for cross-section. The pericycle/periderm cell division was calculated by cell counter plugin of Fiji.

Table S1. Plant Material used in this study.

Plants	Background	Ref.	Obtained from
MYB84::NLS-3xGFP	Col	(Wunderling *et al.*, 2018)	Laura Ragni
UBQ10::eYFP-NPSN12 (W131Y)	Col	(Geldner *et al.*, 2009)	Niko Geldner
PER15::slr-1-GR	*MYB84::NLS-3xGFP; W131Y*	(Xiao *et al.*, 2020)	Laura Ragni
PXY::shy2-2-GR	*W131Y*	(Xiao *et al.*, 2020)	Laura Ragni
pER::3xVenus-N7	Col	(Kai Wang & Sascha Laubinger, 2020)	Martin Bayer
PER15::BIR-ER	*W131Y*	This study	This study
PXY::BIR-ER	*W131Y*	This study	This study
GPAT5::CITRINE	*Col*	(Barberon *et al.*, 2016)	Niko Geldner
GPAT5::shy2-2-GR	*MYB84::NLS-3xGFP; W131Y*	This study	This study
er-105	Col	(Wang *et al.*, 2019b)	Peter Etchells
er erl2	Col	(Wang *et al.*, 2019b)	Peter Etchells
PER15::BP-SRDX-GR	*W131Y*	This study	This study
PXY::BP-SRDX-GR	*W131Y*	This study	This study
PER15::WOX4-SRDX-GR	*W131Y*	This study	This study
PXY::WOX4-SRDX-GR	*W131Y*	This study	This study
PER15::ANT-GR	*W131Y*	This study	This study
PXY::ANT-GR	*W131Y*	This study	This study
PER15::ANT-SRDX-GR	*W131Y*	This study	This study
PXY::ANT-SRDX-GR	*W131Y*	This study	This study

Table S2A. Primers used for molecular cloning.

Element	Primer	Sequence
SRDX-GR	Dr-SDRX-GR part 1 F	GATTTGGATTTGGAATTGAGATTGGGTTTTGCTGAAGCTCGAAAAACA
	Dr-SDRX-GR part 2 F	AACAGGTCTCATCAGGTAAGGGTTTGGATTTGGATTTGGAATTGAGA
BIR-ER	C-BIR3 F	AACAGGTCTCAGGCTCAATGAAGAAGATCTTCATCACAC
	Dr-ER R	AACAGGTCTCACTGACTCACTGTTCTGAGAAATAACTTG
ANT	C-ANT F	AACAGGTCTCAGGCTCAATGAAGTCTTTTTGTGATAATGATGA
	Dr-ANT R	AACAGGTCTCACTGAAGAATCAGCCCAAGCAGC
BP-qPCR	BP-qPCR-F	TCCCATTCACATCCTCAACA
	BP-qPCR-R	CCCCTCCGCTGTTATTCTCT
WOX4-qPCR	WOX4 qPCR F	CCTCCGGCGTCACTTCAG
	WOX4 qPCR R	GGGTTCCACCTTGTCCCTC
ANT-qPCR	ANT-qPCR-F	AAGGAAGAGCAGTGGTTTCTC
	ANT-qPCR-R	ACTCTACCAATCCGTGCTTG
ERF-qPCR	EF1 F	AAGGCTCAAACGCCATCAAAGTTTTAAGAA
	EF1 R	AGGTCACCAAGGCTGCAGTGAAGAA

Table S2B. GG vectors used in this study.

GG modules/vectors	Ref.	Obtained
pGG-A0	(Lampropoulos *et al.*, 2013)	Jan Lohmann
pGG-C0	(Lampropoulos *et al.*, 2013)	Jan Lohmann
pZ03	(Lampropoulos *et al.*, 2013)	Jan Lohmann
pGG-A-pPXY	(Suer *et al.*, 2011)	Thomas Greb
pGG-A-pPER15	(Xiao *et al.*, 2020)	Laura Ragni
pGG-B03 (B-dummy)	(Lampropoulos *et al.*, 2013)	Jan Lohmann

pGG-B05 (NLS)	(Lampropoulos *et al.*, 2013)	Jan Lohmann
pGG-B-H2B	(Ramakrishna *et al.*, 2019)	Alexis Maizel
pGG-C-BIR-ER	This study	This study
pGG-C-*shy-2-2*	(Ramakrishna *et al.*, 2019)	Alexis Maizel
pGG-C-*slr-1*	(Ramakrishna *et al.*, 2019)	Alexis Maizel
pGG-C-WOX4	(Suer *et al.*, 2011)	Thomas Greb
pGG-C-BP/KNAT1	This study	This study
pGG-ANT	This study	This study
pGG-D-GR	(Ramakrishna *et al.*, 2019)	Thomas Greb
pGG-D2 (D-dummy)	(Lampropoulos *et al.*, 2013)	Jan Lohmann
pGG-D-SRDX-GR	This study	This study
pGG-E1 (pea RBCS terminator)	(Lampropoulos *et al.*, 2013)	Jan Lohmann
pGG-F-FR (FASTRED)	(Vilches *et al.*, 2019)	Alexis Maizel

Table 2C. GG Assembly strategy.

Final vector (in pZ03)	A	B	C	D	E	F
PER15::slr-1-GR	*pPER15*	B3	*slr-1*	GR	E1	F12
PXY::shy2-2-GR	*pPXY*	B3	*shy2-2*	GR	E1	F5
PER15::BIR-ER	*pPER15*	B3	BIR-ER	D2	E1	FR
PXY::BIR-ER	*pPXY*	B3	BIR-ER	D2	E1	FR
PER15::BP-SRDX-GR	*pPER15*	B3	BP	SRDX-GR	E1	FR
PXY::BP-SRDX-GR	*pPXY*	B3	BP	SRDX-GR	E1	FR
PER15::WOX4-SRDX-GR	*pPER15*	B3	WOX4	SRDX-GR	E1	FR
PXY::WOX4-SRDX-GR	*pPXY*	B3	WOX4	SRDX-GR	E1	FR
PER15::ANT-GR	*pPER15*	B3	ANT	GR	E1	FR
PXY::ANT-GR	*pPXY*	B3	ANT	GR	E1	FR
PER15::ANT-SRDX-GR	*pPER15*	B3	ANT	SRDX-GR	E1	FR
PXY::ANT-SRDX-GR	*pPXY*	B3	ANT	SRDX-GR	E1	FR

Table S2E. Genes used in this study.

Gene Abbreviation	**Gene Name**	**Gene Number**
MYB84	MYB DOMAIN PROTEIN 84/ REGULATOR OF AXILLARY MERISTEMS 3	AT3G49690
PER15	PEROXIDASE 15	AT2G18150
PXY/TDR	PHLOEM INTERCALATED WITH XYLEM/ TDIF RECEPTOR	AT5G61480
BDL/IAA12	BODENLOS/ INDOLE-3-ACETIC ACID INDUCIBLE 12	AT1G04550
SLR/ IAA14	SOLITARY ROOT/ INDOLE-3-ACETIC ACID INDUCIBLE 14	AT4G14550
BIR3	BAK1-INTERACTING RECEPTOR-LIKE KINASE 3	AT1G27190
WOX4	WUSCHEL RELATED HOMEOBOX 4	AT1G46480
BP/KNAT1	BREVIPEDICELLUS/ KNOTTED-LIKE FROM *ARABIDOPSIS* THALIANA 1	AT4G08150
EF1	ELONGATION FACTOR 1 ALPHA	AT5G60390
ANT	AINTEGUMENTA	AT4G37750
ER	ERECTA	AT2G26330
ERL2	ERECTA-LIKE 2	AT5G07180

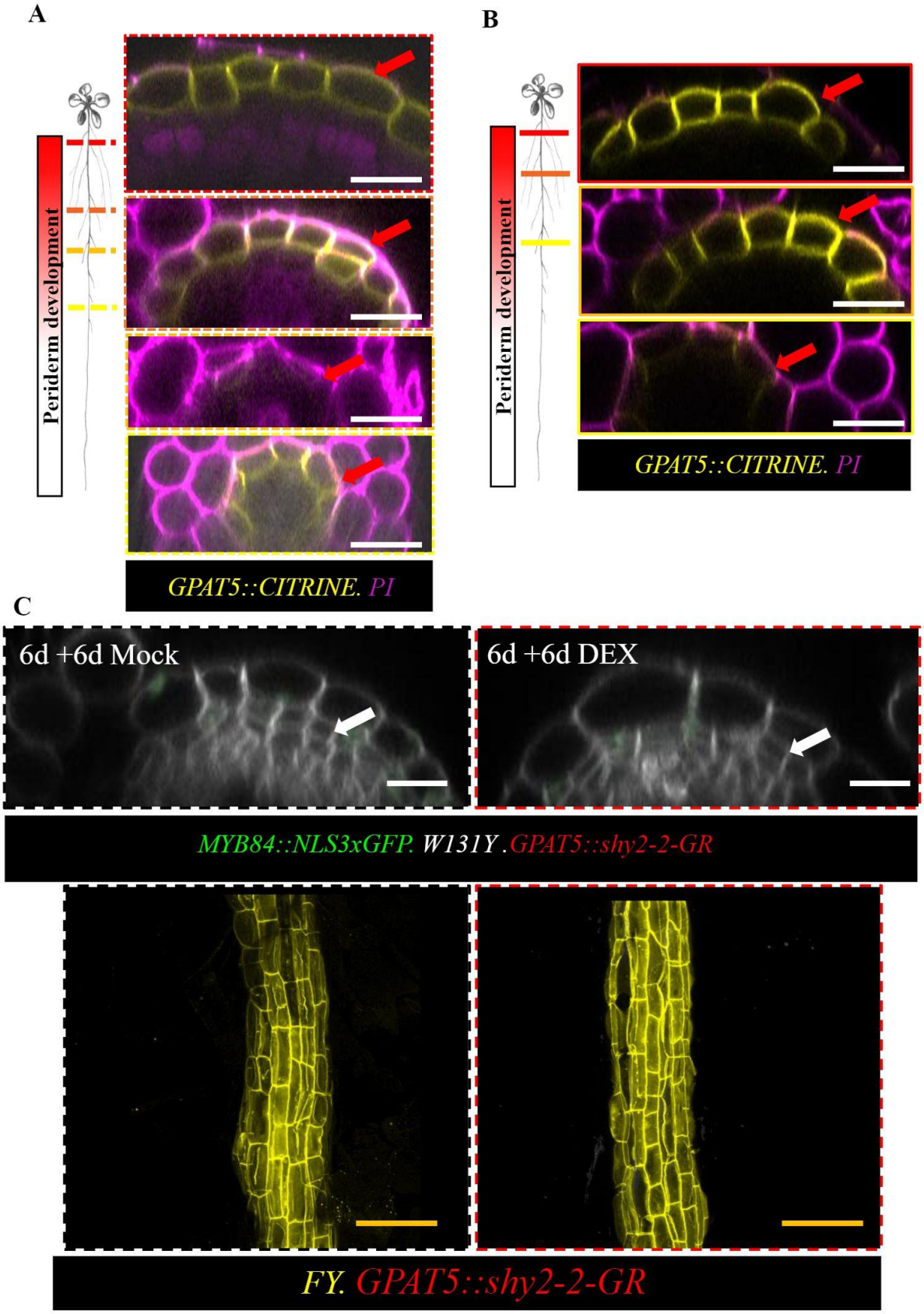
A
Periderm development
GPAT5::CITRINE. PI
B
Periderm development
GPAT5::CITRINE. PI
C
6d +6d Mock
6d +6d DEX
MYB84::NLS3xGFP. W131Y . GPAT5::shy2-2-GR
FY. GPAT5::shy2-2-GR

Figure S1. *GPAT5* expression patterns and phenotypic characterization of *GPAT::shy2-2-GR* roots.

A, Orthogonal view of Z-stacks of *GPAT5::CITRINE* roots at the positions corresponding to stage 1 (lower panel), stage 3/4 (middle panel) and stage 5 (upper panel) (12-d-old). **B**, Orthogonal view of Z-stacks of *GPAT5::CITRINE* roots at 6,8,10 and 20 days (uppermost part of the root). **C,** Upper panels: orthogonal view of Z-stacks of *GPAT5::shy2-2-GR* (in *MYB84::NLS-3xGFP W131Y*) roots at 12 days. Lower panels: 3D reconstruction of Z-stacks of 12-d-old *GPAT5::shy2-2-GR* (in *MYB84::NLS-3xGFP W131Y*) roots stained with Fluorol yellow (FY). 6-d-old plants were treated for 6-d with Mock (left panels) or 10μM DEX (right panels). Red arrows indicate the cork cambium and white arrows indicate *MYB84* expression. White scale bars: 20μm and yellow scale bars: 50μm.

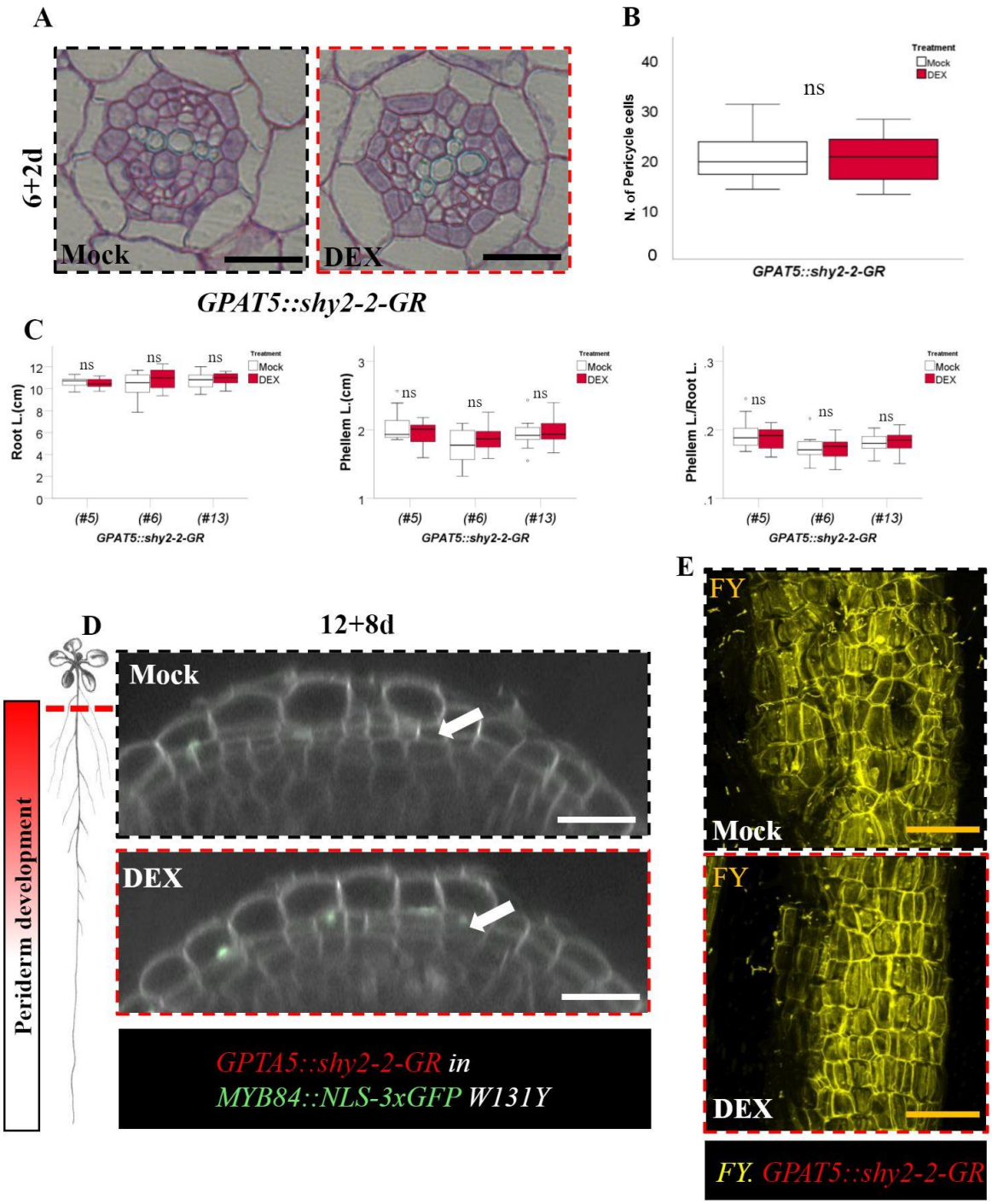
A
6+2d
Mock
DEX
GPAT5::shy2-2-GR
B
Treatment
Mock
DEX
ns
N. of Pericycle cells
40
30
20
10
0
GPAT5::shy2-2-GR
C
Root L.(cm)
Phellem L.(cm)
Phellem L./Root L.
ns
(#5)
(#6)
(#13)
GPAT5::shy2-2-GR
D
12+8d
Mock
DEX
Periderm development
GPTA5::shy2-2-GR in
MYB84::NLS-3xGFP W131Y
E
FY
Mock
DEX
FY. GPAT5::shy2-2-GR

Figure S2. Blocking auxin signalling in no-meristematic tissues does not affect secondary growth initiation and maintaining.

A, Cross-sections (plastic embedding) of the uppermost part of *GPAT5::shy2-2-GR* (in *MYB84::NLS-3xGFP W131Y*) roots. 6-d-old plants were transferred for 2-d on Mock (left panels) or 10µM DEX (right panels). **B,** Quantification of pericycle cell number of the experiment shown in (A). T-test (n =10-15). **C,** Quantification of root length, phellem length, and phellem ratio in 3 independent *GPAT5::shy2-2-GR* (in *MYB84::NLS-3xGFP W131Y*) lines. 7-d-old plants were treated for 5-d with mock or 10µM DEX. T-test (n =15). **D,** Orthogonal view of Z-stacks of *GPAT5::shy2-2-GR* (in *MYB84::NLS-3xGFP W131Y*) roots at 20 days. 12-d-old plants were treated for 8-d with Mock (upper panels) or 10µM DEX (lower panels). **E,** 3D reconstruction of Z-stacks of 20-d-old *GPAT5::shy2-2-GR* (in *MYB84::NLS-3xGFP W131Y*) roots stained with Fluorol yellow (FY). 6-d-old plants were treated for 6-d with Mock (upper panels) or 10µM DEX (lower panels). White arrows indicate *MYB84* expression. White and black scale bars: 20µm and yellow scale bars: 50µm.

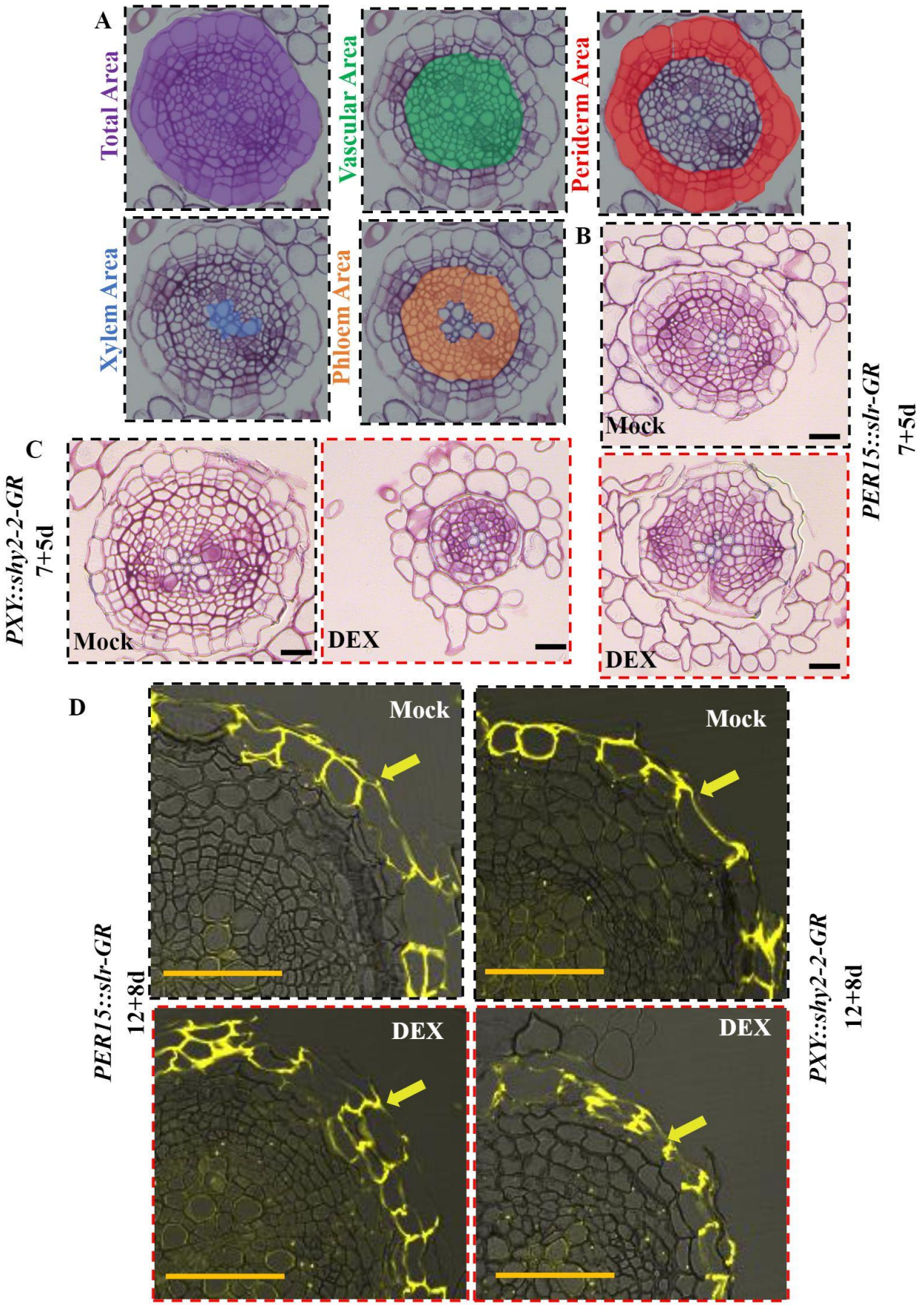
A
Total Area
Vascular Area
Periderm Area
Xylem Area
Phloem Area
B
Mock
DEX
PER15::slr-GR
7+5d
C
PXY::shy2-2-GR
7+5d
Mock
DEX
D
Mock
Mock
DEX
DEX
PER15::slr-GR
12+8d
PXY::shy2-2-GR
12+8d

Figure S3. Auxin is needed for secondary growth and cork cambium establishment.

A, The sketch of area measurement: total area, vascular area, phloem area (including phloem and vascular cambium), xylem area, and periderm area. **B,** Cross-sections (plastic embedding) of the uppermost part of *PER15::slr-1-GR* (in *MYB84::NLS-3xGFP W131Y*; #1) roots. 7-d-old plants were transferred for 5-d on Mock (upper panels) or 10μM DEX (lower panels) plates. **C,** Cross-sections (plastic embedding) of the uppermost part of *PXY::shy2-2-GR* (in *MYB84::NLS-3xGFP W131Y*) roots. 7-d-old plants were transferred for 5-d on Mock (left panels) or 10μM DEX (right panels) plates. **D,** Left panels: collecting the upper most part of *PER15::slr-1-GR* (in *MYB84::NLS-3xGFP W131Y*; #1) roots for cross-sections (plastic embedding) with Fluorol yellow (FY). Right panels: collecting the upper most part of *PXY::shy2-2-GR* (in *MYB84::NLS-3xGFP W131Y*) roots for cross-sections (plastic embedding) with Fluorol yellow (FY). 12-d-old plants were transferred for 8-d on Mock (upper panels) or 10μM DEX (lower panels) plates. Yellow arrows indicate FY. Black scale bars: 20μm and yellow scale bars: 50μm.

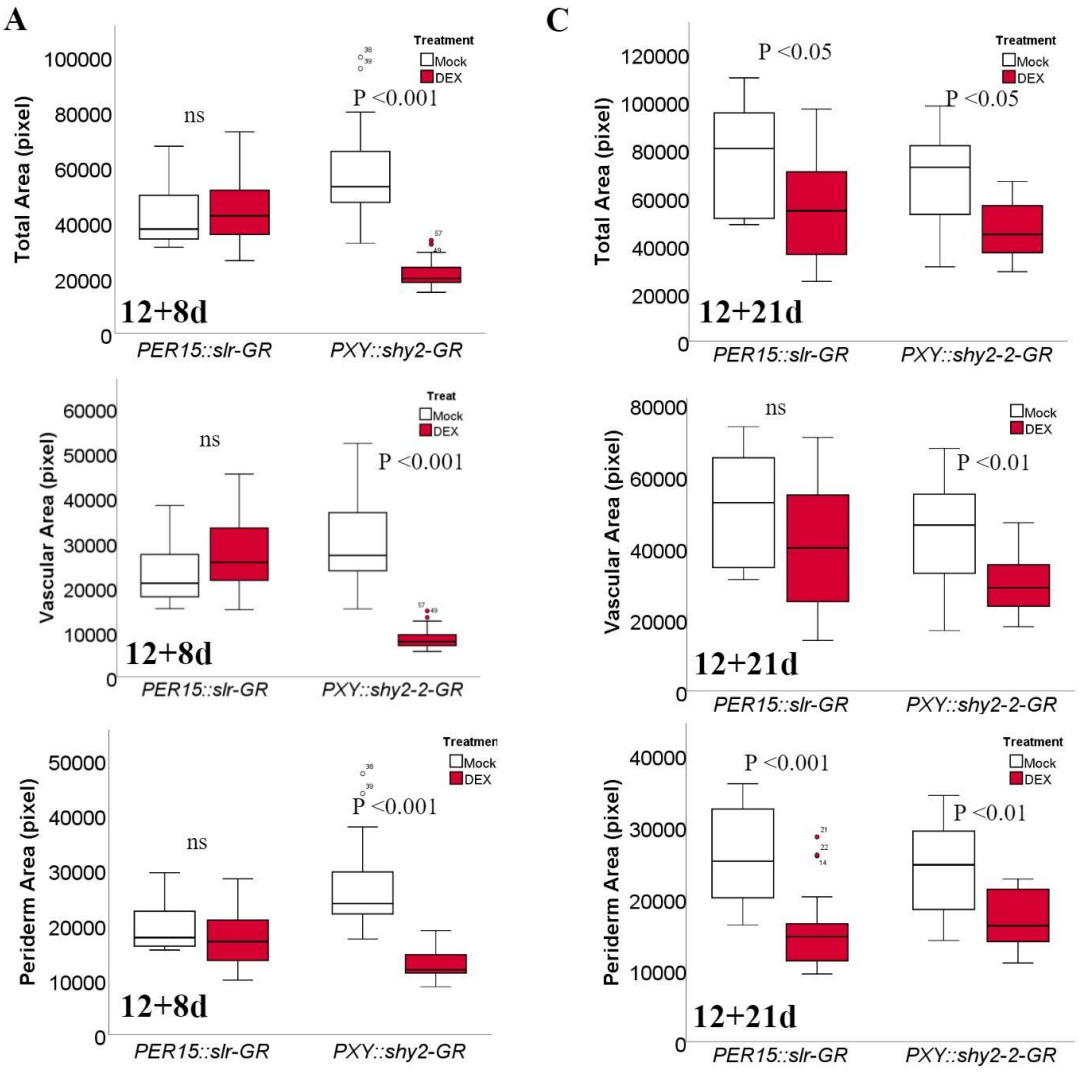
A
Total Area (pixel)
Treatment
Mock
DEX
ns
P <0.001
12+8d
PER15::slr-GR
PXY::shy2-GR
Vascular Area (pixel)
Treat
ns
P <0.001
12+8d
PER15::slr-GR
PXY::shy2-2-GR
Periderm Area (pixel)
Treatmen
ns
P <0.001
12+8d
PER15::slr-GR
PXY::shy2-GR
C
Total Area (pixel)
P <0.05
P <0.05
12+21d
PER15::slr-GR
PXY::shy2-2-GR
Vascular Area (pixel)
ns
P <0.01
12+21d
PER15::slr-GR
PXY::shy2-2-GR
Periderm Area (pixel)
P <0.001
P <0.01
12+21d
PER15::slr-GR
PXY::shy2-2-GR

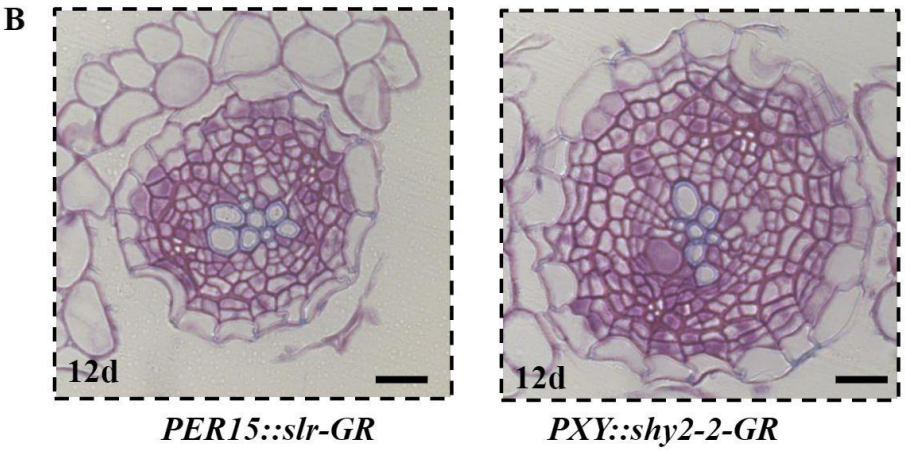
B
12d
12d
PER15::slr-GR
PXY::shy2-2-GR

Figure S4. Blocking auxin signalling in vascular cambium and cork cambium represses secondary growth.

A, Quantification of total area (left panels) and periderm area (right panels) of the experiment shown in (Figure 1A-B). T-test (n =12-13). **B,** Left panels: cross-sections (plastic embedding) of the uppermost part of 12-d-old *PER15::slr-1-GR* (in *MYB84::NLS-3xGFP W131Y*; #1) roots. Right panels: cross-sections (plastic embedding) of the uppermost part of 12-d-old *PXY::shy2-2-GR* (in *MYB84::NLS-3xGFP W131Y*) roots. **C,** Quantification of total area (left panels) and periderm area (right panels) of the experiment shown in (Figure 2A-B). T-test (n =10-13). Black scale bars: 20µm.

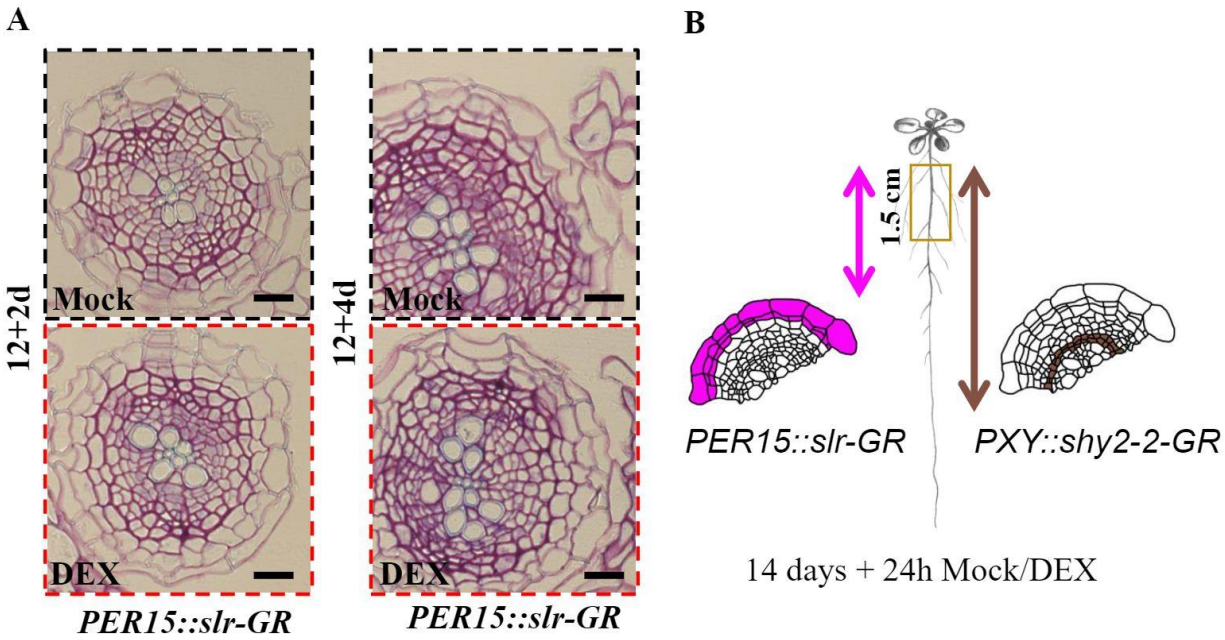

C

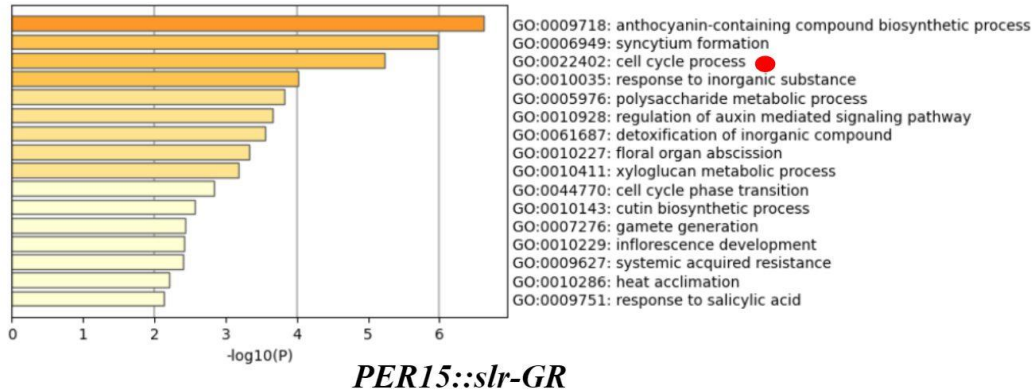

PER15::slr-GR

D

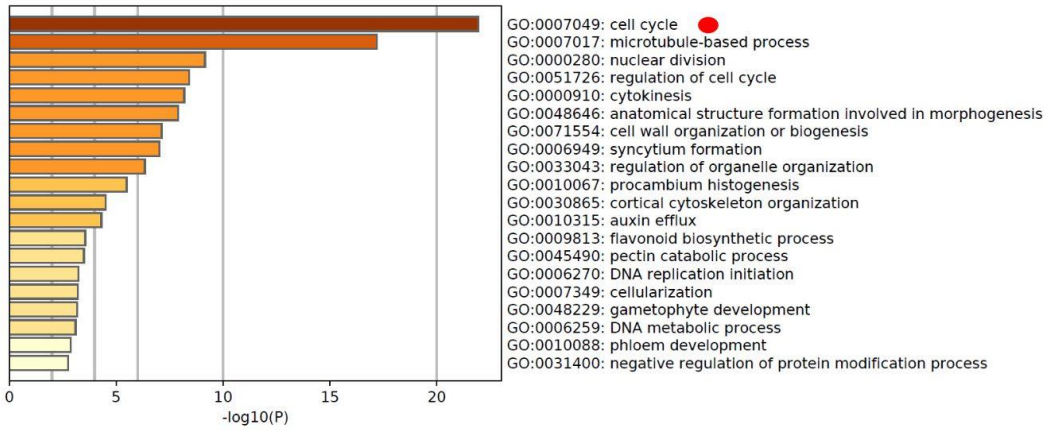

PXY::shy2-2-GR

Figure S5. Blocking auxin signalling helps cork cambium to maintain its cell identity.

A, Left panels: cross-sections (plastic embedding) of the uppermost part of *PER15::slr-1-GR* (in *MYB84::NLS-3xGFP W131Y*; #1) roots. 12-d-old plants were transferred for 2-d on Mock (upper panels) or 10μM DEX (lower panels) plates. Right panels: c cross-sections (plastic embedding) of the uppermost part of *PER15::slr-1-GR* (in *MYB84::NLS-3xGFP W131Y*; #1) roots. 12-d-old plants were transferred for 4-d on Mock (upper panels) or 10μM DEX (lower panels) plates. **B,** The sketch of RNA-seq sample collecting: 12-d-old plants were transferred for 24h on Mock or 10μM DEX plates, and collect up most 1.5 cm- 2cm for each sample. **C-D**， GO analysis of *PER15::slr-1-GR* and *PXY::shy2-2-GR* (log2FC < 0.5; padj < 0.05). Black scale bars: 20μm.

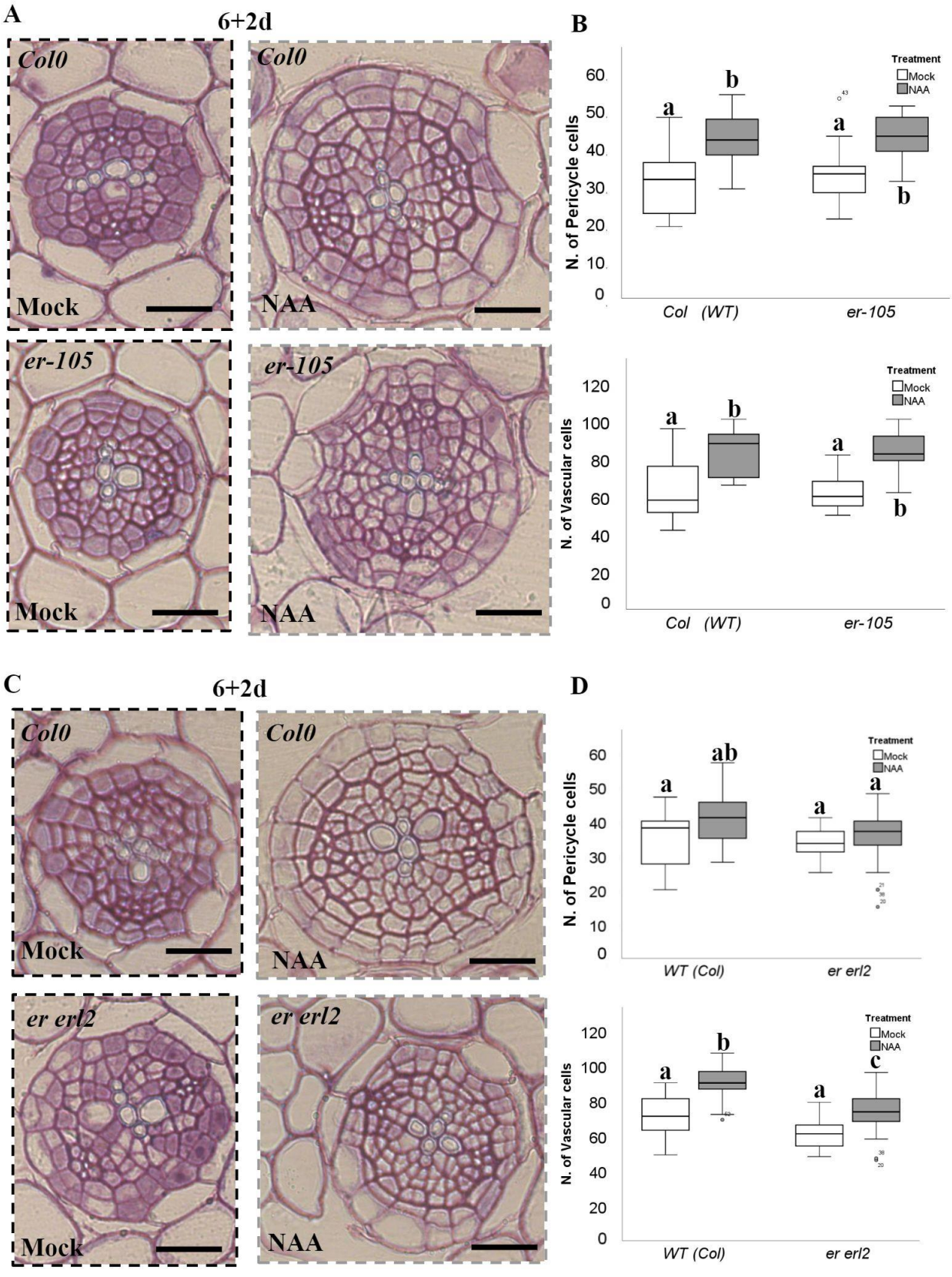
A
6+2d
Col0
Mock
Col0
NAA
er-105
Mock
er-105
NAA
B
Treatment
Mock
NAA
N. of Pericycle cells
Col (WT)
er-105
N. of Vascular cells
Col (WT)
er-105
C
6+2d
Col0
Mock
Col0
NAA
er erl2
Mock
er erl2
NAA
D
Treatment
Mock
NAA
N. of Pericycle cells
WT (Col)
er erl2
N. of Vascular cells
WT (Col)
er erl2

Figure S6. *ERECTA* receptor kinases are related to auxin signalling.

A, Cross-sections (plastic embedding) of the uppermost part of *Col0* (upper panels) and *er-105* (lower panels) roots. 6-d-old plants were transferred for 2-d on Mock (left panels) or 1μM NAA (middle panels) plates. **B,** Quantification of pericycle cell number (upper panels) and vascular cell number (lower panels) of the experiment shown in (A). One-way ANOVA (CI95%, Post-Hoc: Tamhane, n = 10-15). **C,** Cross-sections (plastic embedding) of the uppermost part of *Col0* (upper panels) and *er er2* (lower panels) roots. 6-d-old plants were transferred for 2-d on Mock (left panels) or 1μM NAA (middle panels) plates. **D,** Quantification of pericycle cell number (upper panels) and vascular cell number (lower panels) of the experiment shown in (C). One-way ANOVA (CI95%, Post-Hoc: Tamhane, n = 11-14). Black scale bars: 20μm.

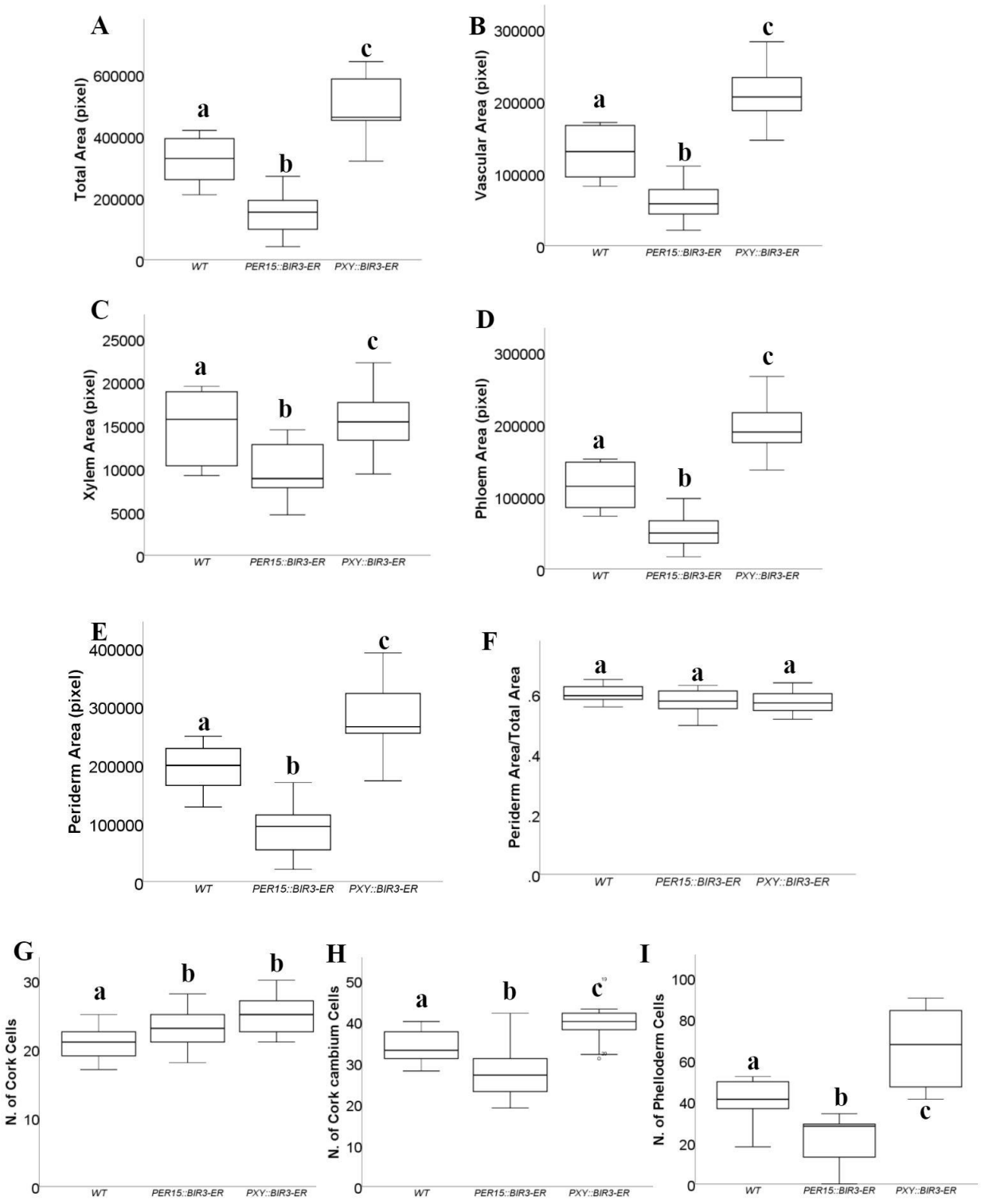
A
Total Area (pixel)
600000
400000
200000
0
a
b
c
WT
PER15::BIR3-ER
PXY::BIR3-ER
B
Vascular Area (pixel)
300000
200000
100000
0
a
b
c
WT
PER15::BIR3-ER
PXY::BIR3-ER
C
Xylem Area (pixel)
25000
20000
15000
10000
5000
0
a
b
c
WT
PER15::BIR3-ER
PXY::BIR3-ER
D
Phloem Area (pixel)
300000
200000
100000
0
a
b
c
WT
PER15::BIR3-ER
PXY::BIR3-ER
E
Periderm Area (pixel)
400000
300000
200000
100000
0
a
b
c
WT
PER15::BIR3-ER
PXY::BIR3-ER
F
Periderm Area/Total Area
.6
.4
.2
.0
a
a
a
WT
PER15::BIR3-ER
PXY::BIR3-ER
G
N. of Cork Cells
30
20
10
0
a
b
b
WT
PER15::BIR3-ER
PXY::BIR3-ER
H
N. of Cork cambium Cells
50
40
30
20
10
0
a
b
c
WT
PER15::BIR3-ER
PXY::BIR3-ER
I
N. of Phelloderm Cells
100
80
60
40
20
0
a
b
c
WT
PER15::BIR3-ER
PXY::BIR3-ER

Figure S7. *ERECTA* receptor kinases are related to secondary growth.

A-E, Quantification of total area, vascular area, phloem area, xylem area, and periderm area of the experiment shown in (Figure 4B). **F,** Quantification of periderm area/total area of the experiment shown in (A and E). T-test (n =12-13). One-way ANOVA (CI95%, Post-Hoc: Tamhane, n = 12-18). **G-I,** Quantification of pericycle cell number (upper panels) and vascular cell number (lower panels) of the experiment shown in (Figure 4B). One-way ANOVA (CI95%, Post-Hoc: Tamhane, n = 12-17).

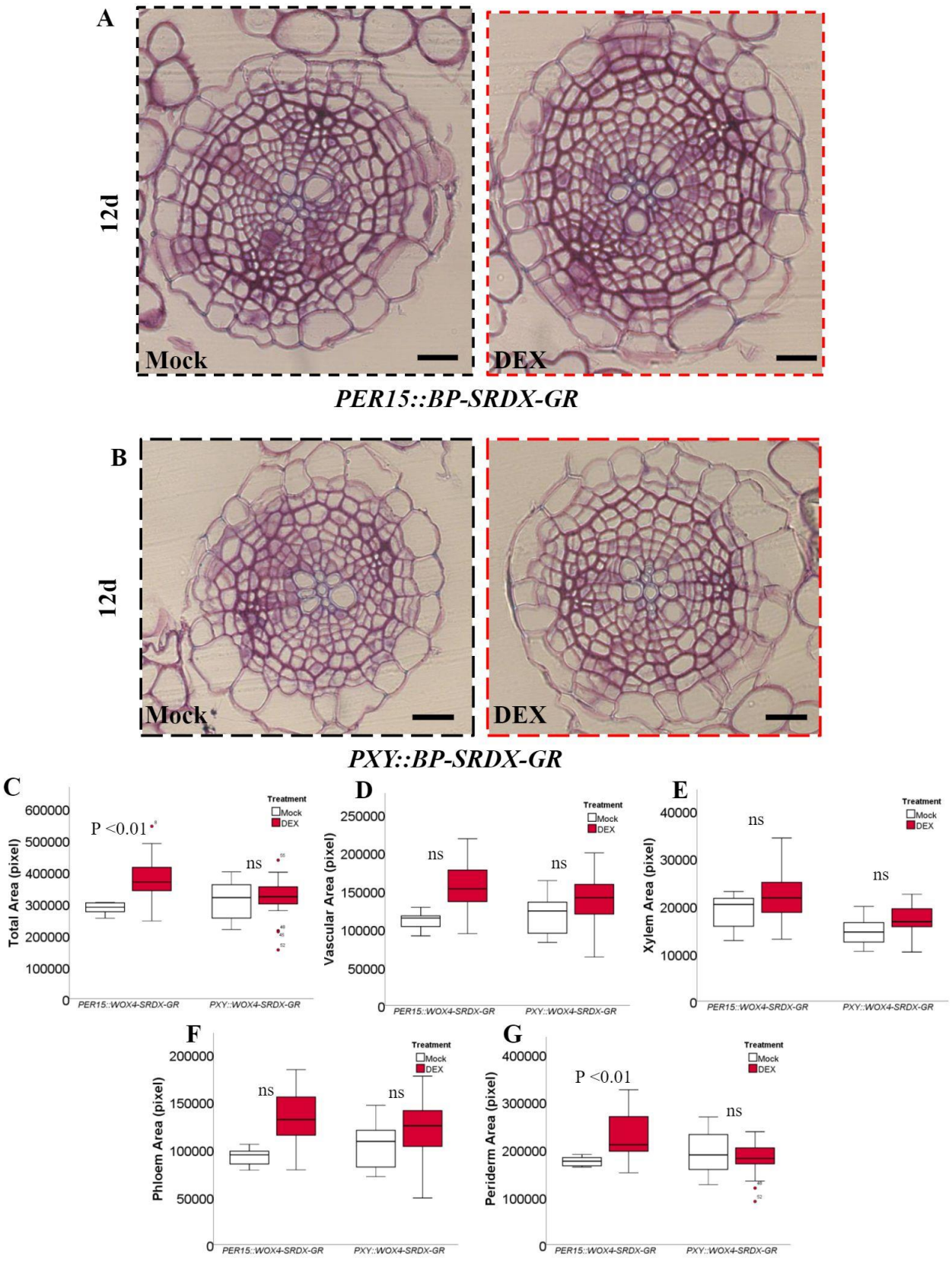
A
12d
Mock
DEX
PER15::BP-SRDX-GR
B
12d
Mock
DEX
PXY::BP-SRDX-GR
C
Total Area (pixel)
P <0.01
ns
Treatment
Mock
DEX
PER15::WOX4-SRDX-GR
PXY::WOX4-SRDX-GR
D
Vascular Area (pixel)
ns
ns
E
Xylem Area (pixel)
ns
ns
F
Phloem Area (pixel)
ns
ns
G
Periderm Area (pixel)
P <0.01
ns

Figure S8. BP-SRDX promotes periderm development.

A, Cross-sections (plastic embedding) of the uppermost part of *PER15::BP-SRDX-GR* (in *W131Y*) roots. 12-d-old plants on Mock (left panels) or 10μM DEX (right panels) plates. **B,** Cross-sections (plastic embedding) of the uppermost part of *PXY::BP-SRDX-GR* (in *W131Y*) roots. 12-d-old plants on Mock (left panels) or 10μM DEX (right panels) plates. **C-G,** Quantification of total area, vascular area, phloem area, xylem area, and periderm area of the experiment shown in (A-B). T-test (n =10-13). Black scale bars: 20μm.

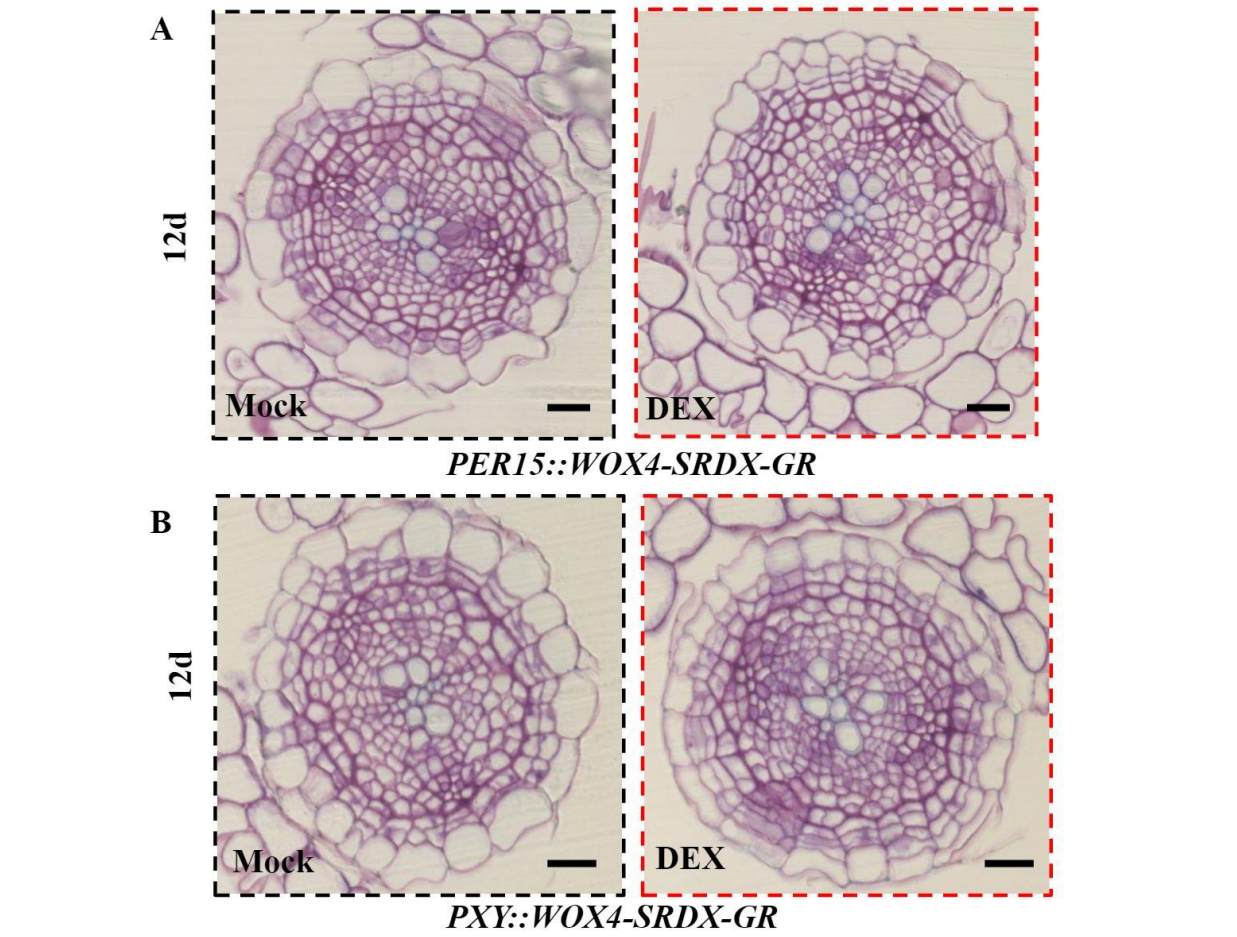
A
12d
Mock
DEX
PER15::WOX4-SRDX-GR
B
12d
Mock
DEX
PXY::WOX4-SRDX-GR

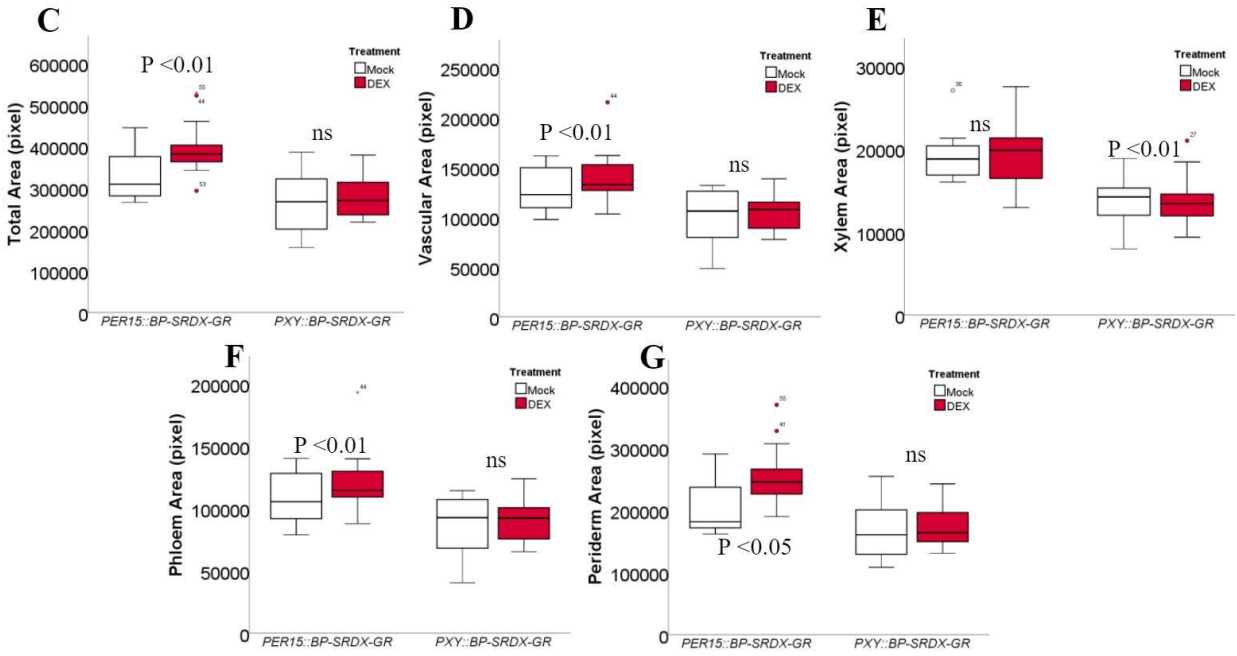
C
Total Area (pixel)
P <0.01
ns
Treatment
Mock
DEX
PER15::BP-SRDX-GR
PXY::BP-SRDX-GR
D
Vascular Area (pixel)
P <0.01
ns
E
Xylem Area (pixel)
ns
P <0.01
F
Phloem Area (pixel)
P <0.01
ns
G
Periderm Area (pixel)
P <0.05
ns

Figure S9. WOX4-SRDX promotes periderm development.

A, Cross-sections (plastic embedding) of the uppermost part of *PER15::WOX4-SRDX-GR* (in *W131Y*) roots. 12-d-old plants on Mock (left panels) or 10µM DEX (right panels) plates. **B,** Cross-sections (plastic embedding) of the uppermost part of *PXY::WOX4-SRDX-GR* (in *W131Y*) roots. 12-d-old plants on Mock (left panels) or 10µM DEX (right panels) plates. **C-G,** Quantification of total area, vascular area, phloem area, xylem area, and periderm area of the experiment shown in (A-B). T-test (n =10-13). Black scale bars: 20µm.

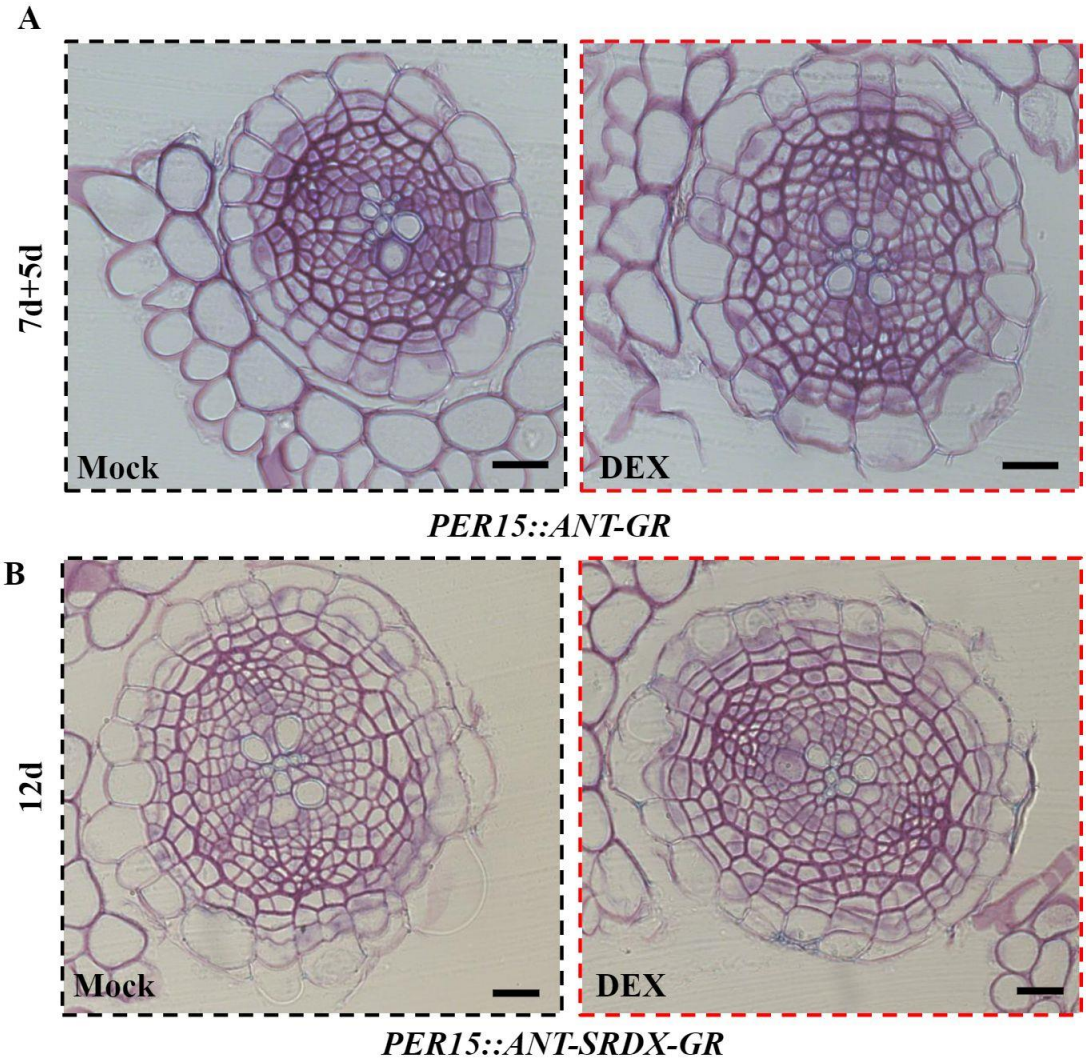
A
7d+5d
Mock
DEX
PER15::ANT-GR
B
12d
Mock
DEX
PER15::ANT-SRDX-GR

Figure S10. ANT is related to secondary growth.

A, Cross-sections (plastic embedding) of the uppermost part of *PER15::ANT-GR* (in *W131Y*) roots. 7-d-old plants were transferred for 5-d on Mock (left panels) or 10μM DEX (right panels) plates. **B,** Cross-sections (plastic embedding) of the uppermost part of *PER15::ANT-SRDX-GR* (in *W131Y*) roots. 12-d-old plants on Mock (left panels) or 10μM DEX (right panels) plates. Black scale bars: 20μm.

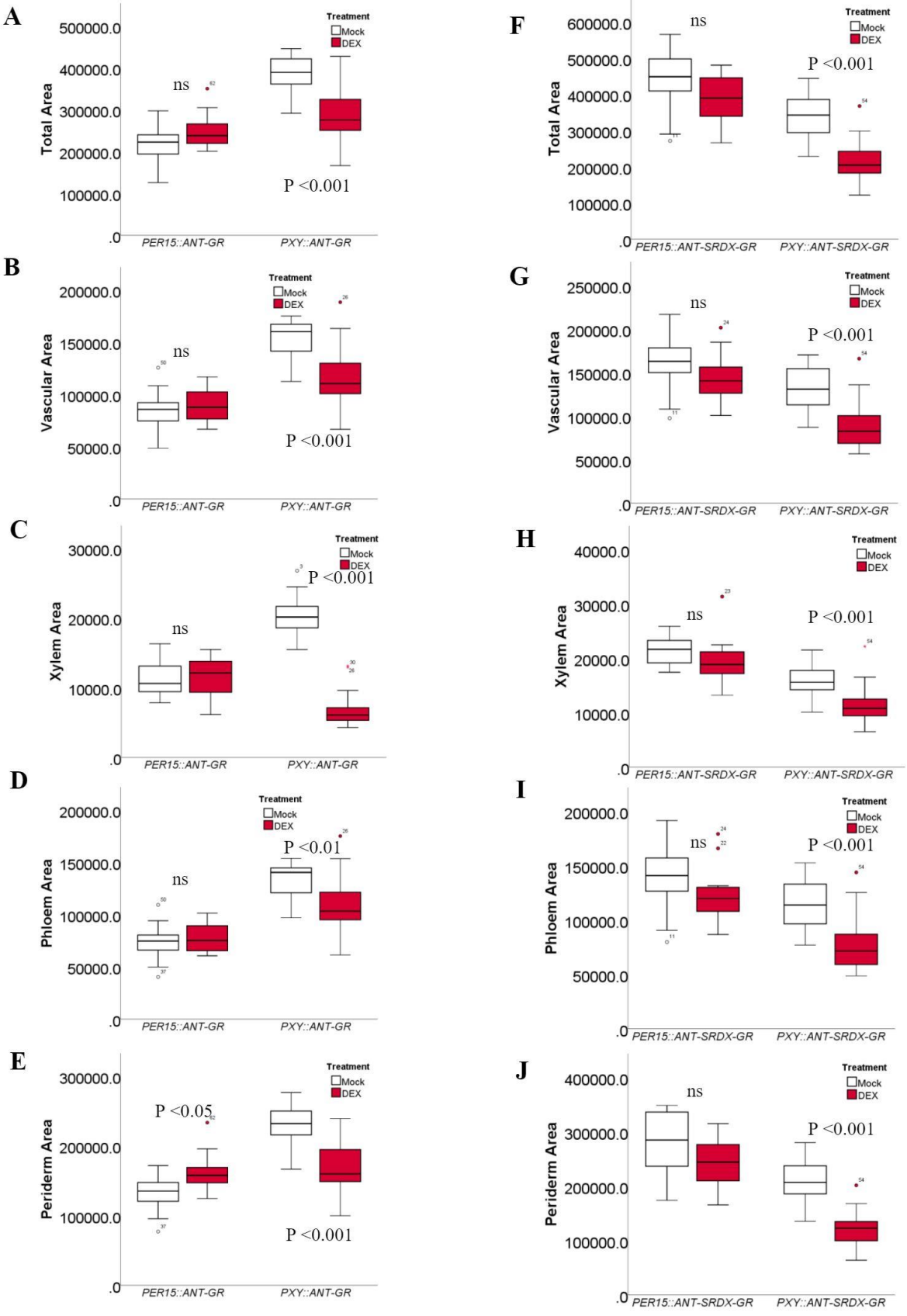
A
Total Area
500000.0
400000.0
300000.0
200000.0
100000.0
.0
Treatment
Mock
DEX
ns
P <0.001
PER15::ANT-GR
PXY::ANT-GR
B
Vascular Area
200000.0
150000.0
100000.0
50000.0
.0
ns
P <0.001
C
Xylem Area
30000.0
20000.0
10000.0
P <0.001
D
Phloem Area
200000.0
150000.0
100000.0
50000.0
P <0.01
E
Periderm Area
300000.0
200000.0
100000.0
P <0.05
P <0.001
F
Total Area
600000.0
500000.0
400000.0
300000.0
200000.0
100000.0
PER15::ANT-SRDX-GR
PXY::ANT-SRDX-GR
G
Vascular Area
250000.0
200000.0
150000.0
100000.0
50000.0
H
Xylem Area
40000.0
30000.0
20000.0
10000.0
I
Phloem Area
200000.0
150000.0
100000.0
50000.0
J
Periderm Area
400000.0
300000.0
200000.0
100000.0

Figure S11. ANT is related to xylem cell formation.

A-E, Quantification of total area, vascular area, phloem area, xylem area, and periderm area of the experiment shown in (Figure 5B and S10A). T-test (n =10-16). **F-J,** Quantification of total area, vascular area, phloem area, xylem area, and periderm area of the experiment shown in (Figure 5C and S10B). T-test (n =10-18).

References:

Barberon M, Vermeer JE, De Bellis D, Wang P, Naseer S, Andersen TG, Humbel BM, Nawrath C, Takano J, Salt DE, Geldner N. 2016. Adaptation of root function by Nutrient-Induced plasticity of endodermal differentiation. *CELL* **164(**3): 447-459.

Barra-Jimenez A, Ragni L. 2017. Secondary development in the stem: When Arabidopsis and trees are closer than it seems. *CURRENT OPINION IN PLANT BIOLOGY* **35**: 145-151.

Ben-Targem M, Ripper D, Bayer M, Ragni L. 2021. Auxin and gibberellin signaling cross-talk promotes hypocotyl xylem expansion and cambium homeostasis. *Journal of Experimental Botany* **72**(10): 3647–3660.

Bergmann DC, Lukowitz W, Somerville CR. 2004. Stomatal development and pattern controlled by a MAPKK kinase. *SCIENCE* **304**(5676): 1494-1497.

Campilho A, Nieminen K, Ragni L. 2020. The development of the periderm: The final frontier between a plant and its environment. *CURRENT OPINION IN PLANT BIOLOGY* **53**: 10-14.

DALBY P. 2021. From solving climate change to building space rockets, ERECTA - a multifaceted Receptor-Like Kinase. Durham theses, Durham University.

de Reuille PB, Ragni L. 2017. Vascular morphodynamics during secondary growth. *Methods in Molecular Biology* **1544**: 103-125.

Etchells JP, Provost CM, Mishra L, Turner SR. 2013. WOX4 and WOX14 act downstream of the PXY receptor kinase to regulate plant vascular proliferation independently of any role in vascular organisation. *DEVELOPMENT* **140(**10): 2224-2234.

Geldner N, Denervaud-Tendon V, Hyman DL, Mayer U, Stierhof YD, Chory J. 2009. Rapid, combinatorial analysis of membrane compartments in intact plants with a multicolor marker set. *PLANT JOURNAL* **59(**1): 169-178.

Hirakawa Y, Kondo Y, Fukuda H. 2010. TDIF peptide signaling regulates vascular stem cell proliferation via the WOX4 homeobox gene in Arabidopsis. *PLANT CELL* **22**(8): 2618-2629.

Hohmann U, Ramakrishna P, Wang K, Lorenzo-Orts L, Nicolet J, Henschen A, Barberon M, Bayer M, Hothorn M. 2020. Constitutive activation of Leucine-Rich repeat receptor kinase signaling pathways by BAK1-INTERACTING RECEPTOR-LIKE KINASE3 chimera. *PLANT CELL* **32**(10): 3311-3323.

Ikematsu S, Tasaka M, Torii KU, Uchida N. 2017. ERECTA-family receptor kinase genes redundantly prevent premature progression of secondary growth in the Arabidopsis hypocotyl. *NEW PHYTOLOGIST* **213**(4): 1697-1709.

Kai Wang HCYM, Sascha Laubinger MB. 2020. Independent parental contributions initiate zygote polarization in Arabidopsis thaliana. *bioRxiv*.

Krizek BA, Bantle AT, Heflin JM, Han H, Freese NH, Loraine AE. 2021. AINTEGUMENTA and AINTEGUMENTA-LIKE6 directly regulate floral homeotic, growth, and vascular development genes in young Arabidopsis flowers. *JOURNAL OF EXPERIMENTAL BOTANY* **72**(15): 5478-5493.

Lampropoulos A, Sutikovic Z, Wenzl C, Maegele I, Lohmann JU, Forner J. 2013. GreenGate---a novel, versatile, and efficient cloning system for plant transgenesis. *PLoS One* **8**(12): e83043.

Liebsch D, Sunaryo W, Holmlund M, Norberg M, Zhang J, Hall HC, Helizon H, Jin X, Helariutta Y, Nilsson O, Polle A, Fischer U. 2014. Class I KNOX transcription factors promote differentiation of cambial derivatives into xylem fibers in the Arabidopsis hypocotyl. *DEVELOPMENT* **141**(22): 4311-4319.

Mahfouz MM, Li L, Piatek M, Fang X, Mansour H, Bangarusamy DK, Zhu JK. 2012. Targeted transcriptional repression using a chimeric TALE-SRDX repressor protein. *PLANT MOLECULAR BIOLOGY* **78**(3): 311-321.

Meng X, Wang H, He Y, Liu Y, Walker JC, Torii KU, Zhang S. 2012. A MAPK cascade downstream of ERECTA receptor-like protein kinase regulates Arabidopsis inflorescence architecture by promoting localized cell proliferation. *PLANT CELL* **24**(12): 4948-4960.

Naseer S, Lee Y, Lapierre C, Franke R, Nawrath C, Geldner N. 2012. Casparian strip diffusion barrier in Arabidopsis is made of a lignin polymer without suberin. *Proceedings of the National Academy of Sciences of the United States of America* **109**(25): 10101-10106.

Ragni L, Greb T. 2018. Secondary growth as a determinant of plant shape and form. *SEMINARS IN CELL & DEVELOPMENTAL BIOLOGY* **79**: 58-67.

Ramakrishna P, Ruiz DP, Rance GA, Schubert M, Vordermaier V, Vu LD, Murphy E, Vilches BA, Swarup K, Moirangthem K, Jorgensen B, van de Cotte B, Goh T, Lin Z, Vobeta U, Beeckman T, Bennett MJ, Gevaert K, Maizel A, De Smet I. 2019. EXPANSIN A1-mediated radial swelling of pericycle cells positions anticlinal cell divisions during lateral root initiation. *Proceedings of the National Academy of*

Sciences of the United States of America **116**(17): 8597-8602.

Randall RS, Miyashima S, Blomster T, Zhang J, Elo A, Karlberg A, Immanen J, Nieminen K, Lee JY, Kakimoto T, Blajecka K, Melnyk CW, Alcasabas A, Forzani C, Matsumoto-Kitano M, Mahonen AP, Bhalerao R, Dewitte W, Helariutta Y, Murray JA. 2015. AINTEGUMENTA and the D-type cyclin CYCD3;1 regulate root secondary growth and respond to cytokinins. *Biology Open* **4**(10): 1229-1236.

Schindelin J, Arganda-Carreras I, Frise E, Kaynig V, Longair M, Pietzsch T, Preibisch S, Rueden C, Saalfeld S, Schmid B, Tinevez JY, White DJ, Hartenstein V, Eliceiri K, Tomancak P, Cardona A. 2012. Fiji: An open-source platform for biological-image analysis. *NATURE METHODS* **9**(7): 676-682.

Schurholz AK, Lopez-Salmeron V, Li Z, Forner J, Wenzl C, Gaillochet C, Augustin S, Barro AV, Fuchs M, Gebert M, Lohmann JU, Greb T, Wolf S. 2018. A comprehensive toolkit for inducible, cell Type-Specific gene expression in arabidopsis. *PLANT PHYSIOLOGY* **178**(1): 40-53.

Shpak ED, Berthiaume CT, Hill EJ, Torii KU. 2004. Synergistic interaction of three ERECTA-family receptor-like kinases controls Arabidopsis organ growth and flower development by promoting cell proliferation. *DEVELOPMENT* **131**(7): 1491-1501.

Shpak ED, McAbee JM, Pillitteri LJ, Torii KU. 2005. Stomatal patterning and differentiation by synergistic interactions of receptor kinases. *SCIENCE* **309**(5732): 290-293.

Smetana O, Makila R, Lyu M, Amiryousefi A, Sanchez RF, Wu MF, Sole-Gil A, Leal GM, Siligato R, Miyashima S, Roszak P, Blomster T, Reed JW, Broholm S, Mahonen AP. 2019. High levels of auxin signalling define the stem-cell organizer of the vascular cambium. *NATURE* **565**(7740): 485-489.

Suer S, Agusti J, Sanchez P, Schwarz M, Greb T. 2011. WOX4 imparts auxin responsiveness to cambium cells in Arabidopsis. *PLANT CELL* **23**(9): 3247-3259.

Torii KU, Mitsukawa N, Oosumi T, Matsuura Y, Yokoyama R, Whittier RF, Komeda Y. 1996. The Arabidopsis ERECTA gene encodes a putative receptor protein kinase with extracellular leucine-rich repeats. *PLANT CELL* **8**(4): 735-746.

Uchida N, Tasaka M. 2013. Regulation of plant vascular stem cells by endodermis-derived EPFL-family peptide hormones and phloem-expressed ERECTA-family receptor kinases. *JOURNAL OF EXPERIMENTAL BOTANY* **64**(17): 5335-5343.

Vilches BA, Stockle D, Thellmann M, Ruiz-Duarte P, Bald L, Louveaux M, von Born P, Denninger P, Goh T, Fukaki H, Vermeer J, Maizel A. 2019. Cytoskeleton

dynamics are necessary for early events of lateral root initiation in arabidopsis. *CURRENT BIOLOGY* **29**(15): 2443-2454.

Wang N, Bagdassarian KS, Doherty RE, Kroon JT, Connor KA, Wang XY, Wang W, Jermyn IH, Turner SR, Etchells JP. 2019. Organ-specific genetic interactions between paralogues of the PXY and ER receptor kinases enforce radial patterning in Arabidopsis vascular tissue. *DEVELOPMENT* **146**(10).

Wunderling A, Ripper D, Barra-Jimenez A, Mahn S, Sajak K, Targem MB, Ragni L. 2018. A molecular framework to study periderm formation in Arabidopsis. *NEW PHYTOLOGIST* **219**(1): 216-229.

Xiao W, Molina D, Wunderling A, Ripper D, Vermeer J, Ragni L. 2020. Pluripotent pericycle cells trigger different growth outputs by integrating developmental cues into distinct regulatory modules. *CURRENT BIOLOGY* **30**(22): 4384-4398.

Yamaguchi N, Wu MF, Winter CM, Berns MC, Nole-Wilson S, Yamaguchi A, Coupland G, Krizek BA, Wagner D. 2013. A molecular framework for auxin-mediated initiation of flower primordia. *DEVELOPMENTAL CELL* **24**(3): 271-282.

Zhang J, Eswaran G, Alonso-Serra J, Kucukoglu M, Xiang J, Yang W, Elo A, Nieminen K, Damen T, Joung JG, Yun JY, Lee JH, Ragni L, Barbier DRP, Ahnert SE, Lee JY, Mahonen AP, Helariutta Y. 2019. Transcriptional regulatory framework for vascular cambium development in Arabidopsis roots. *Nature Plants* **5**(10): 1033-1042.

6 Conclusion and Discussion

Embryonic development transforms the seed into a multicellular organism, whereas the complexity of plant morphogenesis needs post embryonic development. Plants control the processes of embryonic development and post embryonic development by phytohormones including auxin and cytokinin. In the post embryonic development, both auxin and cytokinin signalling affect plant morphogenesis by generating lateral tissues. In the plant root and stem, secondary growth as one of the lateral tissues contributes to root architecture system. Previous studies have shown that auxin and cytokinin are the crucial phytohormones during secondary growth, maintaining the proliferation and directing differentiation of meristematic tissues (Ragni & Greb, 2018; Smetana *et al.*, 2019; Zhang *et al.*, 2019; Campilho *et al.*, 2020). Our results suggest that auxin distribution and activity are mandatory for maintaining phellogen proliferation and leading differentiation.

Auxin is one of the essential phytohormones and is specified pericycle cell differentiation, generating lateral roots development, periderm development and vascular development, respectively. Interestingly, our results demonstrate a complex auxin induced regulatory mechanism on these three plant organs/tissues: blocking lateral roots have a positive effect on periderm initiation; precocious vascular cambium is the prerequisite of periderm initiation. In the meanwhile, both vascular cambium and phellogen are initiated/partially initiated from pericycle cells, which gives us a clue to further dissect the role of auxin independently in these two cambia.

Furthermore, to elaborate root structure against various environment, plants shape plant architecture system by selecting the appropriate plant organs/tissues during the growth by activating distinct auxin-induced modules. *BP* and *WOX4* as master cambium regulators are activated by BDL-MP module, promoting the vascular cambium and phellogen proliferation and division; while *SLR-ARF7ARF19* module regulates *GATA23* and *LBD16*, controlling the lateral roots formation. Altogether, these findings allow us to generate a model (Figure 2) in which elevate auxin signalling in the root development leads different IAAs-ARFs modules with specific downstream targets to initiate and then maintain distinct plant organs/tissues (Fukaki *et al.*, 2002; Lee *et al.*, 2009; De Rybel *et al.*, 2010; Hirakawa *et al.*, 2010; Suer *et al.*, 2011; Fan *et al.*, 2012; Etchells *et al.*, 2013; Ito *et al.*, 2016; Smetana *et al.*, 2019; Zhang *et al.*, 2019; Xiao *et al.*, 2020). In this work, we fully demonstrated how specificity in pericycle stem cell

fate is achieved and vascular cambium establishment is a positive factor on cork cambium initiation (Xiao *et al.*, 2020).

Although we deeply dissect the function of auxin during periderm initiation and different downstream targets of auxin in controlling the establishment of lateral roots, phellogen, the vascular cambium, it is still unclear about the coordinating activity of the phellogen and the vascular cambium. Therefore, we deeply dissect the auxin signalling in both the phellogen and the vascular cambium. Our genetic and gene expression data demonstrate that auxin is essential for maintain cork cambium identity. Next, under stresses on one of the cambia, the plants activate another cambium, suggesting a compensation mechanism between periderm and vascular. Moreover, we found that these two cambia shared many auxin-related regulators including *BP*, *WOX4*, *ANT*, *ER*, and many other peptides like CLE and EPFL peptides, which were involved in secondary growth, enforcing vascular organization and radial patterning (Hirakawa *et al.*, 2010; Suer *et al.*, 2011; Etchells *et al.*, 2013; Ragni & Greb, 2018). *ER* receptor kinase and *ANT* transcriptional factor are expressed in *Arabidopsis* root and positive regulate secondary growth; furthermore, ER-ANT module determines the differentiation of vascular cambium and promotes phloem development (Torii *et al.*, 1996; Bergmann *et al.*, 2004; Shpak *et al.*, 2004; Shpak *et al.*, 2005; Meng *et al.*, 2012; Uchida & Tasaka, 2013; Randall *et al.*, 2015; Ikematsu *et al.*, 2017; Wang *et al.*, 2019). Taken all together, we show that auxin signalling in meristematic tissues triggers proliferation and differentiation in secondary growth patterning, maintaining both fate and rate of proliferation and differentiation through the activation of distinct auxin inducible transcriptional regulators. Finally, we provide insights into the auxin-induced regulatory network underlying secondary growth plasticity in *Arabidopsis*. Eventually, we highlight that distinct signalling pathways, downstream of auxin and cytokinin, orchestrate periderm and vascular formation: *BP*, *WOX4*, *ANT*, and *ER* as key factors are involved in secondary growth.

We demonstrated a compensated mechanism exists on the vascular cambium and phellogen. We suggest that a non-cell-autonomous signal (hormone/peptide/small RNA/mobile TF) between these two cambia. The communication and cooperation between these two cambia allow the plants to keep on recovering and growing even in an unsatisfied growth condition, and produce the next generation. Moreover, the weight of stem could also be the physical forces on the vascular cambium or phellogen, which could drive the vascular or periderm development. It would be interesting to further

decipher how these two cambia connect.

Recently, many studies reported plants manipulate different plants hormones to precisely control the balance of the plant growth and resistance in different developmental stages. We highlighted that ER-ANT module alter the ratio between the phloem and the xylem causing a strong reduction on secondary growth. We suggest that the plants need to keep the balance of the phloem and the xylem to reach best growth condition. Phellogen and vascular cambium specific overexpression of BIR-ER and ANT-SRDX provide a novel approach for disturbing the ratio of the phloem and xylem, a trait that is known to contribute to stress tolerance.

Moreover, many other plant hormones have been shown that they participate in secondary growth including cytokinin, gibberillic acids (GA), strigolactones (SLs), and etc. During secondary growth, we find these plant hormones contain a crosstalk and co-control the development the processes together. It implies a possible cooperation among these plant hormones. For example, *BP*, *WOX4* and *ANT* work as the downstream targets of both auxin and cytokinin; and *ARF6* and *ARF8* are co-regulated by auxin and GA signalling (Randall *et al.*, 2015; Smetana *et al.*, 2019; Zhang *et al.*, 2019; Ben-Targem *et al.*, 2021; Ye *et al.*, 2021). Although, plants control their behaviour through distinct plant hormones interaction by affecting similar downstream regulators.

In our work, we utilize the tissue specific promoters to further point out the vascular cambium, phellogen and phellem, which greatly improve our knowledge on secondary growth (Xiao *et al.*, 2020). However, the xylem, phloem and phelloderm are lack of a functional marker to highlight their precise location. Therefore, it is important to obtain a specific mark on these tissues.

Altogether, our studies dissect auxin regulatory hub during secondary growth and unveil the processes of vascular cambium differentiation and provide an idea to further investigate how the plants shape their own root structure by controlling different phytohormones.

7. References

Agusti J, Herold S, Schwarz M, Sanchez P, Ljung K, Dun EA, Brewer PB, Beveridge CA, Sieberer T, Sehr EM, Greb T. 2011. Strigolactone signaling is required for auxin-dependent stimulation of secondary growth in plants. *Proceedings of the National Academy of Sciences of the United States of America* **108**(50): 20242-20247.

Andersen TG, Naseer S, Ursache R, Wybouw B, Smet W, De Rybel B, Vermeer J, Geldner N. 2018. Diffusible repression of cytokinin signalling produces endodermal symmetry and passage cells. *NATURE* **555**(7697): 529-533.

Atta R, Laurens L, Boucheron-Dubuisson E, Guivarc'H A, Carnero E, Giraudat-Pautot V, Rech P, Chriqui D. 2009. Pluripotency of Arabidopsis xylem pericycle underlies shoot regeneration from root and hypocotyl explants grown in vitro. *PLANT JOURNAL* **57**(4): 626-644.

Barra-Jimenez A, Ragni L. 2017. Secondary development in the stem: When Arabidopsis and trees are closer than it seems. *CURRENT OPINION IN PLANT BIOLOGY* **35**: 145-151.

Beeckman T, De Smet I. 2014. Pericycle. *CURRENT BIOLOGY* **24**(10): R378-R379.

Bennett T, Sieberer T, Willett B, Booker J, Luschnig C, Leyser O. 2006. The Arabidopsis MAX pathway controls shoot branching by regulating auxin transport. *CURRENT BIOLOGY* **16**(6): 553-563.

Brackmann K, Qi J, Gebert M, Jouannet V, Schlamp T, Grunwald K, Wallner ES, Novikova DD, Levitsky VG, Agusti J, Sanchez P, Lohmann JU, Greb T. 2018. Spatial specificity of auxin responses coordinates wood formation. *Nature Communications* **9**(1): 875.

Campilho A, Nieminen K, Ragni L. 2020. The development of the periderm: The final frontier between a plant and its environment. *CURRENT OPINION IN PLANT BIOLOGY* **53**: 10-14.

Carlsbecker A, Lee JY, Roberts CJ, Dettmer J, Lehesranta S, Zhou J, Lindgren O, Moreno-Risueno MA, Vaten A, Thitamadee S, Campilho A, Sebastian J, Bowman JL, Helariutta Y, Benfey PN. 2010. Cell signalling by microRNA165/6 directs gene dose-dependent root cell fate. *NATURE* **465**(7296): 316-321.

Casimiro I, Marchant A, Bhalerao RP, Beeckman T, Dhooge S, Swarup R,

Graham N, Inze D, Sandberg G, Casero PJ, Bennett M. 2001. Auxin transport promotes Arabidopsis lateral root initiation. *PLANT CELL* **13**(4): 843-852.

Che P, Lall S, Howell SH. 2007. Developmental steps in acquiring competence for shoot development in Arabidopsis tissue culture. *PLANTA* **226**(5): 1183-1194.

Crawford S, Shinohara N, Sieberer T, Williamson L, George G, Hepworth J, Muller D, Domagalska MA, Leyser O. 2010. Strigolactones enhance competition between shoot branches by dampening auxin transport. *DEVELOPMENT* **137**(17): 2905-2913.

De Rybel B, Vassileva V, Parizot B, Demeulenaere M, Grunewald W, Audenaert D, Van Campenhout J, Overvoorde P, Jansen L, Vanneste S, Moller B, Wilson M, Holman T, Van Isterdael G, Brunoud G, Vuylsteke M, Vernoux T, De Veylder L, Inze D, Weijers D, Bennett MJ, Beeckman T. 2010. A novel aux/IAA28 signaling cascade activates GATA23-dependent specification of lateral root founder cell identity. *CURRENT BIOLOGY* **20**(19): 1697-1706.

De Smet I, Lau S, Voss U, Vanneste S, Benjamins R, Rademacher EH, Schlereth A, De Rybel B, Vassileva V, Grunewald W, Naudts M, Levesque MP, Ehrismann JS, Inze D, Luschnig C, Benfey PN, Weijers D, Van Montagu MC, Bennett MJ, Jurgens G, Beeckman T. 2010. Bimodular auxin response controls organogenesis in Arabidopsis. *Proceedings of the National Academy of Sciences of the United States of America* **107**(6): 2705-2710.

De Smet I, Tetsumura T, De Rybel B, Frei DFN, Laplaze L, Casimiro I, Swarup R, Naudts M, Vanneste S, Audenaert D, Inze D, Bennett MJ, Beeckman T. 2007. Auxin-dependent regulation of lateral root positioning in the basal meristem of Arabidopsis. *DEVELOPMENT* **134**(4): 681-690.

Dolan L, Janmaat K, Willemsen V, Linstead P, Poethig S, Roberts K, Scheres B. 1993. Cellular organisation of the Arabidopsis thaliana root. *DEVELOPMENT* **119**(1): 71-84.

Esau K. 1977. *Anatomy of seed plants*. New York: Wiley.

Etchells JP, Provost CM, Mishra L, Turner SR. 2013. WOX4 and WOX14 act downstream of the PXY receptor kinase to regulate plant vascular proliferation independently of any role in vascular organisation. *DEVELOPMENT* **140**(10): 2224-2234.

Fan M, Xu C, Xu K, Hu Y. 2012. LATERAL ORGAN BOUNDARIES DOMAIN transcription factors direct callus formation in Arabidopsis regeneration. *CELL*

RESEARCH **22**(7): 1169-1180.

Fischer U, Kucukoglu M, Helariutta Y, Bhalerao RP. 2019. The dynamics of cambial stem cell activity. *Annual Review of Plant Biology* **70**: 293-319.

Fukaki H, Tameda S, Masuda H, Tasaka M. 2002. Lateral root formation is blocked by a gain-of-function mutation in the SOLITARY-ROOT/IAA14 gene of Arabidopsis. *PLANT JOURNAL* **29**(2): 153-168.

Gibbs DJ, Voss U, Harding SA, Fannon J, Moody LA, Yamada E, Swarup K, Nibau C, Bassel GW, Choudhary A, Lavenus J, Bradshaw SJ, Stekel DJ, Bennett MJ, Coates JC. 2014. AtMYB93 is a novel negative regulator of lateral root development in Arabidopsis. *NEW PHYTOLOGIST* **203**(4): 1194-1207.

Goh T, Kasahara H, Mimura T, Kamiya Y, Fukaki H. 2012. Multiple AUX/IAA-ARF modules regulate lateral root formation: The role of Arabidopsis SHY2/IAA3-mediated auxin signalling. *Philosophical Transactions of the Royal Society B: Biological Sciences* **367**(1595): 1461-1468.

Groh B, Hubner C, Lendzian KJ. 2002. Water and oxygen permeance of phellems isolated from trees: The role of waxes and lenticels. *PLANTA* **215**(5): 794-801.

Guilfoyle TJ, Hagen G. 2007. Auxin response factors. *CURRENT OPINION IN PLANT BIOLOGY* **10**(5): 453-460.

Guilfoyle TJ, Ulmasov T, Hagen G. 1998. The ARF family of transcription factors and their role in plant hormone-responsive transcription. *CELLULAR AND MOLECULAR LIFE SCIENCES* **54**(7): 619-627.

Hamann T, Benkova E, Baurle I, Kientz M, Jurgens G. 2002. The Arabidopsis BODENLOS gene encodes an auxin response protein inhibiting MONOPTEROS-mediated embryo patterning. *Genes & Development* **16**(13): 1610-1615.

Hay A, Barkoulas M, Tsiantis M. 2006. ASYMMETRIC LEAVES1 and auxin activities converge to repress BREVIPEDICELLUS expression and promote leaf development in Arabidopsis. *DEVELOPMENT* **133**(20): 3955-3961.

Hirakawa Y, Kondo Y, Fukuda H. 2010. TDIF peptide signaling regulates vascular stem cell proliferation via the WOX4 homeobox gene in Arabidopsis. *PLANT CELL* **22**(8): 2618-2629.

Hirota A, Kato T, Fukaki H, Aida M, Tasaka M. 2007. The auxin-regulated AP2/EREBP gene PUCHI is required for morphogenesis in the early lateral root primordium of Arabidopsis. *PLANT CELL* **19**(7): 2156-2168.

Husbands A, Bell EM, Shuai B, Smith HM, Springer PS. 2007. LATERAL ORGAN

BOUNDARIES defines a new family of DNA-binding transcription factors and can interact with specific bHLH proteins. *NUCLEIC ACIDS RESEARCH* **35**(19): 6663-6671.

Ito J, Fukaki H, Onoda M, Li L, Li C, Tasaka M, Furutani M. 2016. Auxin-dependent compositional change in Mediator in ARF7- and ARF19-mediated transcription. *Proceedings of the National Academy of Sciences of the United States of America* **113**(23): 6562-6567.

Jing H, Strader LC. 2019. Interplay of auxin and cytokinin in lateral root development. *INTERNATIONAL JOURNAL OF MOLECULAR SCIENCES* **20**(3).

Junli T, Alon B, Ilana S, Amnon B, Arnon D, Ran E. 2020. Root structural plasticity enhances salt tolerance in mature olives. *ENVIRONMENTAL AND EXPERIMENTAL BOTANY* **179**.

Lavenus J, Goh T, Roberts I, Guyomarc'H S, Lucas M, De Smet I, Fukaki H, Beeckman T, Bennett M, Laplaze L. 2013. Lateral root development in Arabidopsis: Fifty shades of auxin. *TRENDS IN PLANT SCIENCE* **18**(8): 450-458.

Lee HW, Kim NY, Lee DJ, Kim J. 2009. LBD18/ASL20 regulates lateral root formation in combination with LBD16/ASL18 downstream of ARF7 and ARF19 in Arabidopsis. *PLANT PHYSIOLOGY* **151**(3): 1377-1389.

Lendzian KJ. 2006. Survival strategies of plants during secondary growth: Barrier properties of phellems and lenticels towards water, oxygen, and carbon dioxide. *JOURNAL OF EXPERIMENTAL BOTANY* **57**(11): 2535-2546.

Leyser O. 2018. Auxin signaling. *PLANT PHYSIOLOGY* **176**(1): 465-479.

Li H, Wang B, Zhang Q, Wang J, King GJ, Liu K. 2017. Genome-wide analysis of the auxin/indoleacetic acid (Aux/IAA) gene family in allotetraploid rapeseed (Brassica napus L.). *BMC PLANT BIOLOGY* **17**(1): 204.

Liebsch D, Sunaryo W, Holmlund M, Norberg M, Zhang J, Hall HC, Helizon H, Jin X, Helariutta Y, Nilsson O, Polle A, Fischer U. 2014. Class I KNOX transcription factors promote differentiation of cambial derivatives into xylem fibers in the Arabidopsis hypocotyl. *DEVELOPMENT* **141**(22): 4311-4319.

Mockaitis K, Estelle M. 2008. Auxin receptors and plant development: A new signaling paradigm. *Annual Review of Cell Developmental Biology* **24**: 55-80.

Motte H, Vanneste S, Beeckman T. 2019. Molecular and environmental regulation of root development. *Annual Review of Plant Biology* **70**: 465-488.

Nieminen K, Blomster T, Helariutta Y, Mahonen AP. 2015. Vascular cambium

development. *Arabidopsis Book* **13**: e177.

Okushima Y, Fukaki H, Onoda M, Theologis A, Tasaka M. 2007. ARF7 and ARF19 regulate lateral root formation via direct activation ofLBD/ASL genes inArabidopsis. *The Plant Cell* **19**(1): 118-130.

Okushima Y, Overvoorde PJ, Arima K, Alonso JM, Chan A, Chang C, Ecker JR, Hughes B, Lui A, Nguyen D, Onodera C, Quach H, Smith A, Yu G, Theologis A. 2005. Functional genomic analysis of the AUXIN RESPONSE FACTOR gene family members in Arabidopsis thaliana: Unique and overlapping functions of ARF7 and ARF19. *PLANT CELL* **17**(2): 444-463.

Ori N, Eshed Y, Chuck G, Bowman JL, Hake S. 2000. Mechanisms that control knox gene expression in the Arabidopsis shoot. *DEVELOPMENT* **127**(24): 5523-5532.

Overvoorde PJ, Okushima Y, Alonso JM, Chan A, Chang C, Ecker JR, Hughes B, Liu A, Onodera C, Quach H, Smith A, Yu G, Theologis A. 2005. Functional genomic analysis of the AUXIN/INDOLE-3-ACETIC ACID gene family members in Arabidopsis thaliana. *PLANT CELL* **17**(12): 3282-3300.

Porco S, Larrieu A, Du Y, Gaudinier A, Goh T, Swarup K, Swarup R, Kuempers B, Bishopp A, Lavenus J, Casimiro I, Hill K, Benkova E, Fukaki H, Brady SM, Scheres B, Peret B, Bennett MJ. 2016. Lateral root emergence in Arabidopsis is dependent on transcription factor LBD29 regulation of auxin influx carrier LAX3. *DEVELOPMENT* **143**(18): 3340-3349.

Ragni L, Greb T. 2018. Secondary growth as a determinant of plant shape and form. *SEMINARS IN CELL & DEVELOPMENTAL BIOLOGY* **79**: 58-67.

Rogg LE, Lasswell J, Bartel B. 2001. A gain-of-function mutation in IAA28 suppresses lateral root development. *PLANT CELL* **13**(3): 465-480.

Shang B, Xu C, Zhang X, Cao H, Xin W, Hu Y. 2016. Very-long-chain fatty acids restrict regeneration capacity by confining pericycle competence for callus formation in Arabidopsis. *Proceedings of the National Academy of Sciences of the United States of America* **113**(18): 5101-5106.

Shin J, Seo PJ. 2018. Varying auxin levels induce distinct pluripotent states in callus cells. *Frontiers in Plant Science* **9**: 1653.

Smetana O, Makila R, Lyu M, Amiryousefi A, Sanchez RF, Wu MF, Sole-Gil A, Leal GM, Siligato R, Miyashima S, Roszak P, Blomster T, Reed JW, Broholm S, Mahonen AP. 2019. High levels of auxin signalling define the stem-cell organizer of the vascular cambium. *NATURE* **565**(7740): 485-489.

Smit ME, Weijers D. 2015. The role of auxin signaling in early embryo pattern formation. *CURRENT OPINION IN PLANT BIOLOGY* **28**: 99-105.

Suer S, Agusti J, Sanchez P, Schwarz M, Greb T. 2011. WOX4 imparts auxin responsiveness to cambium cells in Arabidopsis. *PLANT CELL* **23**(9): 3247-3259.

Swarup K, Benkova E, Swarup R, Casimiro I, Peret B, Yang Y, Parry G, Nielsen E, De Smet I, Vanneste S, Levesque MP, Carrier D, James N, Calvo V, Ljung K, Kramer E, Roberts R, Graham N, Marillonnet S, Patel K, Jones JD, Taylor CG, Schachtman DP, May S, Sandberg G, Benfey P, Friml J, Kerr I, Beeckman T, Laplaze L, Bennett MJ. 2008. The auxin influx carrier LAX3 promotes lateral root emergence. *NATURE CELL BIOLOGY* **10**(8): 946-954.

Swarup R, Kramer EM, Perry P, Knox K, Leyser HM, Haseloff J, Beemster GT, Bhalerao R, Bennett MJ. 2005. Root gravitropism requires lateral root cap and epidermal cells for transport and response to a mobile auxin signal. *NATURE CELL BIOLOGY* **7**(11): 1057-1065.

Tatematsu K, Kumagai S, Muto H, Sato A, Watahiki MK, Harper RM, Liscum E, Yamamoto KT. 2004. MASSUGU2 encodes Aux/IAA19, an auxin-regulated protein that functions together with the transcriptional activator NPH4/ARF7 to regulate differential growth responses of hypocotyl and formation of lateral roots in Arabidopsis thaliana. *PLANT CELL* **16**(2): 379-393.

Tian Q, Reed JW. 1999. Control of auxin-regulated root development by the Arabidopsis thaliana SHY2/IAA3 gene. *DEVELOPMENT* **126**(4): 711-721.

Tiwari SB, Hagen G, Guilfoyle T. 2003. The roles of auxin response factor domains in auxin-responsive transcription. *PLANT CELL* **15**(2): 533-543.

Tiwari SB, Wang XJ, Hagen G, Guilfoyle TJ. 2001. AUX/IAA proteins are active repressors, and their stability and activity are modulated by auxin. *PLANT CELL* **13**(12): 2809-2822.

Uehara T, Okushima Y, Mimura T, Tasaka M, Fukaki H. 2008. Domain II mutations in CRANE/IAA18 suppress lateral root formation and affect shoot development in Arabidopsis thaliana. *PLANT AND CELL PHYSIOLOGY* **49**(7): 1025-1038.

Uggla C, Mellerowicz EJ, Sundberg B. 1998. Indole-3-acetic acid controls cambial growth in scots pine by positional signaling. *PLANT PHYSIOLOGY* **117**(1): 113-121.

Ulmasov T, Hagen G, Guilfoyle TJ. 1999. Dimerization and DNA binding of auxin response factors. *PLANT JOURNAL* **19**(3): 309-319.

Van Norman JM, Xuan W, Beeckman T, Benfey PN. 2013. To branch or not to branch: The role of pre-patterning in lateral root formation. *DEVELOPMENT* **140**(21): 4301-4310.

Vanneste S, De Rybel B, Beemster GT, Ljung K, De Smet I, Van Isterdael G, Naudts M, Iida R, Gruissem W, Tasaka M, Inze D, Fukaki H, Beeckman T. 2005. Cell cycle progression in the pericycle is not sufficient for SOLITARY ROOT/IAA14-mediated lateral root initiation in Arabidopsis thaliana. *PLANT CELL* **17**(11): 3035-3050.

Vermeer JE, von Wangenheim D, Barberon M, Lee Y, Stelzer EH, Maizel A, Geldner N. 2014. A spatial accommodation by neighboring cells is required for organ initiation in Arabidopsis. *SCIENCE* **343**(6167): 178-183.

Vilches BA, Stockle D, Thellmann M, Ruiz-Duarte P, Bald L, Louveaux M, von Born P, Denninger P, Goh T, Fukaki H, Vermeer J, Maizel A. 2019. Cytoskeleton dynamics are necessary for early events of lateral root initiation in arabidopsis. *CURRENT BIOLOGY* **29**(15): 2443-2454.

Waldie T, McCulloch H, Leyser O. 2014. Strigolactones and the control of plant development: Lessons from shoot branching. *PLANT JOURNAL* **79**(4): 607-622.

Wilmoth JC, Wang S, Tiwari SB, Joshi AD, Hagen G, Guilfoyle TJ, Alonso JM, Ecker JR, Reed JW. 2005. NPH4/ARF7 and ARF19 promote leaf expansion and auxin-induced lateral root formation. *PLANT JOURNAL* **43**(1): 118-130.

Wunderling A, Ripper D, Barra-Jimenez A, Mahn S, Sajak K, Targem MB, Ragni L. 2018. A molecular framework to study periderm formation in Arabidopsis. *NEW PHYTOLOGIST* **219**(1): 216-229.

Xiao W, Molina D, Wunderling A, Ripper D, Vermeer J, Ragni L. 2020. Pluripotent pericycle cells trigger different growth outputs by integrating developmental cues into distinct regulatory modules. *CURRENT BIOLOGY* **30**(22): 4384-4398.

Xu C, Luo F, Hochholdinger F. 2016. LOB domain proteins: Beyond lateral organ boundaries. *TRENDS IN PLANT SCIENCE* **21**(2): 159-167.

Yoshihara T, Spalding EP. 2017. LAZY genes mediate the effects of gravity on auxin gradients and plant architecture. *PLANT PHYSIOLOGY* **175**(2): 959-969.

Zhang J, Eswaran G, Alonso-Serra J, Kucukoglu M, Xiang J, Yang W, Elo A, Nieminen K, Damen T, Joung JG, Yun JY, Lee JH, Ragni L, Barbier DRP, Ahnert SE, Lee JY, Mahonen AP, Helariutta Y. 2019. Transcriptional regulatory framework for vascular cambium development in Arabidopsis roots. *Nature Plants* **5**(10): 1033-

1042.

8. Acknowledgements

First and foremost, I would like to thank Dr. Laura Ragni for this great opportunity to unveil the secret of secondary growth in her lab. She has provided me with valuable guidance during my PhD study. Without her enlightening instruction, impressive kindness and patience, I could not have completed my PhD study. Her keen and vigorous academic observation enlightens me not only in my PhD study but also in my future study.

I would like to thank Prof. Marja Timmermans and Dr. Martin Bayer for their scientific input during my PhD study.

Many thanks to my colleagues in the lab: Andrea Boch, David Molina, Dagmar Ripper, Xudong Zhang help me in many aspects during my PhD study. Many thanks to Martin-gebhard Boehme for the German abstract. Many thanks to Prof. Jinshun Zhong for his comments on this thesis. Many thanks to all my colleagues in the developmental genetic department and ZMBP as well as all the staff of each facility.

I would like to thank Prof. Klaus Harter and Prof. Claudia Oecking for accepting to be part of my PhD defense.

Wei Xiao

致谢

迎来送往又一年，春去春来总相连。当我是小孩子的时候，总是羡慕大人，总是埋怨时间过得太慢。等长大，才真正发现，光阴似箭，日月如梭，还真的不是说说而已。时光不知何处去，留我依旧笑春风。作为旅居海外的“华侨”，这将会是我在国外要过的第四个春节。在德国图宾根大学度过的三年半求学生涯，是我最后的学生生涯。

我父母和我说，我从两岁便开始“念书”，到今年共计二十七年。从此以后，再也不能以学生自居了。回首二十七年，我总归不是一个“安稳”的人。头十六年与父母一起度过，得到父母无微不至的关爱甚至是溺爱。之后我便开始了我的“瞎跑”。高考成绩不甚理想，但差强人意。我去到了一所还不错的211大学，位于重庆的西南大学。犹记得我为了勉励自己，用手机下载了德语词典，鼓励自己要去德国留学，读到博士。不过这个flag很快我就忘得干干净净。本科四年，算不得优秀，也算不得差劲，仅拿过两次校级奖学金。

本科毕业之后，又开始了我的“瞎跑”，我考研到了一所中国TOP10的高校，位于广州的中山大学。我运气很好，去到了罗达老师课题组。这个课题组很开心，很快乐，每一天都高高兴兴，和隔壁两个课题组形成了鲜明对比。在这里，有超棒的师兄师姐还有同学，也是最有意思的课题。三年下来，不算好，不算差，我拿到了国家研究生奖学金。

一八年，我又开始了我的“瞎跑”。我的博士导师，Dr. Laura Ragni给了我一个合同（德国全奖），因此我来到了德国，德国精英大学之一的图宾根大学，也正是那个大一立下Flag的德国。国外的日子并不好熬，什么事情都要自己扛。但我很幸运，周围的人都很友善，在这里我也结识到了好多好朋友。三年半过去，算不得成功，算不得失败。我发表了一篇SCI文章，也拿到了国家优秀自费留学生奖学金。

感谢我的父母，无私给予我他们能给予我的一切。他们不求什么回报，只希望我能健康快乐的生活下去。有他们，我才能有今天，穿上正装，昂首挺胸地走向博士答辩的舞台，我永远爱我的爸爸妈妈。

感谢我的导师们：罗达教授，姚楠教授和Laura博士。没有你们的一路指导，我不能走到今天。

感谢我的师兄师姐，我的同学，我的朋友的陪伴与帮助。更忘不了那些一路上来帮助过我的人。

最后感谢我的女朋友，杨玲。在我最迷茫的时候，给予我最大的帮助，鼓励和陪伴。

还是用硕士毕业论文中的同样一句话结尾：世界这么大，我想去看看。希望未来的自己，不忘初心，勇往直前，成为了那个我想成为的人，希望世界因为我的存在有一点点好的改变。

写于2021年12月15日23点34分。

肖威